ABSTRACT

Title of Dissertation: NEUROREPAIR PROMOTING CROSSTALK BETWEEN ASTROCYTES & OLFACTORY ENSHEATHING CELLS

Aybike Sağlam, Doctor of Philosophy, 2020

Dissertation directed by: Dr. Susan Wray, Chief, Cellular and Developmental Neurobiology Section NINDS, NIH

Astrocytes within the neurogenic zones of the adult central nervous system (CNS) support the formation and maturation of neurons from progenitor cells throughout life. In contrast, astrocytes outside of neurogenic zones dedifferentiate and contribute to scar tissue formation after injury, creating a physical barrier to regenerating neurons. Moreover, reactive astrocytes can create a chemical barrier and be toxic for neurons after injury. Therefore, understanding the signaling pathways that switch astrocytes from neurogenesis-inhibitory to neurogenesis-supportive is a promising approach to reverse the progression of neurodegenerative diseases and traumatic CNS injuries.

The mammalian olfactory system shows robust neurogenesis throughout life, with neurosensory cells capable of renewal and differentiation. There is growing evidence that a distinct type of glia, olfactory ensheathing cells (OECs), regulate the astrocytic stress response in the olfactory bulb (OB) and is critical for the neuroregenerative properties of the olfactory system. Therefore, OECs can be leveraged as a tool to identify signals pertinent for maintaining neurorepair-promoting characteristics in astrocytes.

Exosomes are extracellular nanovesicles that serve intercellular communication. Our results show that an exosome secreted protein, Alpha-crystallin B chain (CryAB), plays an important role in astrocyte-OEC crosstalk. CryAB was shown to have protective roles for cells against stress conditions. In accordance, our results indicate that OEC-secreted, CryAB positive exosomes are taken up by astrocytes and this intercellular vesicle trafficking plays an anti-inflammatory role in astrocytes by moderating activity of pro-inflammatory factors.

OECs also support astrocyte differentiation via sustained fibroblast growth factor (FGF) signaling. FGFs are crucial factors in CNS development and injury response, and are targets for neuroregenerative strategies. Heparan sulfate proteoglycans (HSPGs) are cell-specific proteins that can be shed from the membrane and regulate FGF signaling in the donor cell. We show OEC-HSPGs differentially activate FGF receptor-1 (FGFR1) signaling in astrocytes and suppress reactivity. Moreover, our results suggest a mechanistic role for OEC-HSPGs in intracellular FGFR1 trafficking and its association with the transcriptional machinery in astrocytes. Together this work shows that OB OECs are integral components of one of the few neurogenic zones in the CNS. Mimicking OEC-astrocyte crosstalk in vivo may provide new approaches to ameliorating CNS injuries by targeting astrocytes.

NEUROREPAIR PROMOTING CROSSTALK BETWEEN ASTROCYTES & OLFACTORY ENSHEATHING CELLS

by:

Aybike Sağlam

Dissertation submitted to the Faculty of the Graduate School of the University of Maryland, College Park, in partial fulfillment of the requirements for the degree of
Doctor of Philosophy
2020

Advisory Committee:

Dr. Susan Wray
Dr. Ricardo Araneda
Dr. Elizabeth Quinlan
Dr. Leonardo Belluscio
Dr. Jens Herberholz

Dedication:

This work would not have been possible without numerous compassionate, brilliant, resilient, and uplifting people who have helped me persevere in my life and academic work. From labmates to committee members, advisors, family, and friends, I'm humbled by the many ways, large and small, you have supported me. I strongly believe that our world is changed for the better by people like you.

I owe a special acknowledgment to my loving family, in particular my mom whose empowering voice is always with me. Even though we are physically far apart, I carry you all with me wherever I go. Your kindness and positivity inspire me. Because of you, I am an optimist who sees obstacles as only temporary and I know that even a small number of people can make a big difference.

Table of Contents

List of Figures

Chapter 1: Background

Introduction

Astrocytes, traditionally identified by intermediate filament protein glial fibrillary acidic protein (GFAP) immunostaining, are the most numerous cell type in the CNS and perform crucial functions for neuronal development and synapse formation (reviewed in Stevens & Muthukumar, 2016). The adult mammalian subventricular zone (SVZ) contains GFAP positive neural stem cells (NSCs) which are also are classified as astrocytes. These cells give rise to neuroblasts and migrate to the OB where they commit to neuronal (and to a lesser degree to glial) lineage (Doetsch *et al.*, 1999; Picard-Riera *et al.*, 2002). Remarkably, local astrocytes can also enter neurogenic program after injury (Magnuson *et al.*, 2014, Nato *et al.*, 2015). Indeed, adult neural stem cells and reactive astrocytes share a number of features (Magnusson & Frisén, 2016), yet instead of repairing and remodeling damaged tissue, reactive astrocytes typically limit recovery. The main motivation behind this thesis work was to better understand the microenvironment maintaining neurorepair promoting astrocytes of the olfactory bulb (OB), with the prospect of applying these cues to astrocytes outside of the neurogenic zones and prevent their conversion to neurotoxic astrocytes after injury.

Astrocyte reactivity in response to injury was noted as early as 1970's shortly after the discovery of GFAP, an astrocyte cytoskeleton protein characterized by its upregulation under pathological conditions (Bignami & Dahl, 1976). Since then, GFAP had been used as a standard marker of astrocyte reactivity which was considered to be detrimental. However, recent studies show that astrocyte reactivity is not a uniform response but rather a heterogenous mixture of activation states (reviewed in Khakh & Deneen., 2019). This context

dependent response is controlled by both intrinsic and environmental signals such as neural activity (Horner & Palmer, 2003).

Significantly higher GFAP expression was observed in the olfactory system, one of the few neurogenic zones in the adult mammalian brain, in particular where regenerating olfactory sensory neurons (OSNs) enter the OB (Mackay-Sim & Kittel, 1991; Nazareth *et al.,* 2018). Notably, this high astrocyte reactivity is correlated with the plastic nature of the OB which is influenced by both peripheral (Carmen Martinez Garcia *et al.,* 1991) and CNS input (Göktaş *et al.*, 2010; Tanık *et al.* 2015; Yaldızlı *et al.*, 2016; reviewed in Huart *et al.*, 2019). These observations suggest that astrocyte reactivity must be tightly regulated in the OB, where neurogenesis continues throughout life.

Regenerating neurons use aligned glial scaffolds for elongation and migration. Olfactory ensheathing cells (OECs) are a specialized type of glia that form continuous open scaffolds into the OB, enabling entry of regenerating axons into the brain. OECs perform numerous functions important for neuroregeneration and migration, and differentiation (Doucette & Words., 1990; Santos-Silva *et al.*, 2007). Moreover, OECs can migrate through scar tissue, moderate astrocyte reactivity, and improve regeneration *in vivo* (reviewed in Roet *et al.*, 2014). Therefore, we hypothesized that studying the crosstalk between the OECs and astrocytes would reveal mechanisms that control astrocyte reactivity and fate decisions.

CNS injury & factors limiting recovery

In the healthy CNS, astrocytes form functional barriers to restrict and regulate the entry of immune cells. Once the integrity of the blood brain barrier (BBB) between the endothelial cells and astrocytes is compromised in response to an insult, the activity of ion pumps,

neuronal membrane potentials and the synthesis of signaling molecules are disrupted (Gulbenkian *et al.*, 2001; Girouard & Iadecola, 2006). This initial damage is followed by a spectrum of astrocytic stress responses. In severe cases, astrocyte reactivity results in glial scar (astrogliosis); characterized by astrocyte misalignment and size increase, in an attempt to maintain BBB integrity and limit the spread of neurotoxic inflammation. Reactive astrocytes forming the glial scar act as a physical barrier to regenerating axons by expressing intermediate filament proteins (Vimentin, GFAP, etc.), and secrete nerve growth-inhibitory chondroitin sulfate proteoglycans (neurocan, phosphacan, versican, etc). While reactive astroglia express some growth-promoting extracellular matrix (ECM) molecules, the growth-inhibitory molecule secretion dominates with increased severity of injury. Thus, astrocytes have the potential to carry both anti-inflammatory and pro-inflammatory functions and are targets for pharmacologic manipulations to reverse CNS damage (Hamby & Sofroniew, 2010).

The nervous system must be able to continuously update functional connections between neurons, indicating it must remain plastic throughout life (Raisman & Li., 2007). Hence, it has been suggested that if severed neurons were guided through the damaged site, they could make new functional connections. This idea drew attention to glial cells due to their regenerative abilities, such as secreting growth-promoting factors and providing topographic guidance. In the peripheral nervous system (PNS), Schwann cells (SCs) support and guide transected neurons through damaged tissue and promote nerve regeneration. Several groups transplanted SCs into the damaged CNS, in an attempt to repair the glial pathway and promote neuroregeneration across the injury site. However, SCs fail to communicate with CNS-specific glia (primarily astrocytes) and cannot build a glial pathway through the scar tissue (Grimpe *et al.,* 2005).

These findings draw attention to OSNs (Figure 1), which are vulnerable to damage and microbial infections (Dando *et al.,* 2016) due to their exposed location in the nasal cavity (PNS) and have a remarkable capacity for regeneration (Calof *et al.*, 1996, Forni *et al.,* 2013). Ensheathing glia of the olfactory system, OECs, wrap and guide olfactory sensory neuron axons into the OB in the CNS, where they establish new connections (Figure 1). Moreover,

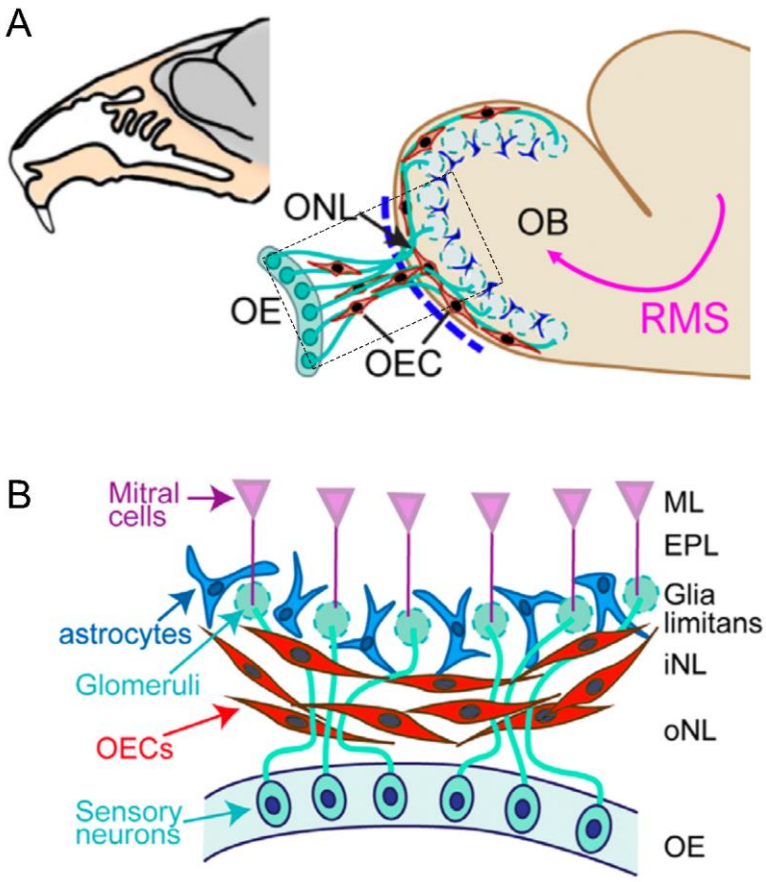

Figure 1: Anatomy of the Olfactory System. (A) OSNs (turquase) send their axons to the OB with the support of OECs (red). OE= olfactory epithelium, ONL= nerve layer, RMS= rostral migratory stream. (B) OECs (red) mingle with astrocytes (blue) in the OB where astrocytes form a defense barrier glia limitans. In the OB, mitral cells (ML), external plexiform layer (EPL) glomerular layer, and internal (iNFL) and outer nerve layer (oNFL) are shown (adopted from Nazareth *et al.*, 2018).

OECs metabolize toxic macromolecules, undergo structural remodeling (Roet *et al.*, 2014), and secrete trophic factors including brain-derived neurotrophic factor, nerve growth factor, glial cell line-derived neurotrophic factor, neuregulins, ciliary neurotrophic factor, integrins, cell adhesion molecules, cadherins and laminin (Franssen *et al.,* 2008, reviewed in Hale, 2011). These observations suggested that OECs are important contributors in directing axons to their correct target and also for maintaining regenerating neurons (Doucette, 1990). Different groups transplanted OECs into CNS injury sites for neuroregenerative purposes and observed therapeutic benefits (Li *et al.*, 1997, Yang *et al.*, 2015), including improved axon sprouting and regrowth (Guntinas-Lichius *et al.*, 2001; Deumens *et al.,* 2006), decreased tissue and neuronal damage (Ruitenberg *et al.*, 2003), formation of myelin sheaths around axons (Barnett *et al.,* 2000), angiogenesis (Richter *et al.*, 2003) and enhanced recovery (Lu *et al.,* 2002; Li *et al.*, 2003; Johansson *et al.*, 2005; reviewed in Chuah *et al.*, 2011).

Notably, OECs directly interact with astrocytes at the entry point into the CNS (Figure 1), enabling regenerating olfactory axons to make new connections (Raisman & Li., 2007). Both transplanted OECs and OECs co-cultured with astrocytes *in vitro* were reported to intermingle with astrocytes and reduce astrocyte activation (Lakatos *et al.*, 2000; Lakatos *et al.*, 2003; Hale *et al.*, 2011). These results suggest a moderating effect of OECs on harmful astrocyte reactivity and is being investigated by several groups. Yet, crosstalk mechanisms between OECs and the surrounding neural-niche cells, including astrocytes, remain to be discovered.

Astrocytes before & after the injury or during a degenerative disease

Glial scar formation is a hallmark of severe brain injuries, where the lesion site is enclosed by a network of astrocytic processes. Although the type of injury varies, in most cases, reactive

astrocytes account for cell death and limited neuroregeneration across the damaged tissue via disruption of metabolic supply and creation of an inhibitory environment, respectively. Insight from transgenic mouse models shows that tumor necrosis factor-alpha (TNF-α) overexpression by astrocytes (Probert *et al.*, 1997) or secretion by microglia (Liddelow *et al.*, 2017) is sufficient to trigger CNS inflammation and neurotoxic astrocyte reactivity. TNF-α is a key pathogenic mediator in inflammatory CNS disorders and induces pro-inflammatory transcriptional factor NFκB production. NFκB is expressed in most mammalian cells, and has 5 subunits, p65, RelA, RelB, p50 and p52. Under basal conditions, NFκB binds to the κB inhibitor IκB in the cytoplasm. After inflammation, IκB phosphorylation causes NFκB to separate from IκB and free NFκB subunits move to the nucleus. This nuclear translocation can directly be detected by immunocytochemistry, providing a readout of this early key event in neurotoxic astrocyte reactivity.

Bacterial endotoxin lipopolysaccharide (LPS) is widely used to mimic pro-inflammatory astrocytes and NFκB translocation in astrocytes *in vitro*. However, a recent study reported that rodent astrocytes in culture do not respond to LPS if the cultures are completely free from microglia (Liddelow *et al.*, 2017). Instead, the study shows astrocytic activation to be induced by the microglial cytokines, primarily interleukin 1α (Il-1α), TNF-α, and complement component 1, subcomponent q (C1q). The results – although vital to understand the progression of CNS inflammation and the role of mitochondria– did not end the use of LPS to mimic astrocyte reactivity *in vitro*, since numerous negative immunopanning steps (selection of cells using an antibody immobilized to the culture dish) are required in order to remove microglia from astrocyte cultures entirely (Foo *et al*, 2011). Moreover, this technique is not efficient to isolate large number of cells and may end up isolating a single astrocyte

subpopulation. An alternative and more cost-effective technique that provides high number of non-reactive astrocytes is magnetic sorting, as previously described (Holt *et al.*, 2019). Certainly, the astrocyte isolation method should be chosen after careful consideration that is most appropriate to distinguish the astrocyte function under investigation.

Upregulation of GFAP (and some other intermediate filaments) is a pan-marker for reactive astrocytes and can also be induced by other CNS injuries such as ischemia. However, in contrast to inflammatory astrocytes, ischemic astrocytes are shown to promote neuronal survival and CNS repair (Bush *et al.*, 1999; Faulkner *et al.*, 2004; Herrmann *et al.*, 2008). Studies strongly suggest that this neurorepair-promoting astrocyte reactivity is mediated by STAT3. This pathway can be activated by tyrosine kinase growth factor receptors and regulates various, functional outcomes such as proliferation, differentiation, expression of intermediate filaments, and multiple other aspects of astrocyte reactivity, via both transcription-dependent and independent mechanisms (reviewed in Ceyzériat *et al.*, 2016). Much remains to be done to understand how these pathways can be targeted to mediate astrocyte reactivity.

Neurogenic potential & heterogeneity of astrocytes

During early stages of development, NSCs go through symmetrical self-renewal divisions, followed by the neurogenic phase which slowly turns into the gliogenic phase. While gliogenesis is still supported in the adult mammalian brain, neurogenesis is restricted to two zones: the SVZ of the lateral ventricle and the dentate gyrus subgranular zone (SGZ) of the hippocampus. NSCs from the SVZ in the adult mammalian brain give rise to neuroblasts and migrate a long distance anteriorly into the OB, where they commit to a lineage (Doetsch *et al.*, 1999). This route is called the rostral migratory stream (RMS, Figure 1) and, notably, cells that

share structural and molecular characteristics of astrocytes along this route can function as stem cells or support the maintenance and differentiation of neuroblasts (Horner & Palmer, 2003). Studies show the crucial role of microenvironment in stem cell self-renewal and progenitor differentiation: while allogenic transplantation of NSCs to SVZ of the host animal generates neurons in the OB, transplantation into nonneurogenic CNS regions results in limited neurogenesis (Alvarez-Buylla & Lim, 2004). In addition, while astrocytes of the neurogenic zones are fundamental players in neurogenesis, astrocytes outside of the neurogenic zones inhibit neurogenesis but support gliogenesis (Horner & Palmer, 2003).

Although the studies described here do not directly focus on the stem cell potential of astrocytes, it should be noted that reactive astrocytes and adult NSCs share many characteristics (Magnusson & Frisén, 2016). Faiz and colleagues (2015) found that NSCs can migrate to injury site, and 4 days after, give rise to neuroblasts which differentiate into neurons, astrocytes, and oligodendrocytes *in vivo*. However, within about 2 months, the majority of these cells turn into reactive astrocytes and contribute to glial scar formation. Unexpectedly, other studies showed that local astrocytes also enter the neurogenic program after injury (Buffo *et al.*, 2008; Magnusson *et al.*, 2014; Nato *et al.*, 2015). Cumulatively, these results indicate that, NSCs that migrate to the injury site cannot functionally integrate into the lesion and instead turn into reactive astrocytes, due to the inhibitory environment (Addington *et al.*, 2015, reviewed in Boccazzi & Ceruti., 2016). Local astrocytic subpopulations also continue to show high plasticity in adulthood – particularly under pathological conditions – and their identity is regulated by cell-cell and cell-ECM interactions (Alvarez-Buylla & Lim, 2004). Numerous studies have focused on using these cells as a pool for new neural cells in the injured brain, yet

more work needs to be done to understand the mechanisms regulating astrocyte reactivity and fate decisions.

Astrocytes exhibit morphological, molecular and functional heterogeneity depending on the CNS region (Doyle *et al.*, 2008, Bachoo *et al.*, 2004, Perego *et al.*, 2000, McKhann, *et al.*, 1997, Poopalasundaram *et al.*, 2000, reviewed in Stevens & Muthukumar, 2016). Similarly, astrocyte reactivity shows great diversity in a location- or injury-specific manner even within the same disorder (Verkhratsky *et al.*, 2012). Exposure to LPS shifts astrocytes towards pro-inflammatory and neurotoxic profiles (Hamby *et al.*, 2012, John *et al.*, 2005), whereas in response to experimental ischaemia, astrocytes upregulate neuroprotective mechanisms (Zamanian *et al.*, 2012). Undoubtedly, the classification of reactive astrocytes into these two; 'helpful versus harmful' groups is a generalization, drawn from a single parameter: survival of neurons. Considering the complex and crucial roles of astrocytes in CNS, this classification— although much needed— is perhaps just the first step towards defining the heterogeneity of astrocyte reactivity.

Neurorepair supportive crosstalk between olfactory bulb glia: astrocytes & OECs

It is well appreciated that astrocytes are key players after injury, that have indispensable roles supporting neuroregeneration (Horner & Palmer, 2003). Nevertheless, adult astrocytes outside of the neurogenic zones of the mammalian brain, support gliogenesis rather than neurogenesis. A striking exception to this general rule of neuroregeneration in the mammalian brain is the olfactory system, which exhibits continuous neurogenesis throughout adulthood. In this study we focused on the communication between the glial cells of the olfactory system, OECs and astrocytes, to identify factors that support this unique microenvironment. In the

PNS, OECs create glial pathways for regenerating OSNs to enter and synapse in the olfactory bulb. In the CNS, OECs and astrocytes are in close proximity and form the glia limitans, contributing to the formation of BBB of the OB. The exact nature of the BBB in the OB, and the cellular organization of OECs and astrocytes in this region has been debated. Nazareth and colleagues (2018) have suggested that the CNS starts at the inner olfactory nerve layer (ONL), and the glia limitans consists of astrocytes alone, in support of earlier work suggesting astrocytes are absent in outer layer of the ONL (Au *et al.*, 2002; Doucette, 1990). These investigators proposed that the BBB start at the inner ONL of the OB and OECs reside in the PNS only.

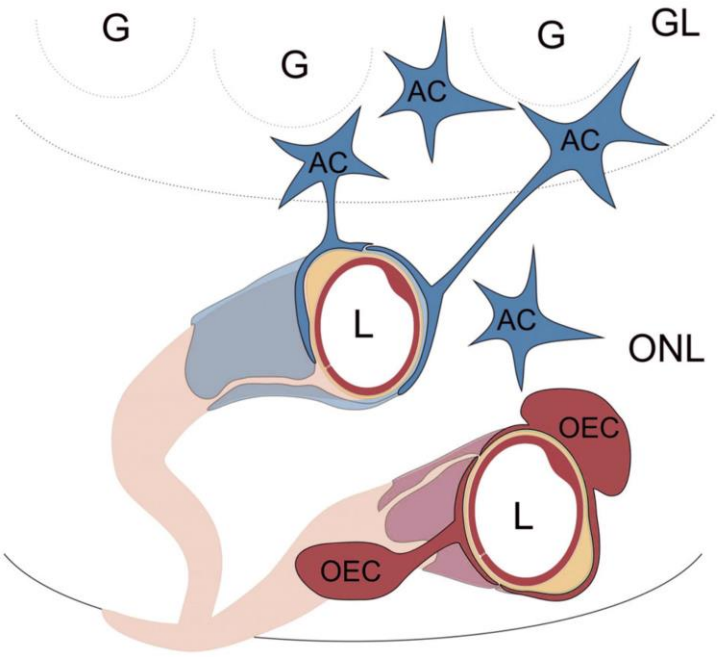

Figure 2: Blood brain barrier in the mouse olfactory nerve layer. OECs (red), AC= astrocytes (blue), ONL= olfactory nerve layer, G= glomeruli, GL= glomerular layer, L= lumen of capillary. (adopted from Beiersdorfer *et al.,* 2019).

However, PNS glia do not make direct contact with blood constituents (Kanda, 2013), hence in the PNS, this barrier is termed blood nerve barrier (BNB). In contrast, in the olfactory system, olfactory axon bundles traversing the cribriform plate are intermingled with arteries and OECs. Indeed, a more recent study presents evidence for the association of OECs and astrocytes with blood vessels in the ONL (Beiersdorfer *et al.*, 2019). Via visualization of blood vessels by lanthanum and electron microscopy, the study shows that in the outer ONL, mainly OECs, while in the inner ONL mainly astrocytes are in contact with blood vessels (Figure 2). Moreover, clonal fate analysis of OB astrocytes using lineage-tracing method confirms the presence of astrocytes throughout the OB, including the outer ONL (García-Marqués & López-Mascaraque, 2017). These results suggest that OECs and astrocytes coexist in the CNS, contributing to the formation of BBB. Independent of whether they are primarily PNS glia or not, it is clear that OECs share properties of both PNS and CNS glia, providing topographic guidance to the regenerating olfactory axons and supporting astrocytes to be neurorepair-promoting, qualities that are suppressed in other parts of the CNS (Smith *et al.*, 2012).

Significance/ Aims

Neurodegenerative diseases and traumatic CNS injuries affect hundreds of millions of people worldwide. Disability-adjusted life-years (DALY) due to these disorders increased 41% (from 182 million to 258 million; where one DALY equals to one lost year of 'healthy' life in the population) between 1990 and 2010 and is expected to grow exponentially. An estimated 9 million people die annually as a result of neurological disorders, and combined with the effects on disability result in an outsized effect of disease burden worldwide (WHO, 2017). Furthermore, the medical costs associated with acute traumatic injuries and chronic degenerative diseases pose a significant financial burden to patients. This burden is six times higher in low- and middle-income countries. Finding a therapeutic strategy for CNS repair would improve the quality of life for these patients dramatically and also ease the economic burden associated with chronic care.

Research over the past century has significantly advanced our understanding of the causes and the prognosis of common neurological disorders such as epilepsy, multiple sclerosis, neuro infections, traumatic brain injuries, Parkinson's, and Alzheimer's disease. These disorders characteristically show different outcomes but convergence in an aspect of their pathology: astrocyte reactivity. Because olfactory ensheathing cells (OECs) regulate the astrocytic stress response in the olfactory bulb (OB) and are critical for the neuroregenerative properties of the olfactory sensory neurons in the olfactory epithelium, we hypothesize that characterizing OEC-astrocyte communication would enable the identification of the molecular mechanisms targeting astrocyte pathology, with the potential to be translated into many distinct CNS injuries and disorders.

Aim 1: Identify OEC-secreted factors which suppress neurotoxic astrocyte reactivity

OEC-secreted factors have been shown to be sufficient to suppress astrocyte reactivity, measured by reduced nuclear translocation of pro-inflammatory factor NFκB (Hale *et al.*, 2011). Our strategy to identify such factors involved assessing the anti-inflammatory capacity of six immortalized OEC lines (OEinfmyc790 lines) that were gifted to our lab by Dr. Anne Calof (Calof & Jose-Guevara., 1993). Conditioned medium (CM) from only two of these lines was successful at mimicking primary OECs, allowing us to select one line as positive control and one line as a negative control for our studies. Mass spectrometry analysis revealed that CryAB, a molecular chaperone protein, was expressed at similar levels by primary OECs and positive control line OEmyc790-C7, and was three times higher compared to the negative control line OEmyc790-C4. This small heat shock protein can bind to misfolded proteins and has been shown to carry protective roles for various cells against stress conditions. Hence, we asked whether OECs from CryAB null ($CryAB^{-/-}$) mice can block astrocyte reactivity. CryAB has been shown to be released via exosomes in several types of glia, possibly coordinating an inter-cellular immune response (Gupta & Pulliam, 2014). Thus, the presence of CryAB was quantified in OEC exosomes compared to astrocyte and oligodendrocyte exosomes. In addition, we examined whether OEC exosomes were sufficient to reduce astrocyte reactivity, measured by nuclear NFκB. Finally, using OEC-CM, $CryAB^{-/-}$OEC-CM or immunoprecipitated CryAB to treat reactive astrocytes, transcripts associated with neurotoxic reactivity were analyzed to determine whether CryAB suppressed astrocyte reactivity. This work identified a novel mechanism for OEC-astrocyte intercellular communication and is presented in Chapter 2.

Aim 2: Investigate the role of FGFR1 in OEC-astrocyte crosstalk

Considering the parallels between developmental and reactive astrocytes, and the importance of FGF signaling for astrocytes in both of these states, we asked whether OECs regulate the FGF pathway in reactive astrocytes to control their stress-response. Our results showed that in the presence of FGFR1 inhibitors, OECs fail to moderate astrocyte stress-response. Consequently, we investigated downstream targets of the FGF/FGFR1 signaling pathway that may play a role in this crosstalk.

Both FGF ligands and receptors, as well as the co-receptor heparan sulfate proteoglycans (HSPGs) can move into the nucleus and carry out signaling functions independent of receptor dimerization on the membrane (Leadbeater *et al.*, 2006). Considering the weak expression of HSPGs in healthy adult CNS, the upregulation of these 'non-traditional nuclear proteins' in reactive astrocytes suggests important roles for HSPGs in the regulation injury response. Using Ext1 (HSPG-synthesizing enzyme) knockout OECs and immunoblotting against NFκB, we investigated whether OEC-secreted HSPGs are a key factor in OEC-CM that blocks astrocyte reactivity. Notably, a regulatory effect for FGFR1 over several transcriptional factors has been reported (Ornitz & Itoh., 2015). Considering that the majority of the nuclear FGFR1 is non-glycosylated (Dunham- Ems *et al.*, 2006; Stachowiak *et al.*, 2015), we asked whether OEC-HSPGs are involved in intracellular FGFR1 trafficking and subsequent association with the transcriptional machinery in astrocytes. This work identified novel mechanisms for astrocyte intracellular changes in the presence of OEC secreted cues and is presented in Chapter 3.

Experiments detailed in this dissertation shows that OEC-astrocyte crosstalk enables astrocytes to be neurorepair-supportive. In vivo studies will be needed to evaluate the overall contribution of OECs for the neurogenic microenvironment in the olfactory system. We will discuss some of our preliminary results related to these experiments in Chapter 4.

Chapter 2: A Novel Factor in Olfactory Ensheathing Cell-Astrocyte Crosstalk: Anti-Inflammatory Protein α-Crystallin B

2.1 Abstract

Astrocytes are key players in CNS neuroinflammation and neuroregeneration that may help or hinder recovery, depending on the context of the injury. Although pro-inflammatory factors that promote astrocyte-mediated neurotoxicity have been shown to be secreted by reactive microglia, anti-inflammatory factors that suppress astrocyte activation are not well-characterized. Olfactory ensheathing cells (OECs), glial cells that wrap axons of olfactory sensory neurons, have been shown to moderate astrocyte reactivity, creating an environment conducive to regeneration. Similarly, astrocytes cultured in medium conditioned by cultured OECs (OEC-CM) show reduced nuclear translocation of Nuclear Factor kappa-B (NFκB), a pro-inflammatory protein that induces neurotoxic reactivity in astrocytes. In this study, we screened primary and immortalized OEC lines to identify these factors and discovered that Alpha B-crystallin (CryAB), an anti-inflammatory protein, is secreted by OECs via exosomes, coordinating an intercellular immune response. Our results showed: 1) OEC exosomes block nuclear NFκB translocation in astrocytes while exosomes from CryAB-null OECs could not; 2) OEC exosomes could be taken up by astrocytes and 3) CryAB treatment suppressed multiple neurotoxicity-associated astrocyte transcripts. Our results indicate that OEC-secreted factors are potential agents that can ameliorate, or even reverse, the growth-inhibitory environment created by neurotoxic reactive astrocytes following CNS injuries.

2.2 Introduction

Damage to the central nervous system (CNS) provokes morphological and molecular changes in astrocytes, causing them to become 'reactive astrocytes' (Liddelow & Barres, 2017). These reactive cells play positive roles during CNS injury, such as confining inflammation by surrounding the damaged tissue and creating a barrier between it and uninjured tissues (Silver, *et al.*, 2015). Reactive astrocytes have been traditionally characterized by increased expression of intermediate filament proteins such as GFAP (Glial Fibrillary Acidic Protein), vimentin, and nestin (summarized in Liddelow & Barres, 2017). Excessive or sustained astrocyte reactivity is characterized by activation of pro-inflammatory pathways such as the NFκB pathway (Liddelow & Barres., 2017; Wheeler 2020). This activity can be deleterious to functional recovery, since it can lead to chronic inflammation and neurotoxicity (Sofroniew, *et al.*, 2010). A better understanding of the molecular mechanisms that govern astrocyte reactivity would therefore be helpful to create environments conducive to regeneration following CNS injury.

The mammalian olfactory system shows robust neurogenesis throughout life. Data suggest that both neural niche signals and the surrounding glia, including olfactory ensheathing cells (OECs), give the olfactory mucosa this unique capability (Li, *et al.*, 2005; Roet & Verhaagen, 2014). Previous investigators have transplanted OECs into CNS injury sites, and observed improved axonal regeneration (Li *et al.*, 1997; Imaizumi *et al.*, 2000), functional recovery (Johansson *et al.*, 2005), reduced astrocytic scar tissue (Ramer *et al.*, 2004), and an attenuated hostile astrocyte response (Lakatos *et al.*, 2003; summarized in Roet & Verhaagen, 2014). Moreover, factors secreted by OECs have been shown to moderate astrocyte reactivity, at least insofar as their presence results in reduction of GFAP expression and nuclear translocation of NFκB (Chuah *et al.*, 2011; O'Toole *et al.*, 2007). Identification of molecules

secreted by OECs, which specifically affect astrocyte reactivity, should lead not only to a better understanding of the crosstalk between astrocytes and OECs; it may also reveal mechanisms that can block the metamorphosis of astrocytes into neurotoxic cells.

To identify such molecules, this study used lipopolysaccharide (LPS)-treated astrocytes, a model for neurotoxic reactive astrocytes, and assessed conditioned medium (CM) from immortalized clonal mouse OEC cell lines (Calof & Guevara, 1993). Nuclear NFκB translocation in astrocytes was measured to determine if CM from these cell lines could mimic primary OEC-CM, which blocked the LPS pro-inflammatory response in astrocytes. Two immortalized cell lines were chosen for further study: one whose CM mimicked the effect of primary OECs (positive control); and a second, whose CM did not block the LPS response in astrocytes (negative control). These two cell lines and primary OECs were challenged with LPS, and the conditioned media screened by mass spectrometry. Using this strategy, the heat-shock protein CryAB (D'Agostino *et al.*, 2013) was identified. Subsequent experiments showed that: 1) CryAB is secreted by OECs via exosomes; 2) exogenous CryAB suppressed LPS-induced astrocyte reactivity; 3) exosomes containing CryAB are taken up by astrocytes; and 4) unlike wildtype (WT) OEC-exosomes, CryAB-null (CryAB−/−) OEC exosomes fail to suppress LPS-induced astrocyte reactivity measured by nuclear NFκB translocation. Finally, examination of transcripts that are associated with neurotoxic-reactive astrocytes (Liddelow *et al.*, 2017) revealed that either exogenous CryAB or OEC-CM can suppress expression of several of these transcripts. Taken together, the data indicate that CryAB secreted by OECs, via exosomes, is an important factor for OEC-astrocyte crosstalk that can block astrocytes from becoming neurotoxic cells. Ultimately, mimicking appropriate astrocyte-OEC crosstalk in vivo may contribute to an environment conducive to regeneration following a broad range of CNS injuries.

2.3 Materials and Methods

2.3.1 Mice

All mice were maintained, and all animal handling procedures were performed according to protocols approved by the National Institutes of Health NINDS Institutional Animal Care and Use Committee. *CryAB*-null (*CryAB*$^{Del(9Hspb2\text{-}Cryab)1Wawr}$, henceforth referred to as *CryAB*$^{-/-}$) mice (Brady *et al.*, 2001) were obtained as homozygous sperm, revived by IVF using eggs from C57bl6/N mice (Jackson Laboratory), and resulting heterozygotes intercrossed to obtain obtain *CryAB*$^{-/-}$ and *CryAB*$^{+/+}$ (wildtype, WT) lines, which were used as the source for OEC primary cultures (see below). Mice were genotyped using a three-primer PCR protocol: 5'-TAGCTTAATAATCTGGGCCA-3', 5'-GGAGTTCCACAGGAAGTACC-3', and 5'-TGGAAGGATTGGAGCTACGG-3' primers were used in 4:1:1 molar ratio. Amplification was performed for 40 cycles at 94^{0}C for 15 sec, 62^{0}C for 30 sec and 72^{0}C at 1 min. PCR produced a 310-bp product for the WT allele and a 600-bp product for the null allele.

2.3.2 Cell culture and reagents

Primary cultures of OECs were generated as described previously (Dairaghi *et al.*, 2018). Briefly, olfactory bulbs of postnatal (PN) day 0-7 mice were collected and placed in an enzyme mix: 30µg/ml hyaluronidase (Sigma, Cat# H3631, St. Louis, MO), 30U/ml dispase I (Sigma, Cat# D4818), 1.2 mg/ml collagenase type 4 (Worthington, Cat# 43E14231, Lakewood, NJ), 10U/ml DNAse I (Worthington, Cat# 54E7315); for 35 min at 37^{0}C with constant agitation (Au & Roskams, 2003). Cells were run through a 40µm cell strainer to remove non-dissociated tissue pieces and then washed with DMEM-F12 medium. Subsequently, cells were purified by the differential cell adhesion method (Nash *et al.*, 2001), which consists of three steps: 1) Cells were seeded into uncoated T75 flasks (4x10^6 viable

cells/flask, VWR, Cat# 734-2788, Radnor, PA) for 18 hrs to remove fibroblasts; 2) the supernatant of the first step was seeded into another uncoated flask for up to 36 hrs to remove astrocytes; and finally 3) the supernatant of the second flask was seeded onto poly-L-lysine (Sigma, Cat# P4707)-coated flasks to grow primary OECs. Cells were cultured for up to 2 weeks and medium was changed every 2–3 days. OECs constituted more than 90% of the cells in the culture based on p75 and S100ß immunostaining consistent with earlier reports (Au & Roskams, 2003). For OECs to be co-cultured with primary astrocytes, the medium was gradually changed to serum-free medium (Klenke & Taylor-Burds, 2012) supplemented with 5ng/ml HB-EGF (PeproTech, Cat# 100-47, Rocky Hill, NJ), and B27 (Thermo Fisher Scientific, Cat# A3582901) to provide a medium compatible with astrocyte culture, since serum has been shown to induce astrocyte reactivity (Foo *et al.*, 2011).

Primary astrocyte cultures were obtained by magnetic sorting as previously described (Holt *et al.*, 2019), with some modifications. Briefly, 10-20 cortices of PN day 2-4 pups were dissociated using the MACS Neural Tissue Dissociation Kit-T (Miltenyi Biotec, Cat# 130-093-231, Auburn, CA) at 37^0C (5% CO^2, 30 min). Non-dissociated tissue was removed using a 40µm cell strainer (Fisher Scientific, Cat# 22-363-547), and the remaining cell solution was centrifuged (300g, 5 min). Next, a discontinuous density gradient, prepared using 1:1 albumin-ovomucoid solution (10mg/ml of each) (Worthington, Cat# OI; GeminiBio, Cat# 700-102P, West Sacramento, CA), was used to remove cell debris and inhibit enzyme activity. The cell pellet was resuspended in 80µl Hank's Balanced Salt Solution (HBSS) (Gibco, Cat# 14025-092) plus 20µl anti-GLAST (ACSA-1) MicroBeads (Miltenyi Biotec, Cat# 130-095-825, Auburn, CA) for up to 10^7 cells, and incubated for 10 min (4^0C). Cells were washed and incubated in 90µl HBSS plus 10µl anti-Biotin MicroBeads for another 15 min (4^0C) before

running through MACS column for positive selection of astrocytes. Cells were cultured for one week and then the same procedure was followed with anti-Prominin-1 MicroBeads (Miltenyi Biotec, Cat# 130-092-564) for the negative selection of radial glia, followed by another positive selection with anti-GLAST antibody the same day, to increase the purity of astrocyte cultures. Sorted cells were cultured in T25 flasks coated with poly-L-lysine, in 5ml serum-free astrocyte culture medium (ACM, described above). In our hands, astrocytes isolated by this method and cultured in ACM were not reactive when stained with NFκB (not shown). The same method was adjusted to obtain oligodendrocyte cultures using anti-O4-MicroBeads (Miltenyi Biotec, Cat# 130-096-670). The immortalized mouse astrocyte line C8D30 (ATCC, VA, USA) was cultured in DMEM-F12 (Gibco, Cat# 10313-02, 11765-054, Long Island, NY) containing 10% Fetal Bovine Serum (FBS) (Gibco, Cat# 10438-026), plus 0.5% antibiotic-antimycotic (Gibco, Cat# 15240-062) at 37^0C in 5%CO2.

2.3.3 Immortalized OEmyc790 Cell Lines

Six immortalized OEC lines (OEmyc790-C7s.D, D6s.AB8, C6s.BG9, D10 and D4), derived from retrovirus-mediated transformation of primary embryonic mouse olfactory epithelium cultures derived from E15 mouse embryos (Calof & Guevara, 1993), were analyzed; two lines, OEmyc790-C7s.D (C7) and OEmyc790-C4 (C4), were used for the studies described below. Cells were plated on cell culture plates (Fisher Scientific, Cat# 130190, Waltham, MA) and cultured in DMEM-F12 as described above. Medium was changed every 3-5 days. When 60% confluent, a 1:4 dilution of trypsin was used (Gibco, Cat# 15400054) to split the cells into thirds.

2.3.4 Primary antibodies and recombinant proteins

The following antibodies were used: CryAB rabbit polyclonal antibody (Millipore, Cat# ABN185, Darmstadt, Germany, 1:1K for WB, 1:4K for immunofluorescence (IF); Histone mouse monoclonal antibody (Fisher Scientific, Cat# AHO1432, Waltham, MA, 1:200 for WB); NFκB rabbit polyclonal antibody (C-20, Santa Cruz, Cat# sc-372, Santa Cruz, CA, 1:650 for WB, 1:750 for IF); Sox10 goat polyclonal antibody (N-20, Santa Cruz, Cat# sc-17342, 1:300 for IF); Alix mouse monoclonal antibody (3A9, Cell Signaling, Cat# 2171T, 1:1K for WB); GFAP chicken polyclonal antibody (Aves, 1:4K for IF); Flotillin-1 rabbit polyclonal antibody (D2V7J, Cell Signaling, Cat# 18634, 1:1K for WB); β-actin mouse monoclonal antibody (AC-74, Millipore, Cat# A2228, 1:1K for WB); Tomm20 rabbit polyclonal antibody (FL-145, Santa Cruz, Cat# sc-11415, 1:1K for WB); CD63 biotinylated antibody (Miltenyi Biotec, Cat# 130-108-922, Auburn, CA, 1:15 for IF); BLBP mouse monoclonal antibody (Abcam, Cat# ab131137, 1:2K for IF) and p75-NGFR rabbit polyclonal antibody (Millipore, Cat# AB1554, 1:5K). Recombinant chicken Anosmin1 (MyBioSource, Cat# MBS963562-COA, San Diego, CA) was used at 5nM while recombinant CryAB protein (MyBioSource, Cat# MBS964495) and recombinant myoglobin (MyBioSource, Cat# MBS142891) were used at 50ng/ml unless stated otherwise.

2.3.5 Mass spectrometry

Primary OECs, and immortalized C7 and C4 OEC cell lines, were established by seeding them in T75 flasks at a concentration of $8x10^5$ cells/flask in regular growth medium. To concentrate secreted proteins, the cells in each flask were rinsed and media replaced with 10ml/flask of Earle's Balanced Salt Solution (EBSS) with 5.5mM D-Glucose (Gibco, Cat# 14155-063);

conditioned medium (CM) was collected after 48 hrs total of incubation. For the last 2 hrs of the 48-hr collection period, either 1µl/ml LPS (Sigma, Cat# L6529) or 5nM recombinant chicken Anosmin1 was added. CM was then collected, centrifuged to remove debris, and frozen at -80^{0}C. Frozen samples were freeze-dried using a lyophilizer (Novalyphe-NL150, Savant Instruments, Holbrook, NY). The pellets were reconstituted in water and bicinchoninic acid (BCA) protein assay was performed. 200µg/60ul protein per group was submitted for mass spectrometry analysis (NINDS Protein Facility, NIH). Each sample was digested with trypsin. Tandem Mass Tag (TMT) labeled samples were mixed together (TMT 126-131). The mixture was separated using hydrophilic interaction liquid chromatography (HILIC) high performance liquid chromatography (HPLC) system. Five HILIC fractions were collected from the mixed sample. One liquid chromatography-tandem mass spectrometry (LC/MS/MS) experiment was performed for each HILIC fraction, using an Orbitrap Fusion Lumos Mass Spectrometer (Thermo Fisher Scientific, Waltham, MA) coupled to a 3000 Ultimate high-pressure liquid chromatography instrument (Thermo Fisher Scientific). Proteome Discoverer 2.2 software used for database search and TMT quantification, and data were mapped against the Sprot mouse database. "Primary OEC+LPS-CM" was used as reference to calculate the ratio for LPS treated samples; "Primary OEC+5nMA1-CM" was used as reference to calculate the ratio for 5nMAnosmin1-treated samples. No normalization was performed. See Supplemental Data 1 and 2 for obtained values.

2.3.6 Immunoblot analysis

As a readout of reactivity, quantitative immunoblot analysis was performed on nuclear fractions of immortalized C8D30 astrocytes treated with 1µl/ml LPS or vehicle control for 2 hrs. For co-culture groups, OECs seeded on porous inserts (0.4µm Millicell Cell Culture Insert,

Millipore, Cat# PICM0RG50) were placed on top of astrocytes for 24 hrs and were discarded at the end of the incubation period, so that only astrocytes were collected for subsequent protein analysis. For the CM treated groups, CM from each line was collected (after 24 hr incubation) and then added to astrocytes for 22 hrs, followed by a 2-hour LPS treatment. Astrocytes were then collected by scraping and the CNMCS Compartmental Protein Extraction Kit (BioChain Cat# K3013010 Hayward, CA) with protease/phosphatase inhibitors (PI, Cell Signaling, Cat# 5872S, Danvers, MA) was used and the nuclear fractions were isolated for each treatment condition. The fractions were run on BioRad Mini-Protean TGX Stain-Free Gels (Cat#4568084), transferred to PVDF stain-free blot (Trans-Blot Turbo Transfer Pack, Cat#1704156) via the Trans-Blot Turbo transfer system (BioRad), and blocked with 5% dry milk (BioRad, Cat #170-6404) prior to staining with NFκB antibody. Membranes were exposed to Clarity enhanced chemiluminescence (ECL) reagent (Cat. # 170–5061, Bio-Rad) for 5 min and the signal was detected using ChemiDoc MP (Cat. # 170–8280, Bio-Rad). Quantification of band intensities was calculated using Image Lab 5.0 software (Bio-Rad) and normalized by the loading control immunostained for Histone on the same sample and the same blot. Three biological replicates were used for statistical analysis.

2.3.7 Quantitative immunofluorescence

Fluorescent immunostaining for nuclear NFκB and cytoplasmic NFκB was quantified in immortalized C8D30 astrocytes following 2-hr treatment with 1μg/ml LPS or a cocktail of 3 cytokines: Il-1α (3ng/ml, Sigma, Cat# I3901), TNFα (30ng/ml, Cell Signaling, Cat# 8902SF) and C1q (400ng/ml, MyBioSource, Cat# MBS143105, San Diego, CA), as follows: After immunofluorescence staining for NFκB, confocal images were taken on a Zeiss LSM 800 Confocal Microscope (Carl Zeiss, Thornwood, NY). A defined area was measured in both

nuclear and cytoplasmic compartments for each astrocyte, and the fluorescence intensity was quantified for each area in each cell using Imaris software. The ratio of nuclear to cytoplasmic fluorescence intensity was used as a quantitative readout of astrocyte reactivity. Median values were calculated for each biological replicate (N=3) obtained from multiple images (2-3/well) containing a total of ~100 cells/treatment (Figure 1C) or ~50 cells/treatment (Figure 2B). Values greater than one indicate that the NFκB value was higher in the nucleus compared to cytoplasm, and cells were reactive. Statistics (ANOVA) were performed and the average median value ±standard deviation (SD) per treatment plotted.

2.3.8 Isolation of exosomes and exosome uptake experiments

For isolation of exosomes, the protocol of Adolf and colleagues (2018) was used with slight modifications. Briefly, 24 hr prior to exosome collection, cells were washed and medium changed to exosome depleted medium (EDM) containing 10% exosome-depleted FBS (Gibco, Cat# A27208-03). CM was collected, (protease inhibitor (PI) was added immediately for immunoblotting) and samples kept at 4^0C until exosome isolation. Exosomes were isolated through three centrifugation steps: 1) CM was spun for 10 min at 2,000*g* to remove debris; 2) the resulting supernatant was centrifuged for 30 min at 10,000*g* to pellet microvesicles; and 3) this second supernatant was centrifuged for 4 hrs at 100,000*g* (Optima MAX-XP ultracentrifuge, TLA-100.3 rotor, Beckman Coulter). Following ultracentrifugation, pelleted exosomes were re-suspended in buffer (for ELISA and immunoblotting) or cell culture medium, as required. For astrocyte uptake experiments, isolated OEC-exosomes were resuspended by pipetting and added directly to the culture medium of *CryAB*$^{-/-}$ astrocytes for 4 hrs. Cultures were then fixed with 4% paraformaldehyde and stained for markers of interest.

Images were taken on a stimulated emission depletion (STED) confocal microscope (Leica, Wetzlar, Germany) for the visualization of internalized exosomes in astrocytes.

2.3.9 CryAB Immunoprecipitation

CryAB was immunoprecipitated (IP-CryAB) from isolated OEC-exosome fractions that were lysed in RIPA buffer. Briefly, 200µl Protein A Dynabeads (30mg/ml, Invitrogen, Cat# 10001D, Carlsbad, CA) were washed 3 times in PBS+ 0.1% Tween (PBST) using a magnetic stand (Millipore, PureProteome Cat# LSKMAGS08), CryAB antibody (400µl, 1:50 (10 µg/mL) in PBST) was added to the beads, and the mixture was incubated (30 min, RT) with constant agitation. The antibody solution was removed, beads washed (3x), exosome fractions resuspended in PBS were added, and the mixture was incubated overnight (4^0C). Beads were then washed (4x) and CryAB protein eluted by addition of 60µl of 0.2M Glycine (pH 2.5); the pH of the eluate was neutralized by addition of 5µl of 1M Tris (pH 8.5). Cell culture, immunoblotting or ELISA was performed.

2.3.10 ELISA

CryAB concentration was measured in exosome fractions using a competitive ELISA kit (MyBioSource, Cat# MBS7239470, San Diego, CA) according to manufacturer's instructions. Isolated exosomes were sonicated and lysed in Buffer M (containing NP40) plus PI from Protein Extraction Kit (BioChain). Equivalent quantities of total exosomal protein or supernatant CM protein, determined by BCA protein assay, were brought to equivalent volumes in EDM. 100µl of samples were added to each well and measured with a microplate reader (FlexStation 3; Molecular Devices, Sunnyvale, CA). Results were analyzed with SoftMax Pro Software (Molecular Devices).

2.3.11 Quantitative RT-PCR (q-RT-PCR)

cDNA synthesis was performed using Superscript™ III reverse transcriptase (Invitrogen), and PCR carried out using the ViiA7 Real-Time PCR System (Applied Biosystems, Waltham, MA) in 20µl final volume, containing 10µl of SsoAdvanced Universal SYBR Green Supermix (BioRad Cat#1725271), 2µl of a primer mix with a concentration of 1µM of each primer and 1µl of cDNA and 7µl water. Samples were run in triplicate. The expression levels of genes of interest were normalized using the primers (forward; reverse) (AGTGCCAGCCTCGTCCCGTA; TGAGCCCTTCCACAATGCCA), for expression of GAPDH. All other primer sequences are detailed in (Liddelow *et al.*, 2017; Clarke *et al.,* 2018). Data were analyzed by one-way ANOVA followed by Dunnett's multiple post hoc test.

2.3.12 Statistical analysis and cell counting

All statistical analyses were done using GraphPad Prism 8.00 software. The results are shown as mean ± SD. Statistical analysis was performed using one-way or two-way ANOVA, unless otherwise stated. Probability values of 0.05 ($p \leq 0.05$) were considered to indicate statistical significance. N=biological replicates, n=technical replicates.

2.4 Results

2.4 Results

2.4.1 OECs secrete anti-inflammatory factor(s) that reduce astrocyte reactivity

Nuclear translocation of the pro-inflammatory protein NFκB was used as a readout of astrocyte reactivity evoked by bacterial endotoxin LPS (Rothhammer *et al.*, 2016), as measured by immunoblot analysis of the nuclear fraction of astrocyte lysates (Figure 3A, inset). As expected, NFκB increased in the nuclear fraction of immortalized C8D30 astrocytes treated with LPS (Figure 3A, gray bars, $p \leq 0.05$). Co-culture of astrocytes with OECs blocked nuclear translocation of NFκB in response to LPS, as previously reported (Hale *et al.*, 2011; Figure 3A, purple bars). Adding CM from untreated OEC monocultures, (OEC-CM), also decreased NFκB translocation into nuclei of astrocytes exposed to LPS (Figure 3A, red bars,), indicating that anti-inflammatory factor(s) are secreted by OECs even in the absence of a stress signal.

To facilitate identification of OEC factors of interest, the anti-inflammatory capacity of six immortalized OEC lines (Calof & Guevara, 1993) were screened. Immortalized astrocytes (C8D30) were treated with CM from the different OEC lines, treated with LPS, immunostained for NFκB (Figure 3B), and the nuclear/cytoplasmic ratio of NFκB immunostaining was determined. As shown in Figure 1C, CM from two of the immortalized OEC lines, C7 and D6, significantly reduced nuclear NFκB translocation in C8D30 astrocytes compared to LPS treatment alone (Figure 3C, red bars, $p \leq 0.05$), while D4 and C4 CM were similar to LPS alone. Original characterization of these immortalized OEC lines had been based on morphology and immunostainining with markers expressed by primary OECs (Calof & Guevara, 1993). Characterization of the re-grown lines was consistent with earlier reports,

with C7 cells, for example, showing heterogeneous morphologies depending on culture conditions and density (Figure 3D): these included Schwann Cell spindle-like (majority; Figure 3Da), astrocyte-like type1 (Figure 3Db), and astrocyte-like type2 (Figure 3Dc) morphologies (Huang *et al.,* 2008). Cell lines were re-examined by immunofluorescence for expression of OEC-specific markers, such as p75, Sox10, and brain lipid-binding protein (BLBP). Both C7 and C4 cell lines were positive for these OEC markers (Figure 3E). Since C7-CM significantly suppressed nuclear NFκB translocation in astrocytes, whereas C4-CM did not (Figure3B, C), and both lines expressed the OEC markers tested, C7-CM was used as a positive control, and C4-CM as a negative control in further experiments.

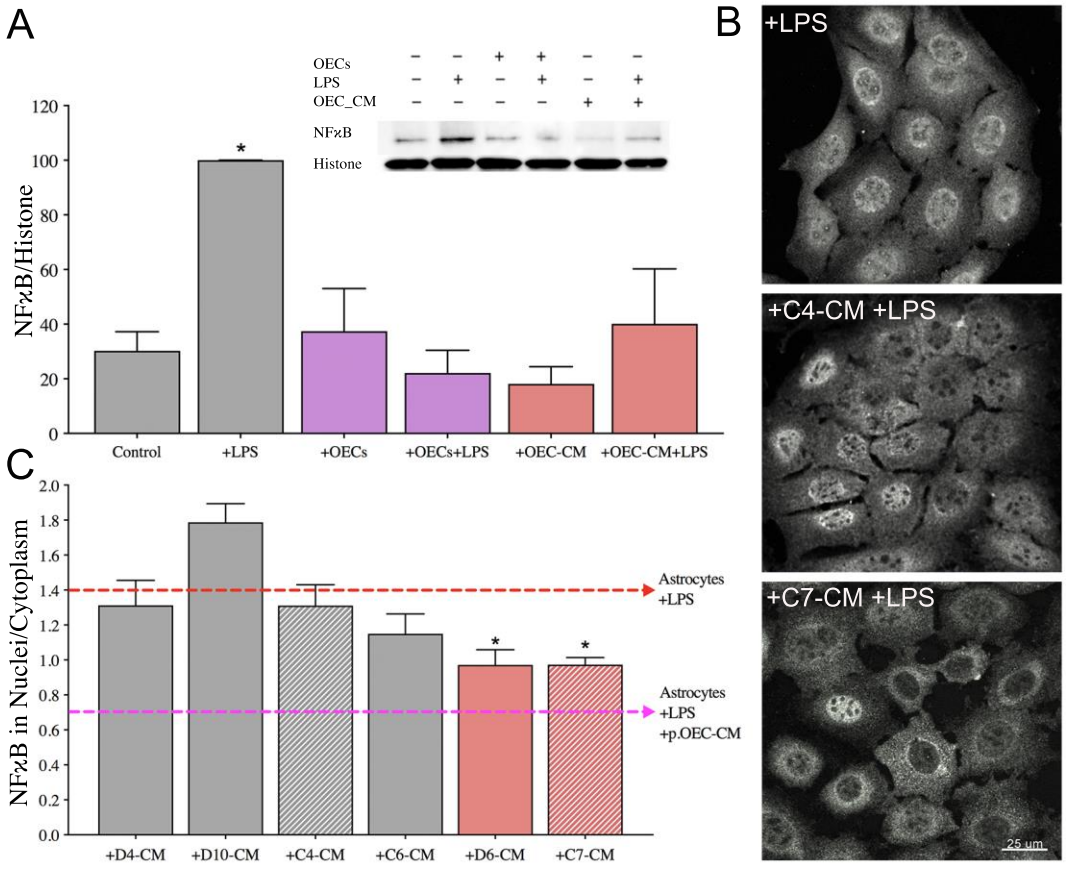

Figure 3 *(figure continued on next page)*

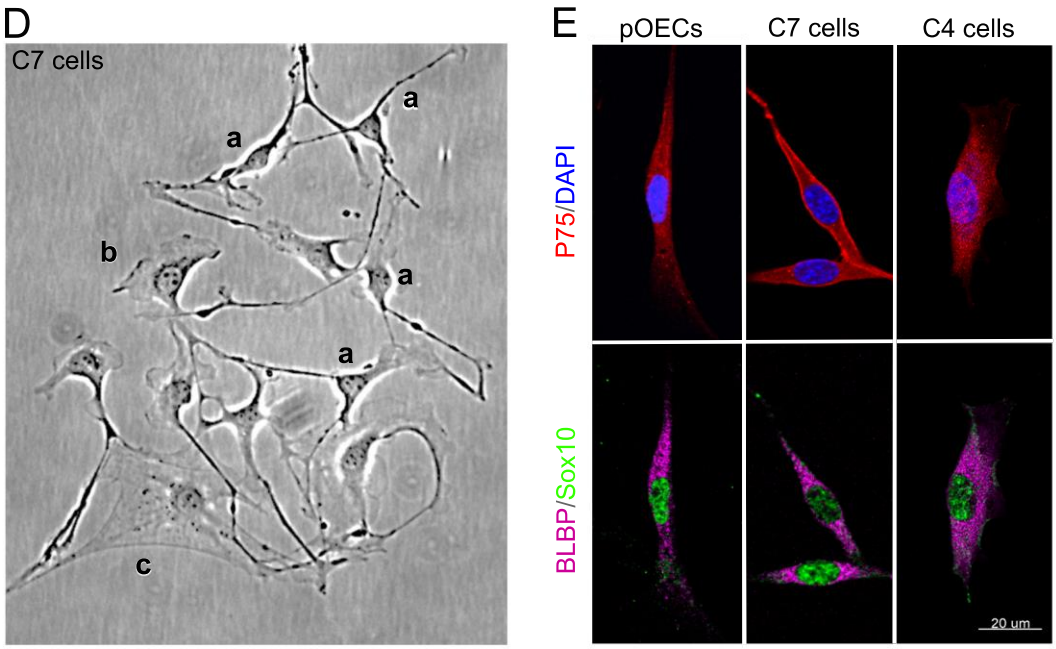

Figure 3: OEC-CM alone is sufficient to suppress LPS-induced astrocyte reactivity, an effect mimicked by a subset of immortalized OEC lines. (A) Quantitative immunoblotting for NFκB was performed on the nuclear fraction of C8D30 astrocyte lysates (inset). All groups were compared using a one-way ANOVA (N=3). Treatment with LPS for 2 hrs significantly increased NFκB activity (* indicates $p \leq 0.05$, gray bars). The presence of OECs blocked the effect of LPS (purple bars). OEC conditioned medium (OEC-CM) alone also blocked the increase in nuclear NFκB (red bars). (B and C) CM from six immortalized OEC lines were investigated for their ability to block the effect of LPS on nuclear NFκB translocation in C8D30 astrocytes, as measured by the ratio of fluorescence intensity of nuclear to cytoplasmic NFκB. (B) Photomicrograph of images of C8D30 astrocytes cocultured with CM of immortalized cell lines. (C) Fluorescent NFκB nuclear and cytoplasmic intensities were measured and ratios plotted. Pink dashed line depicts value of astrocytes treated with primary OEC-CM +LPS and red dashed line depicts value of astrocytes +LPS. A median value was calculated from ~100 cells per field, and then a mean/group was calculated. C7-CM and D6-CM decreased NFκB nuclear translocation (N = 3; * $p \leq 0.05$; one-way ANOVA), while C4-CM treated groups was not significantly different than astrocytes +LPS alone (N = 3; * $p \leq 0.05$; one-way ANOVA). (D) Photomicrograph from line C7. Multiple morphologies were found in all the OEC cell lines: (a) Schwann Cell-like, (b) astrocyte-like type1, and (c) astrocyte-like type2. Schwann cell-like spindle cells (a) predominated in C7. (E) C7 and C4 olfactory cell lines share multiple markers with OECs including BLBP (magenta), Sox10 (green) and P75 (red). Scale bars represent 25 and 20μm.

2.4.2 OEC-secreted CryAB suppresses LPS-induced astrocyte reactivity

To identify OEC-derived molecules potentially involved in crosstalk between OECs and astrocytes, secreted proteins from primary OEC-CM, C7-CM and C4-CM were compared by mass spectrometry. Before collection of CM, LPS was added to cultures as a stress signal. Secreted proteins from LPS-treated cells were ranked based on 1) their abundance in C7-CM compared to C4-CM; 2) their abundance in C7-CM compared to primary OEC-CM; and 3) absence from C4-CM (Figure 4A). Proteins that were secreted at similar levels by C7 cells and primary OECs (Figure 4A, horizontal dashed line), but are not likely to be present in C4-CM (Figure 4A, X axis) were determined. Based on these criteria, we identified two proteins of particular interest: the heat shock protein alpha crystallin B chain (CryAB), and the cell surface glycoprotein MUC18 (MCAM). To identify OEC secreted molecules in response to an endogenous signal from astrocytes, similar experiments were performed after treatment with Anosmin1, an extracellular binding protein secreted by mature astrocytes (Gianola *et al.,* 2009) and shown to act on OECs (Hu *et al.,* 2019). Even though the ortholog is yet to be identified for this protein in mice, we observed a robust migration of primary mouse OECs towards recombinant Anosmin-1 (personal observation). Notably, both CryAB and MCAM were identified as major secreted proteins in this screen as well (Figure 4B). CryAB was selected for further study because of its known role as an anti-inflammatory protein involved in stress responses by CNS glia (e.g., Ousman *et al*., 2007; Kuipers *et al*., 2017), and because it was the most abundant protein fitting our criteria in screens of both LPS (Fig. 4A) and Anosmin-1 (Fig. 4B) treated samples. Recombinant CryAB protein mimicked the effect of OEC-CM or C7-CM on astrocyte reactivity, as measured by suppressed nuclear translocation of NFκB, following either LPS- or cytokine-induced inflammation (Figure 4C).

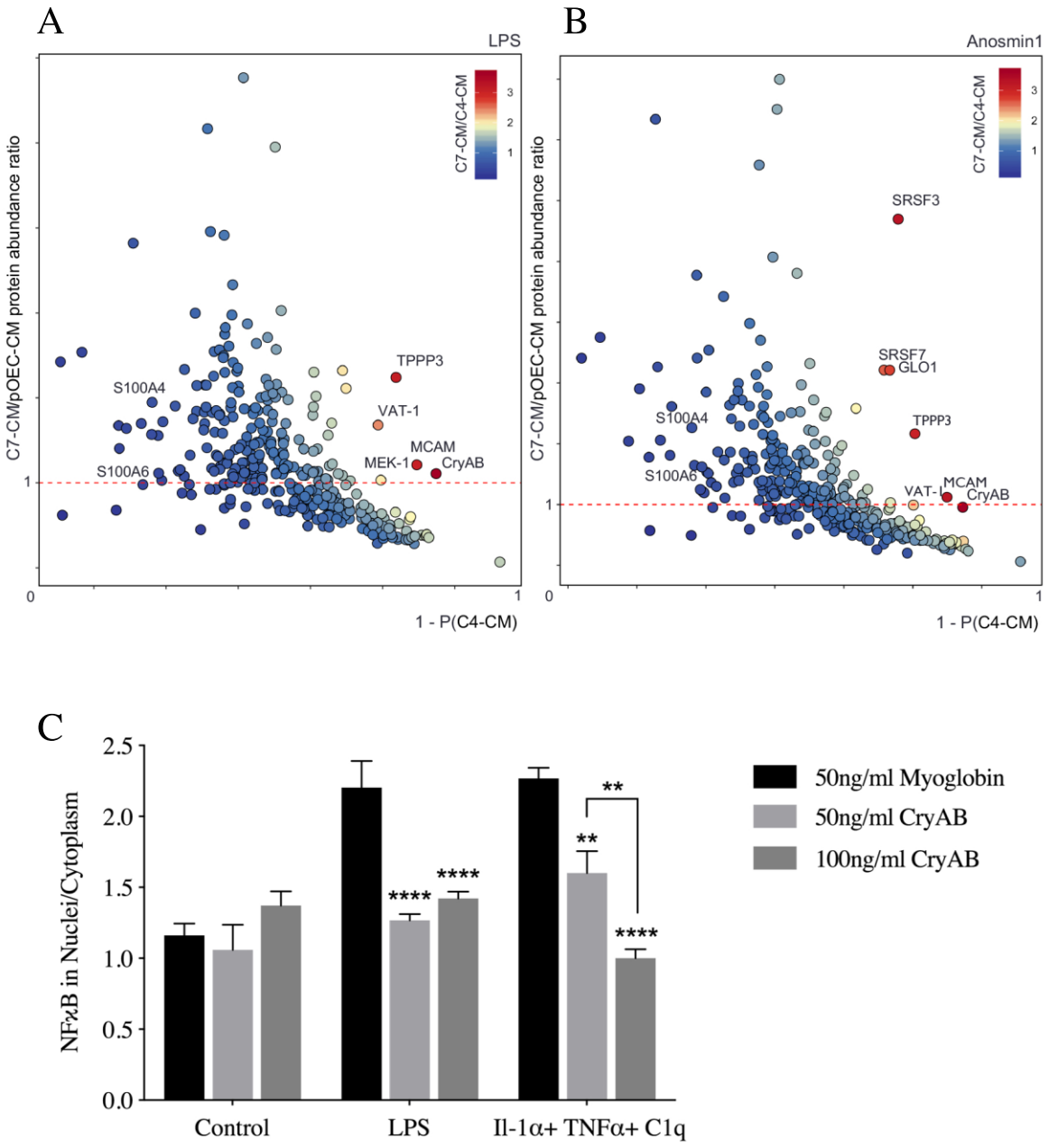

Figure 4: OEC-secreted anti-inflammatory protein CryAB and recombinant CryAB is sufficient to suppress astrocyte reactivity measured by NFκB. (A, B) Comparison of factors secreted from C7 line, C4 line and primary OECs (pOECs), analyzed by mass spectrometry. Proteins detected in CM following LPS treatment (A) or Anosmin1 treatment (B) were ranked by their relative abundance indicated by color code (heat map, inset). Relative abundance of detected proteins in C7-CM compared to pOEC-CM is graphed on the Y axes, and relative absence of the same proteins from C4-CM (1-P(C4-CM) = probability of not being found in C4-CM) is graphed on the X axes. Proteins of similar abundance in CMs from C7 cells and pOECs (horizontal red-dashed lines), and not likely to be present in C4-CM (Y axes) were identified. Alpha crystallin B chain (CryAB) had the highest C7/C4 expression ratio and was equally abundant in CM from C7 cells and pOECs. (C) Recombinant CryAB alone

suppressed the inflammatory response, quantified as the ratio of nuclear to cytoplasmic NFκB (Y axis) in astrocytes exposed to either LPS or a cocktail of the cytokines Il-1α, TNFα and C1q for 2 hrs. Group values were obtained from triplicate wells in which a median value was calculated from ~50 cells per field. N = 3; (*p ≤ 0.05; **p ≤ 0.01; ****p ≤ 0.0001;) two-way ANOVA.

2.4.3 Exosomes secreted by OECs contain CryAB, which moderates intercellular immune response

Since it has been shown that CryAB secretion can occur via exosomes (Sreekumar *et al.*, 2010; Kore *et al.*, 2014; Guo *et al.*, 2019), exosomes were isolated from OECs to determine whether they were positive for CryAB and whether the CryAB secreted via OEC-exosomes had the ability to attenuate astrocyte reactivity. For these experiments, exosome fractions were isolated from culture supernatants of OECs generated from both *CryAB*$^{-/-}$ mice and WT (*CryAB*$^{+/+}$) controls. To ensure the quality of fractions used, exosomes and whole cell lysates (CL) from WT OECs were analyzed by immunoblotting for the following proteins: the structural protein, β-actin; a mitochondrial protein, Tomm20; a nuclear protein, histone H3; and the extravesicular protein Flotilin-1. The exosome fraction was devoid of β-actin, Tomm20 and histone H3, but was positive for Flotilin-1 (Figure 5A), consistent with published information for exosome fractions (Jeppesen *et al.*, 2019).

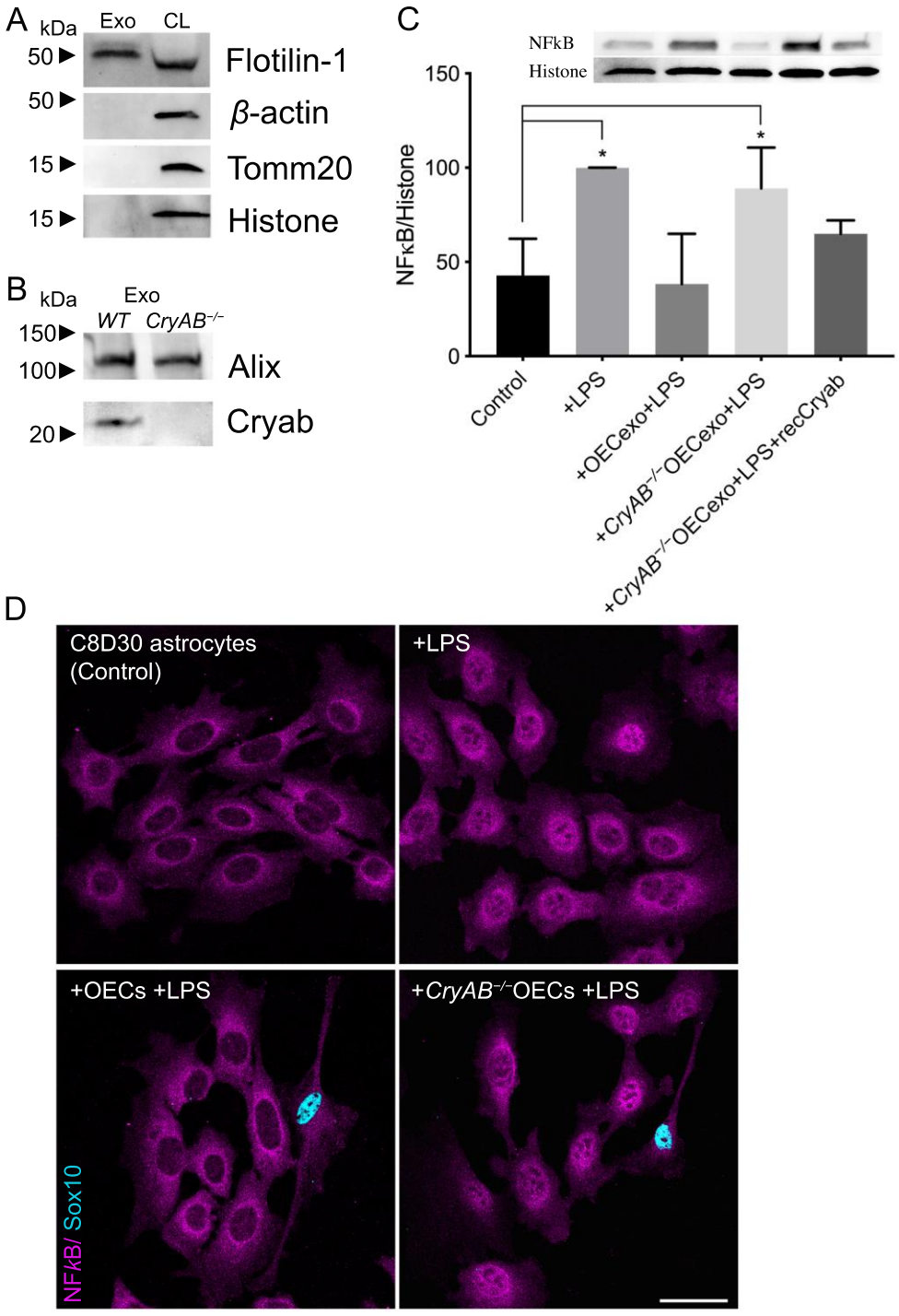

Figure 5: CryAB, secreted by primary OECs into exosomes, suppresses inflammatory response in an astrocyte cell line. (A) Immunoblot of exosome (Exo, left) and whole cell lysate (CL, right) fractions from WT primary OECs were screened for β-actin, Tomm20,

histone H3, and Flotilin-1. The exosome fraction from WT exosomes was devoid of cellular β-actin, Tomm20 and histone H3, but contained the extravesicular protein Flotilin-1. (B) Immunoblots for CryAB and the exosome marker Alix were performed on exosome fractions made from *CryAB*$^{-/-}$ and WT (*CryAB*$^{+/+}$) OEC cultures. CryAB was absent in exosome fractions from *CryAB*$^{-/-}$ OEC culture medium, whereas the exosome marker Alix was present. (C) C8D30 astrocytes were treated for 24 hours with exosomes isolated from WT or *CryAB*$^{-/-}$ OECs. Astrocytes were exposed to 1μg/ml LPS for the last 2 hrs of exosome treatment. Nuclear fractions of astrocytes were analyzed via quantitative immunoblotting for NFκB and Histone H3. Inset shows a representative immunoblot and graph shows mean ± SD of NFκB/histone ratio. All conditions were compared to astrocyte alone group (Control, N = 3; $p \leq 0.05$; one-way ANOVA). Treatment of astrocytes with WT OEC-exosomes (exo) + LPS, blocked nuclear NFκB translocation. In contrast, *CryAB*$^{-/-}$OEC-exosomes failed to suppress nuclear NFκB translocation. Recombinant CryAB (50ng/ml) added to *CryAB*$^{-/-}$OEC-exosomes was sufficient to attenuate NFκB translocation induced by LPS, with levels comparable to WT OEC-exo +LPS. (D) C8D30 astrocytes treated with LPS for 2 hrs (top right: "+ LPS") showed stronger immunostaining for NFκB in the nucleus (magenta) compared to untreated controls (top left). Astrocytes co-cultured with *CryAB*$^{-/-}$ OECs (Sox 10-positive cells with blue nuclei) had increased levels of NFκB immunostaining in the nucleus (bottom right: "+*CryAB*$^{-/-}$OECs +LPS") compared to astrocytes co-cultured with WT OECs (bottom left: "+OECs +LPS"). Scale bar represents 40μm.

Competitive ELISA against CryAB confirmed the presence of CryAB in OEC exosomes. Exosomes derived from $1x10^6$ OECs contained 9.22 ± 0.2 ng CryAB, whereas CryAB protein was undetectable in CM from which exosomes were depleted (Figure 6A). Next, exosomes from both genotypes were immunoblotted for CryAB and the endocytosis protein, Alix, which is concentrated in exosomes (Figure 5B; Jeppesen *et al.*, 2019). CryAB was present in WT OECexo fractions but was absent in *CryAB*$^{-/-}$OECexo fractions; while the exosome marker Alix was present in exosome fractions from OECs of both genotypes. Finally, to assay whether CryAB present in OEC exosomes could suppress astrocyte reactivity, the exosomes were added to immortalized C8D30 astrocytes for 24 hrs, and treated with LPS for the last 2 hours of this incubation. As shown in Figure 3C, quantitative immunoblotting demonstrated that: a) exosomes from WT OECs were able to suppress astrocyte reactivity, as measured by reduced nuclear translocation of NFκB; b) astrocytes treated with *CryAB*$^{-/-}$OECexo remained reactive; and c) the reactivity of astrocytes treated with *CryAB*$^{-/-}$OECexo was reduced by the presence

of recombinant CryAB protein. Immunostaining OEC-astrocyte co-cultures for NFκB further showed strong nuclear NFκB immunostaining exhibited by astrocytes co-cultured with *CryAB*$^{-/-}$OECs (Figure 5D, lower right). whereas astrocytes co-cultured with WT OECs showed little if any nuclear NFκB immunostaining (Figure 5D, lower left). Together, these results are consistent with CryAB, secreted by OECs in exosomes being an important protein for OEC-astrocyte crosstalk, and functioning as an anti-inflammatory molecule for astrocytes.

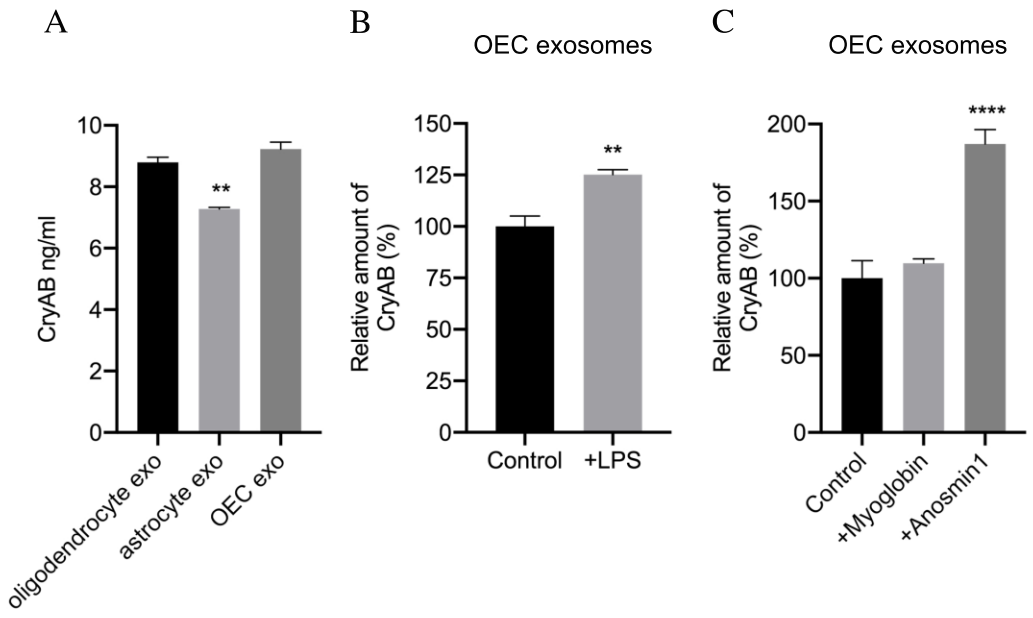

Figure 6: Competitive ELISA against CryAB was used to examine exosomes. (A) Exosomes (exo) derived from 1x10^6 OECs were determined to have 9.22 ± 0.2 ng CryAB. CryAB in OEC secreted exosomes was not significantly different than the concentration in oligodendrocyte exosomes but %21.1 higher than that of astrocyte exosomes. (B) Exposure to LPS increased OEC secreted CryAB concentration by 25.17% (C). Although OECs' exposure to LPS or astrocytic signals were not necessary for the suppressive effect of OECs on NFκB translocation in C8D30 astrocytes, whether the CryAB secretion would be facilitated by external signals was investigated by stimulating with LPS or Anosmin1. Exposure to Anosmin-1 increased CryAB concentration by 77.17%, compared to control protein recombinant myoglobin.

2.4.4 Astrocytes internalize CryAB-containing OEC exosomes

To determine whether astrocytes take up CryAB-containing exosomes secreted by OECs, *CryAB*$^{-/-}$ astrocytes were cultured with exosome fractions from OEC cultures generated from WT mice. Uptake was visualized by immunostaining of GFAP-positive astrocytes (Figure 7, magenta); colabeled with antibodies to endosome/exosome marker CD63 (red) and CryAB (green). CryAB and CD63 colocalized in *CryAB*$^{-/-}$ astrocytes treated with exosomes for 4 hrs (Figure 7, insets). Neither untreated *CryAB*$^{-/-}$ astrocytes (Figure 7B) nor WT astrocytes (Figure 7C) showed such specific colocalization, consistent with the uptake of CryAB-containing OEC exosomes by astrocytes.

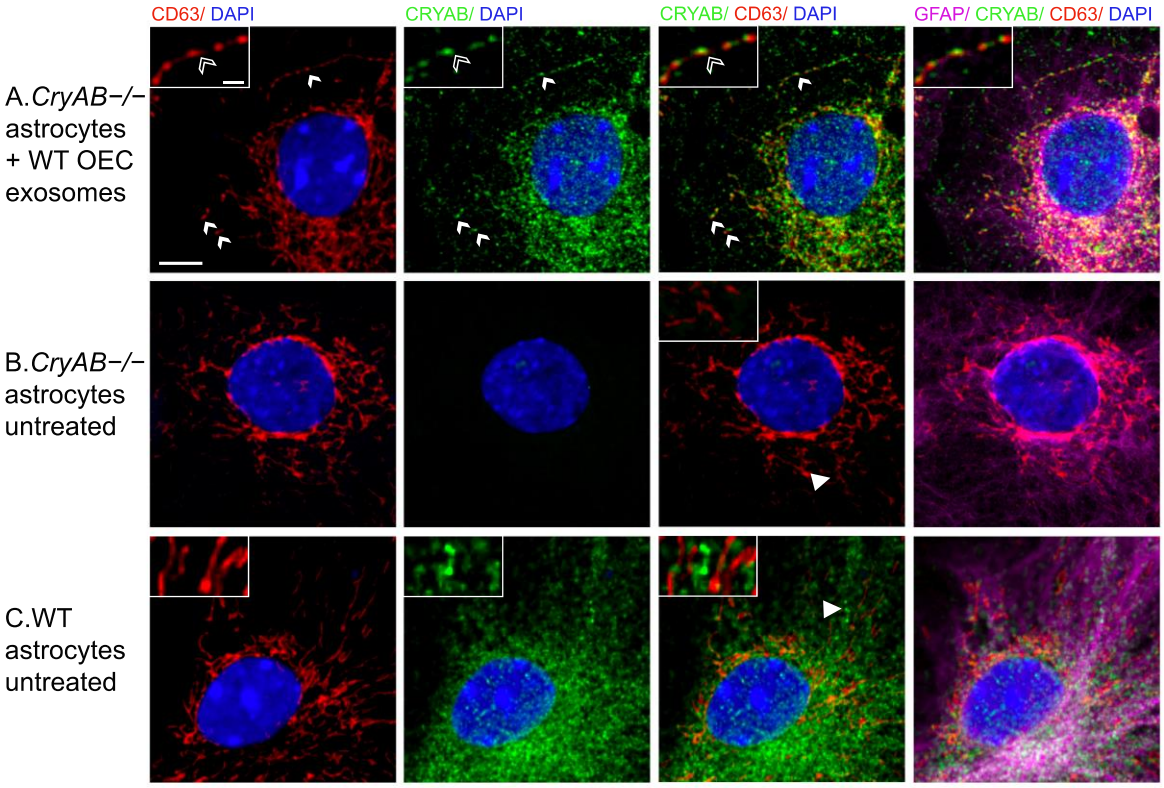

Figure 7: CryAB in OEC exosomes is internalized by astrocytes. (A) OEC exosomes from WT mice were co-cultured with primary astrocytes from CryAB KO mice. (B) Untreated astrocytes from CryAB KO. (C) Untreated astrocytes from WT mice. All groups were stained for CD63 (endosomes; red), CryAB (green), GFAP (magenta) and Dapi (blue). Uptake of OEC secreted CryAB (green) is detected in CryAB$^{-/-}$ astrocytes and is often associated with endosomes (red) (A, arrows, top arrow area shown in inset, arrowhead points to CryAB

positive endosome). No CryAB staining (green) is detected in untreated astrocytes from CryAB KO (B, inset). CryAB (green) is present in untreated astrocytes from WT mice but rarely associated with endosomes (C, inset, arrowhead). Scale bar represents 5μm in low mag and 1μm in insets.

2.4.5 OEC secreted factors, including CryAB, reduce astrocytes' expression of genes associated with neurotoxic reactivity

To evaluate the effects of OEC-secreted CryAB on expression of "neurotoxic" genes, astrocytes were exposed to LPS alone; or WT OEC-CM, *CryAB*$^{-/-}$OEC-CM, or CryAB immunoprecipitated from isolated OEC-exosome fractions (IP-CryAB) together with LPS. mRNA from treated astrocytes was then analyzed for 12 transcripts known to be associated with neurotoxic astrocyte reactivity (Liddelow *et al.*, 2017). Q-RT-PCR analysis (Figure 8) showed that all tested transcripts were reduced in expression in the presence of WT OEC-CM, and this effect was significant for 9 of the 12 (Figure 8, second row, white arrows, $p \leq 0.05$ A vs B). In contrast, 4 of the transcripts showed increased expression when treated with *CryAB*$^{-/-}$OEC-CM (Figure 8C, black arrows). The analysis also suggests that suppression of expression of *Ggta1*, *Serping1*, *ligp1*, *Gbp2* and *Amigo2* was CryAB-dependent, for the following reasons: a) suppression of expression failed to occur with *CryAB*$^{-/-}$OEC-CM treatment, while still taking place with IP-CryAB treatment (Figure 8, C vs D); or b) expression was upregulated in the *CryAB*$^{-/-}$OEC-CM group (Figure 8, C vs A). Suppression of expression of 4 genes (*H2-T23, Srgn*, *H2D1*and *C3*) appeared to be independent of CryAB, since it still occurred in astrocytes treated with *CryAB*$^{-/-}$OEC-CM (Figure 8, C vs A). In contrast to either OEC-CM treatments (*CryAB*$^{-/-}$or WT), a significant increase in *Fbln5* was detected in astrocytes treated with IP-CryAB (Figure 8, D vs A). These results are consistent with the finding that CryAB,

secreted by OECs, functions as an anti-inflammatory agent for astrocytes. In addition, comparison of OEC-CM treatment to IP-CryAB for transcripts *Ugt1a1*, *C3* and *Fbln5* suggest that there are factors in OEC-CM, in addition to CryAB, that suppress neurotoxic astrocyte reactivity.

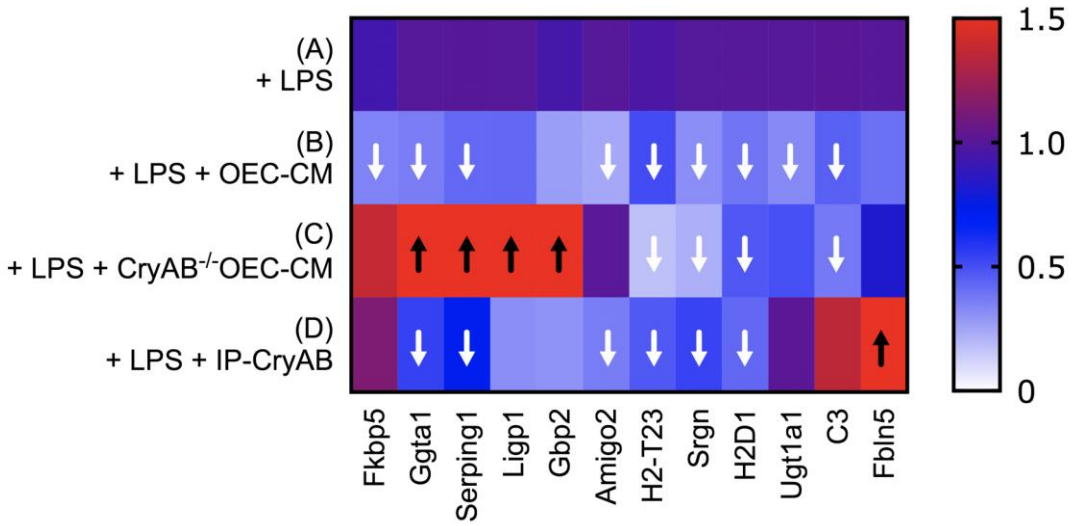

Figure 8: OEC-CM suppresses multiple transcripts associated with neurotoxic astrocyte reactivity in LPS-treated astrocytes. Heat map illustrating results of Q-RT-PCR to detect neurotoxic astrocyte transcripts in primary astrocytes treated with LPS (A); LPS plus WT OEC-CM (B); LPS plus *CryAB*$^{-/-}$OEC-CM (C); or IP-CryAB for 24 hrs (D). Compared to LPS, OEC-CM (B) significantly suppressed 9 transcripts, whereas *CryAB*$^{-/-}$OEC-CM (C) significantly suppressed 4. (D) IP-CryAB suppressed 6 of the 9 transcripts suppressed by OEC-CM. In addition, *CryAB*$^{-/-}$OEC-CM+LPS caused a significant increase in 4 transcripts, while IP-CryAB caused a significant increase in one. Finally, one transcript, C3, was significantly suppressed by both OEC-CM treatments (*CryAB*$^{-/-}$ or WT) but was elevated by IP-CryAB treatment. Q-RT-PCR experiments were analyzed by one-way ANOVA followed by Dunnett's multiple post hoc test (n= 3; arrows $p \leq 0.05$).

2.5 Discussion

2.5.1 OEC-secreted factors that moderate astrocyte reactivity

Astrocyte reactivity is a pathological response that occurs in a wide range of CNS injuries, inflammation and diseases. *In vivo* studies show that some reactive astrocytes induced by ischemia can promote neural recovery and repair (reviewed in Rossi *et al.*, 2007); in contrast, reactive astrocytes induced by bacterial endotoxins such as LPS are neurotoxic (Zamanian *et al.*, 2012). This harmful, neurotoxic astrocyte reactivity appears to be driven by pro-inflammatory cytokines secreted by activated microglia (Liddelow *et al.*, 2017). However, anti-inflammatory factors that suppress neurotoxic astrocyte reactivity are largely unknown. Olfactory system is one of the few niches in the mammalian CNS that supports neuronal regeneration (Forni *et al.*, 2013). Olfactory sensory neurons are vulnerable to damage due to their exposed location in the nasal cavity and have a remarkable capacity for regeneration (Calof *et al.*, 1996, Forni *et al.*, 2013), suggesting the presence of robust anti-inflammatory factors in the olfactory system. OECs wrap and guide axons of the olfactory sensory neurons en route to the OB, where they establish new connections. Moreover, OECs directly interact with astrocytes at the entry point into the CNS, enabling regenerating olfactory axons to make new connections (Williams *et al.,* 2004; Li *et al.*, 2005; Raisman & Li, 2007). Notably, both transplanted OECs (Lakatos *et al.*, 2003; reviewed in Roet & Verhaagen, 2014) and co-cultured OECs (Hale *et al.*, 2011) have been shown to intermingle with astrocytes and to moderate astrocyte activation.

The studies in this report investigate anti-inflammatory factors secreted by OECs participating in OEC-astrocyte crosstalk. Mass spectrometry was used to analyze proteins in CM from primary OECs and compared to the CM of immortalized OEC lines with different

anti-inflammatory capacities. Two proteins were identified as potential factors that could suppress neurotoxic astrocyte reactivity: MCAM and CryAB. MCAM (also called CD146 or MUC18) is a signaling receptor that can be cleaved from the cell membrane, generating a soluble form that is associated with increased cell migration and invasion (Seftalioglu & Karakoc, 2000), and primarily has been studied in endothelial cell angiogenesis and cancer metastasis (reviewed in Dye *et al.*, 2013). Studies on Multiple Sclerosis (MS) patients showed no association between MCAM expression and disease activity (Petersen *et al.*, 2019). In contrast, CryAB treatment of MS patients was associated with a therapeutic outcome, downregulation of T cell proliferation and pro-inflammatory cytokine production (Quach *et al.*, 2013; van Noort *et al.*, 2015). In addition, CryAB has been shown to have neuroprotective and regenerative effects in neuroinflammatory animal model systems (Arac *et al.*, 2011; Ousman *et al.,* 2007; van Noort *et al.*, 2015). Moreover, there is a correlation between glial activation and increased CryAB levels in Alexander, Alzheimer's and Parkinson's diseases, as well as traumatic brain injury and stroke (reviewed in Dulle & Fort, 2016). Thus, we investigated the role of OEC-secreted CryAB in OEC- astrocyte crosstalk.

2.5.2 Exosomal release of CryAB

Our results show that OECs secrete CryAB via exosomes, and that these exosomes produce an intercellular anti-inflammatory effect following their uptake by astrocytes. Exosomes are small vesicles packaged inside multivesicular endosomes (MVE) and released into the extracellular matrix when MVE fuse with the plasma membrane (Jeppesen *et al.*, 2019). Subsequent uptake by a neighboring cell initiates intercellular communication. Notably, released exosomes are functional components of the extracellular matrix that can be induced by stress signals but are associated with cell-cell communication rather than apoptosis

(Jeppesen *et al.*, 2019; Gupta & Pulliam, 2014). Consistent with our findings, recent studies suggest that CryAB can be secreted by glia in an autocrine manner (Kore *et al.*, 2014; Guo *et al.*, 2019) and play a protective role (Ousman *et al.*, 2007). Although the downstream effects of CryAB in astrocytes that we demonstrate have yet to be fully explored, one important role of CryAB may be its interaction with transcription factors, including NFkB, to suppress inflammation by inhibition of their nuclear translocation (Shao *et al.,* 2013; Zhang *et al.,* 2015; Qiu *et al.*, 2016). However, exosome-mediated regulation of the astrocytic immune response by OECs may also be a unique interaction, as membrane composition and protein content of exosomes is cell type (Kalra *et al.*, 2012; Keerthikumar *et al.*, 2015; Kim *et al.,* 2015) and context specific (György *et al.,* 2011; Müller *et al.*, 2012).

The robust anti-inflammatory response induced by OEC-secreted CryAB, shown in the present report, may also be a function of concentration, as our results indicate the concentration of CryAB in OEC exosomes to be higher than that found in astrocyte exosomes. We found that CryAB in OEC secreted exosomes was ~21% higher than that of astrocyte exosomes (Figure 6A) and exposure to LPS increased OEC secreted CryAB concentration by ~25% (6B), indicating OECs actively respond to stress by either secreting more exosomes or increasing CryAB concentration in exosomes, or both. In addition, exposure to Anosmin1 increased CryAB concentration by ~77% (Figure 6C), compared to control protein recombinant myoglobin, suggesting OECs can actively respond to extracellular astrocyte signals by increasing CryAB concentrations.

2.5.3 CryAB, as well as other factors secreted by OECs, can suppress neurotoxic astrocyte reactivity

Stress causes denaturation of correctly folded proteins that can result in their aggregation and binding to CryAB (Muranova *et al.,* 2018) and subsequent changes in gene expression (Singh *et al.,* 2019). Our results show that OEC-secreted CryAB suppressed expression of a number of genes associated with neurotoxic astrocyte reactivity and suggest there are additional factor(s) in OEC-CM that further suppress this harmful reactivity. In fact, complement component-3 (C3) expression in IP-CryAB +LPS-treated astrocytes, although not significantly different than that observed in astrocytes treated with LPS alone, was significantly greater than expression in astrocytes treated with either OEC-CM groups (Figure 5). C3 is an important marker for neurotoxic astrocytes, evident by knockout mice showing reduced activity in microglia and astrocytes, as well as neuron loss (Shi *et al.*, 2017). Moreover, C3 is found colocalized with astrocyte markers in regions of neurodegeneration in human post-mortem tissue (Liddelow *et al.*, 2017). Therefore, more experiments are required to identify OEC-secreted factor(s) that can suppress C3. In this regard, other proteins identified in our mass spectrometric screen, showing smaller changes, may be worthwhile to evaluate. Certainly, crosstalk mechanisms between OECs and surrounding niche cells, including astrocytes, are highly complicated (Chuah *et al.*, 2011). In addition to unidentified anti-inflammatory factors, absence or suppression of pro-inflammatory factors might also play a role in OEC-CM's effect on astrocyte reactivity. For example, our mass spectrometry screening showed higher concentration of S100A4 and S100A6 proteins in C4-CM compared to pOEC-CM or C7-CM (Figure 4, Supplemental Data-1 & 2). S100 proteins are known to modulate neuroinflammation (Donato, 2001), and as such are also candidate molecules that

may contribute to the observed difference in the inflammatory reactivity of astrocytes treated with C4-CM versus pOEC-CM or C7-CM.

Recent studies have transformed our perception of astrocytes from a passive structural support network for neurons, to active effectors in the regulation of synaptic transmission, neural excitability, plasticity and recovery. In this paper, we identify OEC secreted CryAB as an anti-inflammatory factor that can moderate astrocyte reactivity, suppressing both transcription of neurotoxic classified genes and nuclear translocation of pro-inflammatory factor NFκB. Improving our understanding of the crosstalk between astrocytes and OECs may inform strategies to identify other endogenous repair mechanisms that facilitate CNS repair, and consequently impact function, in the injured nervous system.

Chapter 3: OEC-HSPGs moderate astrocyte reactivity, proliferation, and differentiation via FGFR1 signaling

3.1 Abstract

FGFR1 signaling pathway is important in astrocyte fate determination and reactivity. However, the contribution of specific downstream signaling components has been difficult to identify due to compensation/feedback mechanisms between FGFRs and other pathways. In this study, we show that olfactory ensheathing cell (OEC)-secreted factors moderate astrocyte reactivity by suppressing pro-inflammatory transcription factor (TF) NFκB. In addition, (OEC)-secreted factors induce the expression of differentiation and neuro-repair promoting TF STAT3 in astrocytes. FGF signaling is one of the few known pathways that can block harmful astrocyte reactivity in vitro. In accordance, when FGFR1 RTK activity was chemically inhibited in cocultures, OECs failed to suppress stress-induced nuclear translocation of pro-inflammatory transcription factors in astrocytes. OEC-secreted heparan sulfate proteoglycans (HSPGs) are strong candidates for factors that play a role in this crosstalk, since they are cell-specific ECM proteins known to support and regulate FGF signaling. Moreover, a regulatory role in intracellular FGFR trafficking has also been shown for HSPGs. Our results indicate that differential FGF/FGFR1 signaling can directly and rapidly impact the binary choice of astrocytes to proliferate or differentiate. These changes are mediated by differential membrane activity in the presence of OEC-HSPGs and may also reflect nuclear FGFR-mediated regulation of transcription. OEC-HSPGs, or synthetic heparan sulfate oligosaccharides that mimic OEC-HSPGs, may guide new therapies for traumatic CNS injury and other neurological disorders by targeting astrocytes.

3.2 Introduction

Astrocytes are one of the most abundant and heterogeneous cell types in the central nervous system (CNS), yet, in contrast to many other CNS cell types, changes in gene-expression profiles of astrocytes during development and pathological states remain poorly defined. Studies in the developing spinal cord, and *in vitro* human astrocytes, identify two gene-expression patterns: an early, developmental phase characterized by cell cycle, cytoskeletal and axon guidance genes and a late, differentiated phase characterized by channels, neuronal signaling and metabolic genes (Chaboub *et al.,* 2016; Molofsky *et al.,* 2013). Differentiated astrocytes exhibit regionally distinct and unique properties that are maintained by local signals (Morel *et al*., 2017). Under pathological conditions, differentiated astrocytes become reactive and demonstrate key features of developmental phase astrocytes, such as upregulation of structural proteins (glial fibrillary acidic protein (GFAP), Nestin and Vimentin), rounded morphologies and in some cases increased proliferation (Sirko *et al.,* 2013; Lepore *et al.,* 2008; Anderson *et al.,* 2016, reviewed in Liddelow & Barres, 2017). The return to a less mature genotype/phenotype is referred to as "dedifferentiation" (Buffo *et al*., 2008; Sirko *et al*., 2013). Indeed, astrocytes can re-acquire stem cell properties both *in vitro*, upon FGF2 stimulation (Kleiderman *et al*., 2016), and *in vivo* after injury (Faiz *et al*., 2015). All together, these results suggest that under pathological conditions, reactive astrocytes turn on developmentally encoded genes and dedifferentiate due to unsuitability, or absence of, extracellular signals in the microenvironment.

Dedifferentiation includes the upregulation of intermediate filaments, which enables reactive astrocytes to surround and isolate inflamed tissue, creating the 'glial scar'. Glial scar can prevent the tissue from secondary damage but also limits access for regenerating neural

cells to repair the damaged tissue after injury (Faiz *et al.,* 2015). The mechanism(s) responsible for dedifferentiation of reactive astrocytes and the contribution of transcriptional regulation to the harmfulness of astrocyte reactivity remain enigmatic. Our study focusses on aspects of astrocyte differentiation that are regulated by extracellular signals to test the hypothesis that activation of these signaling pathways could be used to support astrocytes for a therapeutic outcome following CNS injury.

Astrocytes display plasticity in protein expression, gliotransmitter release, calcium activity, changes of morphology or gap junction (Doetsch *et al.,* 1999; Alvarez-Buylla & Lim., 2004; Farmer *et al.,* 2016, reviewed in Pirttimaki & Parri, 2013). Astrocyte plasticity can have profound effects on neuronal network activity and also can be induced by local activity, in parallel with their reactive nature to pathological changes (Pirttimaki & Parri, 2013, Khakh & Deneen, 2019). Support for this observation comes from a recent study in the olfactory bulb (OB) where layers of morphologically distinct astrocytes are shaped by local interactions rather than clonal relationships (García-Marqués & López-Mascaraque, 2017). Astrocytes in the outermost layer of the OB, olfactory nerve layer (ONL), commingle with a distinct type of glia that is unique to the olfactory system, olfactory ensheathing cells (OECs). Astrocytes and OECs form the glia limitans of the OB and protect CNS against inflammation (Beiersdorfer *et al*., 2019). Notably, astrocytes of the ONL show the most differentiated morphology in the OB (García-Marqués & López-Mascaraque, 2017).

The olfactory system is one of the few regions in the adult mammalian CNS that supports the differentiation of new neurons and glia throughout life. Both neural niche signals and the surrounding glia, including OECs, give the olfactory mucosa this capability (Li *et al*., 2005, Roet, 2014). OECs transplanted into CNS injury sites for neuroregenerative purposes show

therapeutic benefits (Lakatos, 2003; reviewed in Roet, 2014). Similarly, astrocytes cultured in medium conditioned by cultured OECs (OEC-CM) show reduced nuclear translocation of Nuclear Factor kappa-B (NFκB), a pro-inflammatory protein that is a hallmark of harmful astrocyte reactivity (Hale *et al.*, 2011, Liddelow & Barres, 2017, see Chapter 2, Figure 5). Moreover, our own work shows that OEC-secreted factors suppress multiple neurotoxicity-associated transcripts in astrocytes (see Chapter 2, Figure 8).

FGFs are a family of critically important growth factors for CNS development, homeostasis and after injury; regulating neurogenesis, gliogenesis and also regeneration. FGF1 and FGF2 are significantly upregulated following CNS injuries (Woodbury & Ikezu, 2014; Ornitz & Itoh, 2015). FGF2 enhances neural stem cell proliferation (Newman *et al.*, 2000) and is upregulated in astrocytes in neurodegenerative disorders and following traumatic brain injury (Kirby *et al.*, 2013). While FGF2 signaling via FGFR1 is primarily known for its mitogenic effect and role in dedifferentiation, FGF2/FGFR1 has also been shown to be crucial for cell differentiation. These conflicting observations regarding the role of FGFR1 in cell-fate control of neural stem cells (NSCs) and reactive astrocytes has been contentious (Reuss *et al.,* 1998; Fahmy & Moftah, 2010). This controversy was settled by a loss- and gain- of function study showing that FGF signaling inhibits astrocyte reactivity in both normal and injured CNS (Kang *et al.,* 2014). Indeed, *in vitro*, FGF signaling significantly decreases expression of transcripts associated with neurotoxic astrocyte reactivity (Liddelow *et al.*, 2017). Curiously, both the gain, and loss of FGFR function decreases scar tissue formation *in vivo* (Kang *et al.,* 2014). Although compensation between FGFR members cannot be excluded (Oh *et al.,* 2003; Pringle *et al.,* 2003; Kang *et al.,* 2014), these findings suggest developmentally contrasting roles of pathways downstream of FGFR activation, as well as positive and negative feedback mechanisms

regulating FGFR signaling. However, the downstream effectors of FGF/FGFR signaling that enable astrocyte differentiation and their potential role in prevention of astrocyte metamorphosis into harmful reactive astrocytes remain to be identified.

FGFR1 is one of the most crucial signaling pathways that govern nervous system development (Stachowiak *et al.*, 2016) and FGF signaling is one of the few known pathways that can block harmful astrocyte reactivity *in vitro* (Liddelow *et al.*, 2017). An interesting partner of regulation for differential FGFR1 activity is heparan sulfate proteoglycan (HSPG). HSPGs are cell-specific extracellular matrix (ECM) proteins known to support and regulate FGF signaling. Barnett and colleagues suggest a role for OEC-secreted HSPGs in suppressing astrocyte reactivity, measured by GFAP expression (Santos-Silva *et al.*, 2007) and astrocyte-OEC mingling (Higginson *et al.*, 2012), with chemical blockage of FGF receptors promoting cell mingling. In agreement, Leadbeater and colleagues (2006) suggest that HSPGs regulate cell-specific injury responses through FGF2 after CNS injury.

Here we used OEC-astrocyte cultures to characterize FGFR1 downstream targets that can block harmful astrocyte reactivity. Experimental results showed that OEC-secreted HSPGs block astrocyte reactivity and suggest that this effect is mediated via increased FGFR1 phosphorylation initiated on the astrocyte membrane. On the other hand, FGF2 potentiated proliferation in astrocytes was neutralized in the presence of OEC-secreted factors. These results are consistent with a role for OEC-HSPGs in intracellular FGFR1 trafficking via association with the transcriptional machinery in astrocytes. Novel treatment strategies designed to mimic this crosstalk, targeting astrocytes, may enable improved recovery following CNS injuries.

3.3 Materials and Methods

3.3.1 Mice

All mice were maintained, and all animal handling procedures were performed according to protocols approved by the National Institutes of Health NINDS Institutional Animal Care and Use Committee. *Ext1*$^{floxed/floxed}$ mice were kindly gifted by Dr. Yu Yamaguchi. Mice were genotyped using primers 5'-GGAGTGTGGATGAGTTGAAG-3' and 5'-CAACACTTTCAGCTCCAGTC-3', using the PCR protocol previously described (Chen *et al.*, 2008). Male mice were obtained as heterozygous both for the *Ext1*^{floxed} allele and also the BLBP-Cre allele (Hegedus *et al.*, 2007). Female mice were obtained as homozygous for the *Ext1*^{floxed} allele. All mice were transgenic for the reporter S100ß-DsRed (Windus *et al.*, 2007). *Ext1*-CKO *(Ext1*^{BLBP}KO S100ß-DsRed) mice had developmental defects including diminished or absent olfactory bulbs and severe arrest of limb development, in particular in the hindlimbs, and did not survive postnatally. Absence of olfactory bulbs was previously reported for Nestin conditioned *Ext1*-KO mice which also does not survive postnatally, however these embryos are reported to grossly look normal (Inatani *et al.*, 2003). Even though BLBP expression is restricted in the nervous system in adults, *BLBPCre-RosaTom* mice showed reporter expression in the early limb buds. Thus, the most likely explanation for the severely impaired limb development phenotype we observed is due to the transient expression of BLBP during limb development. This skeletal defect allowed us to distinguish mutant mice from heterozygous or WT littermates without PCR genotyping. Embryos were collected from time mated females between E16- 21 for future experiments.

3.3.2 Cell culture and reagents

Olfactory Epithelium (OE) OECs were obtained via fluorescence activated cell sorting (FACS). Unless otherwise stated, OB derived OECs were used for the experiments as previously described (Dairaghi *et al.*, 2018). Briefly, olfactory bulbs of postnatal (PN) day 0-7 mice were collected and enzymatically digested at 37^0C for 35 min using 30µg/ml hyaluronidase (Sigma, Cat# H3631, St. Louis, MO), 30U/ml dispase I (Sigma, Cat# D4818), 1.2 mg/ml collagenase type 4 (Worthington, Cat# 43E14231, Lakewood, NJ), 10U/ml DNAse I (Worthington, Cat# 54E7315) (Au & Roskams, 2003; Richter *et al.*, 2008). Enzymes were deactivated by adding fresh medium (DMEM:F12) and the cell suspension was centrifuged for 7 minutes at 1000rpm. The cell pellet was resuspended in fresh medium and the cells were run through a 40-micron cell strainer (Falcon) before the three steps of differential cell adhesion method (Nash *et al.*, 2001). Initially cells were seeded into uncoated T75 flasks ($4x10^6$ viable cells/flask, VWR, Cat# 734-2788, Radnor, PA) for 18 hrs. This initial seeding helps to remove fibroblasts. Unattached cells were collected and seeded into another uncoated flask for up to 36 hrs to remove astrocytes, followed by a final step where unattached cells were seeded onto poly-L-lysine (Sigma, Cat# P4707)-coated flasks to grow primary OECs. The first medium was changed at day 4 and every 2-3 days after the initial medium change. Cells were cultured for up to 2 weeks. More than 90% of the cells in the culture were OECs based on p75 and S100ß immunostaining consistent with earlier reports (Au & Roskams, 2003). For OECs to be co-cultured with primary astrocytes, the medium was gradually changed to serum-free medium (Klenke & Taylor-Burds, 2012) supplemented with 5ng/ml HB-EGF (PeproTech, Cat# 100-47, Rocky Hill, NJ), and B27 (Thermo Fisher Scientific, Cat# A3582901) to provide a medium compatible with astrocyte cultures, since serum has been shown to induce astrocyte reactivity (Foo *et al.*, 2011).

Primary astrocytes were obtained by magnetic sorting as previously described (Holt *et al.*, 2019), with some modifications. Briefly, 10-20 cortices of PN day 2-4 pups were dissociated using the MACS Neural Tissue Dissociation Kit-T (Miltenyi Biotec, Cat# 130-093-231, Auburn, CA) at 37^0C (5% CO^2, 30 min). Non-dissociated tissue was removed using a 40µm cell strainer (Fisher Scientific, Cat# 22-363-547), and the remaining cell solution was centrifuged (300g, 5 min). Next, a discontinuous density gradient, prepared using 1:1 albumin-ovomucoid solution (10mg/ml of each) (Worthington, Cat# OI; GeminiBio, Cat# 700-102P, West Sacramento, CA), was used to remove cell debris and inhibit enzyme activity. The cell pellet was resuspended in 80µl Hank's Balanced Salt Solution (HBSS) (Gibco, Cat# 14025-092) plus 20µl anti-GLAST (ACSA-1) MicroBeads (Miltenyi Biotec, Cat# 130-095-825, Auburn, CA) for up to 10^7 cells, and incubated for 10 min (4^0C). Cells were washed and incubated in 90µl HBSS plus 10µl anti-Biotin MicroBeads for another 15 min (4^0C) before running through MACS column for positive selection of astrocytes. Cells were cultured for one week and then the same procedure was followed with anti-Prominin-1 MicroBeads (Miltenyi Biotec, Cat# 130-092-564) for the negative selection of radial glia, followed by another positive selection with anti-GLAST antibody the same day, to increase the purity of astrocyte cultures. Sorted cells were cultured in T25 flasks coated with poly-L-lysine, in 5ml serum-free astrocyte culture medium (ACM, described above). In our hands, astrocytes isolated by this method and cultured in ACM were not reactive when stained with NFκB (not shown). The immortalized mouse astrocyte line C8D30 (ATCC, VA, USA) was cultured in DMEM-F12 (Gibco, Cat# 10313-02, 11765-054, Long Island, NY) containing 10% Fetal Bovine Serum (FBS) (Gibco, Cat# 10438-026), plus 0.5% antibiotic-antimycotic (Gibco, Cat# 15240-062) at 370C in 5%CO2. FGFR1 inhibitor SU5402 (Tocris, Cat# 3300) was

used at 30nM and PD173074 (Tocris, Cat# 3044) was used at 20nM. Inhibitors were added 1 hr before the 2 hr LPS treatment.

3.3.3 Collection and heparinase treatment of OEC-CM

Once primary OECs reached 70% confluency, medium was replaced with fresh medium and collected 24 hours after. This OEC-conditioned medium (OEC-CM) was spun down (30 min) to remove cell debris and then directly used on astrocyte cultures unless otherwise stated. For the heparinase treatment, primary OECs were gradually adapted to serum free medium (ACM) prior to medium collection. Heparin containing proteins in OEC-CM were digested as previously described (Higginson *et al.,* 2012) with slight modifications. Briefly, the OEC-CM received 3 consecutive treatments of a cocktail of Heparinase I and III (Sigma, Cat# H3917) and Heparinase II (Biolabs, Cat# SP0736S), containing 3mU/ml of each heparinase enzyme. The first treatment was for 10 hrs (37°C). The second treatment was for 24 hrs (37°C) and the final treatment was for 5 hrs (37°C). The conditioned medium was then mixed 1:1 with serum containing medium (DMEM-F12 + 10% FBS) to inactivate the enzymes and added on to immortalized C8D30 astrocytes for 24 hrs. The last 2 hours of this incubation, cells were stimulated with LPS as described earlier. Nuclear compartments of astrocytes were isolated, and immunoblotting was performed (described below).

3.3.4 Primary antibodies

The following antibodies were used: NFκB rabbit polyclonal antibody (C-20, Santa Cruz, Cat# sc-372, Santa Cruz, CA, 1:650 for WB, 1:750 for IF); Histone mouse monoclonal antibody (Fisher Scientific, Cat# AHO1432, Waltham, MA, 1:200 for WB); Sox10 goat polyclonal antibody (N-20, Santa Cruz, Cat# sc-17342, 1:300 for IF); FGFR1 mouse monoclonal antibody (Santa Cruz, Cat# sc-57132, 1:1K for IF); FGFR1 rabbit polyclonal

antibody (Abcam, Cat# ab10646, 1:400 for WB); FGFR1 (phospho-Tyr653/654) rabbit polyclonal antibody (Cell Signaling, Cat# 3471, 1:1K for IF); FGFR1 (phospho-Tyr766) rabbit polyclonal, biotinylated antibody (Biorbyt, Cat# orb501512, 1:50 for IF); O4 mouse monoclonal antibody conjugated to APC (Miltenyi Biotec, Cat# 130-119-155, 1:50 for FACS); F4/80 mouse monoclonal antibody conjugated to PE-Cyanine7 (Invitrogen, Cat# 25-4801-82, 1:50 for FACS); CD45.2 mouse monoclonal antibody conjugated to FITC (BioLegend, Cat# 109805, 1:100 for FACS); pERK mouse monoclonal antibody (Millipore, Cat# M8159, Darmstadt, Germany) was used at 1:5K for WB; GFAP chicken polyclonal antibody (Aves, 1:4K for IF); p75-NGFR rabbit polyclonal antibody (Millipore, Cat# AB1554, 1:5K for IF) and p75-NGFR goat polyclonal antibody (R&D Systems, Cat# AF1157, 1:200 for FACS).

3.3.5 FACS

Dissociated OE tissue obtained from WT (*Ext1*$^{floxed/floxed}$ S100ß-DsRed) and *Ext1*-CKO (*Ext1*^{BLBP}KO S100ß-DsRed) E16- 21 mouse embryos was subjected to FACS for single cell sorting of S100ß-DsRed expressing cells. Cells were dissociated using trypsin according to manufacturer's protocol (Miltenyibiotech, Cat#130-093-231) and were filtered through 35mm cell strainers (Falcon, Cat#352235) to remove cell clumps before sorting. The single cell suspensions were then incubated with 1mg/ml DAPI (1:500, Thermo Scientific, Cat#62248) for a few minutes to label dead cells before loading samples to FACS (MoFlo Astrios EQ high speed cell sorter; Beckman Coulter). Flow data setting of sorting gates on DsRed-expressing cells that are DAPI-negative were carried out using Summit software V6.3.016900 (Beckman Coulter). Determination of the optimum time point for sorting after dissociation was established using antibodies against OECs (p75-NGFR or O4-APC) and tissue resident

macrophages (F480 and CD45.2). For OE cell dissociates that were sorted on the day of dissociation (acute sorting), trypsin was preferred instead of papain in order to preserve the F4/80 epitope. However, trypsin dropped the cell viability (from ~70% to 40%). Moreover, acute sorting revealed that a considerable percentage of S100ß-DsRed cells were positive for tissue resident macrophage markers (also called monocytic cells, Smithson & Kawaja., 2010) (Chart 1). However, these cells were eliminated when the cell suspension was plated and maintained in serum containing culture medium (Bohlen *et al.*, 2017) for 25-35 days (DIV). In addition, these established cells were more resilient against trypsin. As can be seen in Chart 1, both cell viability and the percentage of S100ß-DsRed positive OE cells that were OECs dramatically increased when the cells were sorted after culturing. The purity of OECs (S100ß-DsRed+ cells) obtained by FACS after culturing was similar to our primary OEC cultures obtained via differential-attachment method described above. Therefore, for future experiments, primary OECs were obtained via FACS from embryonic OE cultures (25-35 days DIV) by relying solely on the S100ß-DsRed signal. Following this protocol, typically ≥1K cells were obtained from 4 mouse embryos. After sorting, cells were grown for ~1 week on poly-L-lysine (Sigma, Cat# P4707)-coated flasks before conducting experiments.

Chart 1	Live cells (% of All)	S100ß + cells % of Hist	S100ß – cells % of Hist	S100ß + cells that are OECs % of Hist	S100ß + cells tissue resident macrophages % of Hist
E18 OE Acute sorting	36.39%	8.11%	88.61%	7.79%	65.82%
E18 OE Sorted at 31 DIV	78.02%	25.28%	75.21%	85.48%	0.1%

3.3.6 Immunoblot analysis

Nuclear fractions of immortalized C8D30 astrocytes were used for quantitative immunoblot analysis. To be able to collect astrocytes alone for the analysis, OECs were cultured on porous inserts (0.4μm Millicell Cell Culture Insert, Millipore, Cat# PICM0RG50), that were discarded at the end of the experiment. For the CM treated groups, OEC-CM was collected (24 hr-old medium). Treatment was 24 hours for all groups and the last 2 hours of this incubation, all groups were stimulated with 1μl/ml LPS (Sigma, Cat# L6529). Astrocytes were then scraped and the CNMCS Compartmental Protein Extraction Kit (BioChain Cat# K3013010 Hayward, CA) plus protease/phosphatase inhibitors (PI, Cell Signaling, Cat# 5872S, Danvers, MA) was used for the nuclear fractionation of each treatment condition. The fractions were run on BioRad Mini-Protean TGX Stain-Free Gels (Cat#4568084), transferred to PVDF stain-free blot (Trans-Blot Turbo Transfer Pack, Cat#1704156) via the Trans-Blot Turbo transfer system (BioRad), and blocked with 5% dry milk (BioRad, Cat #170-6404) prior to staining with NFκB, FGFR1 or pErk1/2 antibodies. Membranes were exposed to Clarity enhanced chemiluminescence (ECL) reagent (Cat. # 170–5061, Bio-Rad) for 5 min and the signal was detected using ChemiDoc MP (Cat. # 170–8280, Bio-Rad). Quantification of band intensities was calculated using Image Lab 5.0 software (Bio-Rad) and normalized by the loading control Histone.

3.3.7 Quantitative immunofluorescence

Following immunofluorescence staining for antibodies of interest, confocal images were taken on Zeiss LSM 800 Confocal Microscope (Carl Zeiss, Thornwood, NY). Imaging was done on a single plane and the same parameters (gain, pin size, etc.) were used between the groups while imaging. On the images, intensity median for each channel that overlaps with

FGFR1 staining (magenta, threshold=30) was calculated using Imaris software. Statistics (two-way ANOVA) were performed and the average median value ±standard deviation (SD) per treatment plotted. To calculate the covariance of two fluorescent signals independently of fluorescence intensity, pixels colocalized or Pearson's colocalization coefficient was used. For quantifications, the thresholds were determined automatically using Imaris 9.1.0; based on the maximum threshold of intensity for each channel that shows any statistical correlation (Costes *et al.*, 2004). Fiji was used for the quantification of factorial Markov random field (FMRF) signal on a single plane and the FGFR1 signal was scaled up x3 to enable selection of individual spots of correlation.

3.3.8 Cell proliferation

Cell proliferation was analyzed continually every day over a period of up to 3 days using the Alamar blue assay (Nikolaychik *et al.* 1996) and 50ng/ml FGF2 was used to stimulate the cells. Briefly, at the day of measurement, the cells were rinsed with PBS and then incubated for 2 hr with their respective growth medium supplemented with 5% Alamar blue reagent (Thermo Fisher Scientific, Cat# DAL1025). At the end of incubation time, supernatant was collected and Alamar blue absorbance was measured (NanoDrop, Thermo Fisher Scientific), using the appropriate filter set (570 nm and 600 nm). The data, expressed as means ± SD, are presented in arbitrary fluorescence units.

3.3.9 Quantitative RT-PCR (q-RT-PCR)

cDNA synthesis was performed using Superscript™ III reverse transcriptase (Invitrogen), and PCR carried out using the ViiA7 Real-Time PCR System (Applied Biosystems, Waltham, MA) in 20µl final volume, containing 10µl of SsoAdvanced Universal SYBR Green Supermix (BioRad Cat#1725271), 2µl of primer mix (1µM of each primer) 1µl of cDNA and 7µl water.

For samples that were mixed with FGFR1 primers, a different template was used containing 3µl of cDNA and 5µl water. Samples were run in triplicate. The expression levels of FGFR mRNA were determined using primers (forward; reverse) TCTGGAAGCCCTGGAAGAGAGA; TCTTAGAGGCAAGATACTCCAT for FGFR1 (Verheyden *et al.*, 2005), CAAAGGCAACTACACCTGCC; CAGCCATGACTACTT-GCCCG for FGFR2 (Yu *et al.,* 2003), GCTGTAGGCTTAACACTTCC; GCTGACAAACCATGTGCTAGG FGFR3, GGACTAGCTGCAAAACTTATGC; CCATGTCTTCTGTCGTTCC for FGFR4 and were normalized using the primers (forward; reverse) (AGTGCCAGCCTCGTCCCGTA; TGAGCCCTTCCACAATGCCA), for expression of GAPDH. Data were analyzed by a one-way ANOVA followed by Dunnett's multiple post hoc test.

3.3.10 Statistical analysis

All statistical analyses were done using GraphPad Prism 8.00 software. The results are shown as mean ± SD. Statistical analysis was performed using one-way or two-way ANOVA, unless otherwise stated. Probability values of 0.05 ($p \leq 0.05$) were considered to indicate statistical significance. N=biological replicates, n=technical replicates.

3.4 Results

3.4.1 OEC-HSPGs suppress harmful astrocyte reactivity and promote astrocyte differentiation.

Previous studies, as well as our own work (see Chapter 2) shows that OECs secrete anti-inflammatory factors that reduce neurotoxic-astrocyte reactivity. Expression of neurotoxicity associated genes in astrocytes are understood to be mediated by the pro-inflammatory factor NFκB (Lian *et al.*, 2015; Liddelow *et al.*, 2017). In contrast, recovery-promoting astrocytes are mediated by activation of STAT3, a transcription factor (TF) shown to moderate reactivity and support differentiation of astrocytes (Anderson *et al.*, 2016; Hong & Song, 2014). We analyzed mRNA expression of immortalized C8D30 astrocytes for NFκB and STAT3 2 hr after LPS exposure, with or without OEC-cultured inserts. As expected, NFκB expression was blocked by factors secreted from OEC-cultured inserts. Moreover, OEC-secreted factors increased STAT3 expression (Figure 1A). These results indicate that OEC-astrocyte crosstalk suppresses early transcriptional changes associated with neurotoxic astrocytes and upregulates changes associated with neurorepair-promoting astrocytes. Here, this crosstalk was used to characterize FGFR1 downstream targets that play a role in astrocyte reactivity. First, mRNA expression of different FGFR subtypes at this time point was examined (Figure 1B). Studies suggest that FGFR3 and FGFR2 upregulation correlates with glial lineage commitment while FGFR1 is crucial for both self-renewal and differentiation (Maric *et al.*, 2007; Zhang *et al.*, 2015;). Our results show that under LPS-induced stress conditions, astrocytes cultured with OECs express significantly higher FGFR expression for FGFR1-3, but not 4. The absence of increased FGFR4 expression is not surprising given it is expressed mostly during development (Lichtenstein *et al.*, 2012) (Figure 1A, 1B). Notably FGFR1 expression increased over 100-fold

in the presence of OECs (Figure 1B). In accordance to the observed increase in STAT3; FGFR2 and FGFR3 expression were also significantly upregulated, pointing out increased astrocyte differentiation (Hong & Song, 2014; cite FGFRs).

To assess whether the change in FGFR1 activity plays a role in the suppression of harmful TFs in astrocytes, two different inhibitors to block receptor tyrosine kinase (RTK) activity, 30nM SU5402 or 20nM PD173074, were used. Stimulation with LPS treatment for 2 hrs increased nuclear translocation of NFκB in astrocyte monocultures (Figure 9C, left panel). Addition of neither FGFR1 inhibitor impacted nuclear NFκB translocation, but significantly slowed the proliferation of C8D30 cells measured by a viability test consistent with earlier reports (Reilly *et al.*, 2004). Presence of OECs (distinguished by Sox10 staining, Figure 9C middle panel) blocked the inflammatory reactivity in C8D30 cells stimulated with LPS (arrowheads, middle panel, notice weak nuclear NFκB staining). However, this effect disappeared when FGFR1 activity was chemically inhibited using SU5402 (arrowheads, right panel) or PD173074 (data not shown). These results are consistent with our hypothesis that astrocyte FGFR1 signaling, activated via OEC secreted factors, suppresses harmful astrocyte reactivity and support a more differentiated phenotype in astrocytes.

Candidates for the OEC-secreted factors, enabling observed changes in astrocyte reactivity via FGFR1 1) should be secreted into the extracellular space, and 2) act as FGFR co-receptors and moderate downstream signaling. Heparan sulfate proteoglycans (HSPGs) are strong candidates for such OEC-secreted factors since they are cell-specific ECM proteins known to support and regulate FGF signaling; and have been suggested to play a role in suppressing astrocyte reactivity (Higginson *et al.*, 2012). To examine the contribution of OEC-HSPGs, we enzymatically degraded secreted HSPGs in the OEC conditioned medium with heparinase

(OEC-CM). Heparinase-treated (Hase) OEC-CM (see material & methods) failed to block nuclear NFκB translocation in astrocytes, as measured by quantitative immunoblotting in nuclear fractions of C8D30 cells (Figure 9D). To confirm these results, transgenic animals with conditional ablation of the HSPG-synthesizing enzyme Ext1 (Irie *et al.,* 2012; Yamaguchi *et al*., 2010) in OECs ($Ext1^{BLBP}KO$) were used. $Ext1^{BLBP}KO$-OECs (± WT OEC-CM) and WT-OECs were grown on hanging inserts and moved to multi-well plates containing C8D30 astrocytes 24 hrs before the experiment. Cells were treated with LPS for the last 2 hours of this incubation. Inserts were discarded at the end of experiment and nuclear fractions of C8D30 cells were collected for immunoblotting. Factors secreted from WT OECs on inserts brought nuclear NFκB levels down, comparable to the control group (Figure 9E). Similar to HaseOEC-CM, $Ext1^{BLBP}KO$-OECs failed to block nuclear NFκB translocation in astrocytes. Notably, addition of WT OEC-CM to astrocytes co-cultured with $Ext1^{BLBP}KO$-OECs also showed NFκB levels comparable to the control group, ruling out the role of negative factors that may have been upregulated by conditional ablation of HSPG in OECs (Figure 9E). These results are consistent with our hypothesis that observed changes in astrocytes are mediated by OEC-secreted HSPGs.

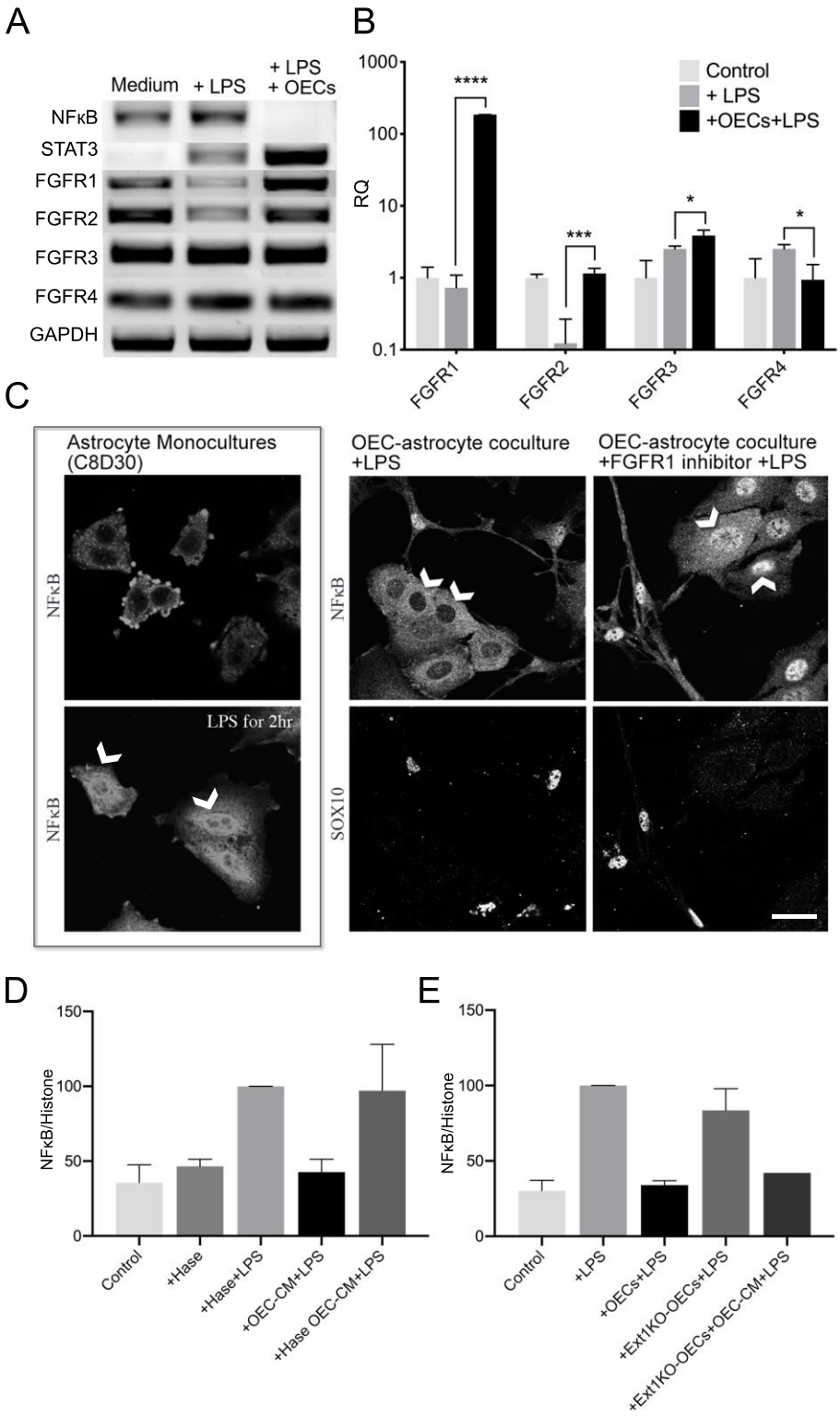

Figure 9: Role of HSPGs in OEC-dependent suppression of astrocyte reactivity via FGFR1. (A) Representative images show mRNA expression of 6 transcript of interest in immortalized C8D30 astrocytes 2 hr after LPS exposure, with or without OECs. Presence of OECs blocked expression of pro-inflammatory TF NF𝓀B and increased expression of STAT3.

(B) In the presence of OECs, quantitative PCR revealed increased expression for all FGFR subtypes, but developmental subtype FGFR4, in cultured C8D30 astrocytes 2 hr after LPS exposure (n=3, one-way ANOVA ($F(2, 6) = 297732$, $P<0.0001$ for FGFR1; $F(2, 6) = 35.86$, $p=0.0005$ for FGFR2; $F(2, 6) = 16.35$, $p=0.0037$ for FGFR3; $F(2, 6) = 6.153$, $p=0.0352$ for FGFR4 * $p \leq 0.05$, *** $p \leq 0.001$, **** $p \leq 0.0001$; followed by Dunnett's multiple comparisons test). (C) Immunofluorescence staining of C8D30 astrocytes treated with LPS for 2 hr (left bottom) shows nuclear NFκB translocation compared to untreated astrocytes (left top image). In contrast, LPS treated OEC-astrocyte co-cultures block NFκB translocation (middle). This effect is lost when co-cultures treated with FGFR1 inhibitors (right). Bottom middle and right panels images show OEC nuclei stained with neural crest marker Sox10. (D) Heparinase-treated (Hase) OEC-CM+LPS impaired OEC-astrocyte crosstalk measured by nuclear NFκB; relative to control OEC-CM+LPS (N=2). C8D30 astrocytes were treated with OEC-CM for 24 hr. Cells were exposed to 1μg/ml LPS for the last 2 hours of this treatment. Nuclear fractions of astrocytes were analyzed via quantitative immunoblotting for NFκB. (E) Ext1KO-OECs fail to prevent nuclear accumulation of NFκB ($N \leq 2$). Scale bar represents 30μm.

3.4.2 FGFR-1 signaling differentially activates primary astrocytes cultured in OEC-CM

FGF/FGFR signaling pathways have been proposed to differentially regulate proliferation and differentiation of cells through interactions with downstream targets (Figure 10A). Our results suggest that OEC-secreted factors support astrocyte differentiation via FGFR1 in a HSPG dependent mechanism. To investigate the regulation of FGFR1 phosphorylation sites as a possible target of astrocyte-fate regulation we isolated primary astrocytes and challenged in the presence of OEC-secreted factors.

Tyrosine autophosphorylation of FGFR1 induced by extracellular cues can occur on seven phosphorylation sites: Y463, Y583, Y585, Y653, Y654, Y730, and Y766 (Figure 10A). Structural and biochemical studies have shown that, FGFR1 phosphorylation sequence follow a precise order independent of the proximity of these tyrosines to each other (Mohamadi *et al.*, Bae *et al.*, 2009; Furdui *et al.*, 2006). The identity and the ratio of tyrosines phosphorylated along this activation determines which proteins are recruited and pathways are stimulated (Furdui *et al.*, 2006).

Activation by FGFR-1 leads to the phosphorylation of fibroblast growth factor receptor substrate 2 (Frs2a) on several sites that results in activation of extracellular signal regulated kinase 1/2 (Erk1/2), which is necessary both for self-renewal (Ma *et al.*, 2009) and for differentiation (Lanner & Rossant., 2010). Briefly, FRS2a, Src homology region 2 domain containing phosphatase 2 (Shp2; also known as Ptpn11) and growth factor receptor-bound protein 2 (GRB2) complex initiates son of sevenless homology (SOS)-RAS activation (Figure 10A). RAS protein activation regulates multiple downstream pathways of which one is included in the schematic model: MEK-Erk1/2 pathway. This pathway can be activated via FGFR1 kinase function on the activation loop Y653/Y654. Both phospholipase-C γ (PLCγ) and SH2 domain-containing adapter protein-B (Shb) bind to phosphorylated Y766 (serves as a docking site) following FGF/FGFR1 signaling and result in the activation of PKC. Shb can also regulate FRS2 phosphorylation via Shp-2. Other structural motifs may also activate the FRS2/Ras pathway (Cross *et al.*, 2002). These pathways can directly or indirectly regulate numerous genes via activation of transcriptional factors. The balance between their phosphorylation levels induce the expression of cell proliferation, survival and differentiation related genes; in a cell type and stimulus dependent manner (Zarubin & Han., 2005).

The Erk1/2 is pathway is most well-known for its mitogenicity. In contrast, PLCγ is not responsible for cell proliferation (Mohammadi *et al.*, 1992; Peters *et al.*, 1992) but maintains differentiation (Ma *et al.*, 2009). Thus, antibodies recognizing specific phosphorylation sites for Erk1/2 (Y653/654) and PLCγ (Y766) were used to evaluate differential FGFR1 activation in the presence of OEC-secreted factors. GFAP positive primary astrocytes (Figure 10 B-D magenta), ±LPS ±OEC-CM, were stained with anti-pY653/654 antibody (red) and anti-pY766 antibody (green) (Figure 10B-D). In the control group (Figure 10B), pY653/654 signal

was detected throughout the cell, including the perinuclear area (Figure 10B, red). In contrast the signal was less robust and appeared diffuse and distant from the nucleus following LPS treatment (Figure 10C, red). The signal appeared more clustered in astrocytes cultured with OEC-CM +LPS (Figure 10D, red). Notably, astrocytes cultured with OEC-CM showed enhanced phosphorylation on Y766 (Figure 10D, green) compared to control and also LPS-stimulated astrocytes Figure 10B and C).

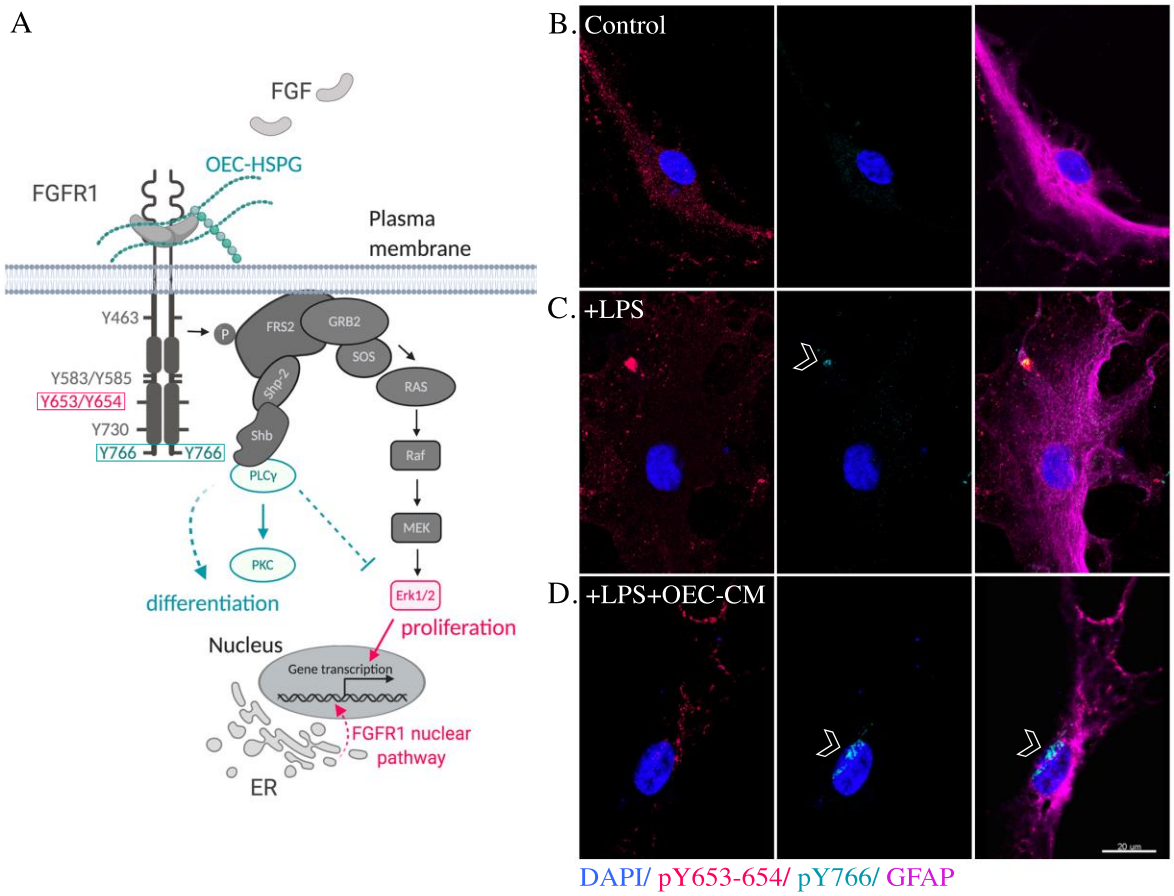

Figure 10: Differential FGFR-1 signaling in GFAP positive primary astrocytes. (A) Schema summarizing the functional outcomes of differential FGFR-1 signaling in astrocytes demonstrating how the presence of OEC-HSPGs can change astrocyte fate decision (shown in green; HSPG-pY766-PLCγ/PKC-differentiation). The schema was adapted from Cross *et al.,* 2002; and created using biorender. (B) Differential FGFR1 signaling in GFAP positive(magenta) primary astrocytes (B) compared to (C) primary astrocytes+ LPS or (D) LPS+OEC-CM visualized with phosphorylated FGFR1 Y653/654 (red) or Y766 (green) antibodies. Primary astrocytes cultured with OEC-CM show enhanced phosphorylation at Y766 (D, open arrowheads)(N=2).

3.4.3 OEC-CM stabilizes FGFR1 signaling at pY766.

Next, C8D30 astrocytes were used to quantify differential FGFR1 signaling in response to LPS ±OEC-secreted factors (Figure 11). Cells were stained with antibodies against phosphorylated FGFR1 Y653/654 (red), Y766 (green), FGFR1 (magenta) and DAPI. C8D30 astrocytes showed a similar pattern to primary astrocytes (Figure 11A). Quantifications for each antibody (normalized to control value for each channel) confirmed that 1) Y653/654 phosphorylation in +LPS +OEC-CM group (Figure 11B, red rhombus) was lower, compared to either +LPS (Figure 11B, red triangle), or control groups (Figure 11B, red circles) and 2) Y766 was significantly increased in +LPS +OEC-CM group (Figure 11B, green rhombus) compared to control (Figure 11B, green circles). In accordance, quantitative immunoblotting performed on the nuclear fraction of C8D30 astrocyte lysates showed that pErk1/2 was significantly suppressed by the presence of OECs cocultured on hanging inserts, confirming the observed suppression on pY653/654 reflects Erk1/2 phosphorylation (Figure 11B, inset).

Erk1/2 phosphorylation is linked to different outcomes of cellular fate. While some studies indicate that Erk1/2 signaling suppresses self-renewal, (Li *et al.*, 2006, Chan *et al.*, 2013, reviewed in Lanner & Rossant, 2010); other studies show that it is involved in regulating proliferation (Ma *et al.*, 2009). Hence, the Alamar blue test was performed on C8D30 astrocytes ±FGF2 ±OECs (Figure 11C). This widely used viability test is often interpreted as a readout of cell proliferation. Higher proliferation rates in astrocyte monocultures that were treated with 50ng/ml FGF2 were observed (Figure 11C, grey triangles), consistent with previous studies (Gomez- Pinilla *et al.*, 1995). The presence of OECs neutralized this effect (Figure 11C, green rhombus).

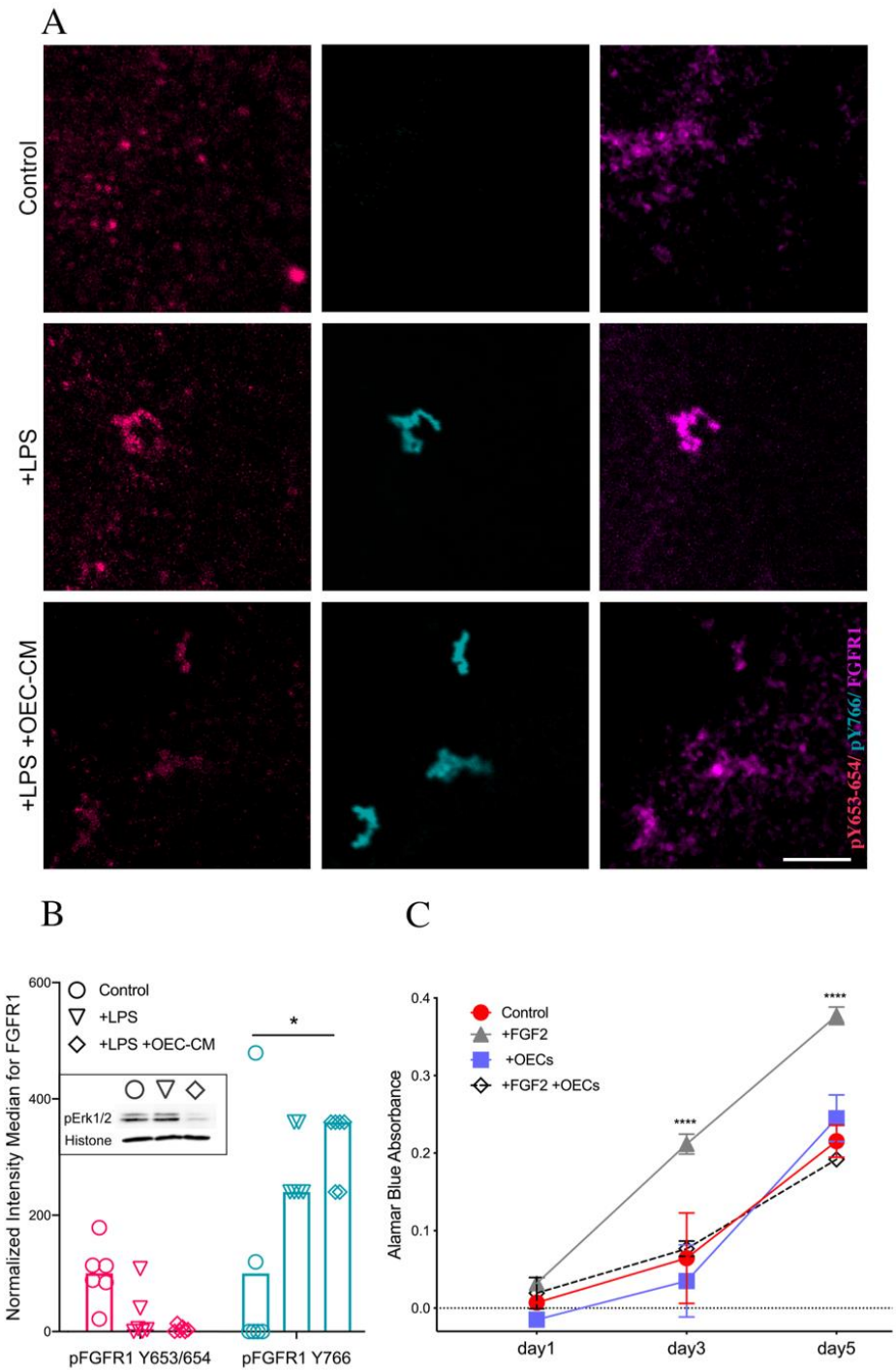

Figure 11: OEC-CM preferentially stabilizes pY766 FGFR1 signaling. (A) Representative images of differential FGFR1 signaling in immortalized astrocyte line C8D30 in response to LPS or LPS+OEC-secreted factors, stained with phosphorylated FGFR1 Y653/654 (red), Y766 (green), FGFR1 (magenta) and DAPI. (B) Quantification of differential FGFR1 signaling in C8D30 line shows lower FGFR1 phosphorylation at Y653/654 and significantly higher phosphorylation at Y766 compared to control. Notably LPS-induced stress signal significantly increased intensity median for nuclear signal colocalized with FGFR1 and

presence of OEC-CM suppressed this increase (N=3, * $p \leq 0.05$; two-way ANOVA). C8D30 astrocytes with or without OECs for 24 hours were exposed to 1μg/ml LPS for the last 2 hours of this treatment. Nuclear fractions of astrocytes were analyzed via immunoblotting for NFκB, FGFR1 and pErk1/2. While LPS treatment upregulated NFκB translocation in astrocyte monocultures, the presence of OECs blocked this effect. (Figure 9B inset) (C) Viability test results on C8D30 line treated with FGF2 showed significantly increased proliferation for +FGF2 group (gray line, triangle), while the presence of OECs neutralized this effect, consistent with the suppression of FGFR1 pY653/654 signaling (green line, rhombus) (N=3, **** $p \leq 0.0001$; two-way ANOVA).

3.4.4 Role of OEC-HSPGs for astrocyte intracellular FGFR1 trafficking.

To further quantify differential FGFR1 signaling in Figure 11B (magenta), intensity median for DAPI that overlaps with FGFR1 was calculated (Figure 12A, left). Intensity of the DAPI signal (normalized to control group) showed a significant increase following LPS treatment, and this increase was suppressed by the presence of OEC-CM. Next, we asked whether the same pattern applies when the colocalization is quantified for FGFR1 and DAPI by pixels colocalized (Figure 12A, middle) or by the Pearson's colocalization coefficient (Figure 12A, right). These two quantifications showed no significant difference between treatments, suggesting that the observed increase in intensity median for DAPI, colocalized with FGFR1, may be due to its colocalization on brighter DAPI-stained regions within the astrocyte nuclei. Histones block the access of DAPI to DNA, therefore, heterochromatin loci are known to show weaker DAPI staining, while in the euchromatin loci, DNA is open and ready for transcription, revealing DAPI binding sites in the DNA (De Cecco *et al.*, 2011). Thus, the observed difference in the quantifications related to nuclear FGFR1 & DAPI may be a consequence of differential association of FGFR1 with DNA under different treatments. A second analysis was made by setting the threshold to select euchromatin loci (using DAPI signal) which had a similar distribution, where LPS treatment augmented FGFR1 in the

euchromatin, although not significant (p= 0.34). We also observed a non-significant increase in overall DAPI signal in LPS stimulated cells. Thus, whether the increased DAPI intensity (colocalized with FGFR1) in the presence of LPS-induced stress is due to a change in chromatin organization or FGFR1 trafficking to the euchromatin loci remains to be determined.

Next, the nuclear fractions of astrocytes were analyzed by quantitative immunoblotting against FGFR1. A significant increase in nuclear FGFR1 in the LPS treated group was detected (Figure 12B). In accordance with previous observations (Irschick *et al.*, 2013., Stachowiak *et al.*, 2015; Stachowiak *et al.*, 2016), neither stimulation of membrane FGFR signaling by FGF2 nor the inhibition by FGFR inhibitor SU5402 cause nuclear accumulation of the receptor. Moreover, SU5402 did not prevent the observed nuclear FGFR1 accumulation in the presence of LPS, consistent with earlier reports (Reilly *et al.*, 2004), providing further evidence that the LPS-induced stress signal itself is the primary cause for the nuclear FGFR1 accumulation. LPS-induced increase in nuclear FGFR1 was suppressed in the presence of OECs but not $Ext1^{BLBP}$KO-OECs. Notably addition of WT OEC-CM was sufficient to suppress the increase observed in the astrocytes cocultured with $Ext1^{BLBP}$KO-OECs (Figure 12B). Glycosylation of proteins causes a size change with varying degrees, preventing the total amount to be detected via immunoblotting. In contrast, the total protein can still be detected via immunostaining. Considering that nuclear colocalization of FGFR1 and DAPI (either by pixels colocalized or by the Pearson's colocalization coefficient) was similar between different treatment groups, we hypothesize that the differences in quantitative immunoblots reflect non-glycosylated forms of FGFR1. This may also explain how OEC

secreted HSPGs may play a role in intracellular FGFR1 trafficking in astrocytes, and their association with the DNA.

To further assess our hypothesis that injury signal increasing nuclear FGFR1 association with DNA in the euchromatin, the colocalization of FGFR1 as a function of DAPI intensity was quantified (Figure 12C). In the control group, FGFR1 was predominantly located in heterochromatin loci (arrowheads) where DAPI signal is weaker (left image). FGFR1 was observed to colocalize with bright euchromatin regions following LPS treatment, indicating that regions of DNA that are available for active transcription are associated with FGFR1 (middle image, arrowheads). In the presence of OEC-CM; FGFR1 showed a similar pattern to controls, colocalized with regions of low DAPI signal, indicative of condensed chromatin that is not available for transcription (right image, arrowheads). To quantify this, a plane was selected based on strongest distribution of the FMRF signal per image (Figure 12C, dashed lines). Quantification of the fluorescence intensity for DAPI (blue) and FGFR1 (yellow) on these planes showed FGFR1 signaling was correlated with DAPI intensity in LPS treated group (overlap of blue/yellow lines in bottom middle panel). These findings suggest the association of FGFR1 with DNA may explain how astrocytes dedifferentiate in the presence of LPS-induced stress signal; and are consistent with the role of FGFR1 as a master regulator of transcription. Whether such association can be responsible for the harmful astrocyte reactivity is an interesting hypothesis for future investigations.

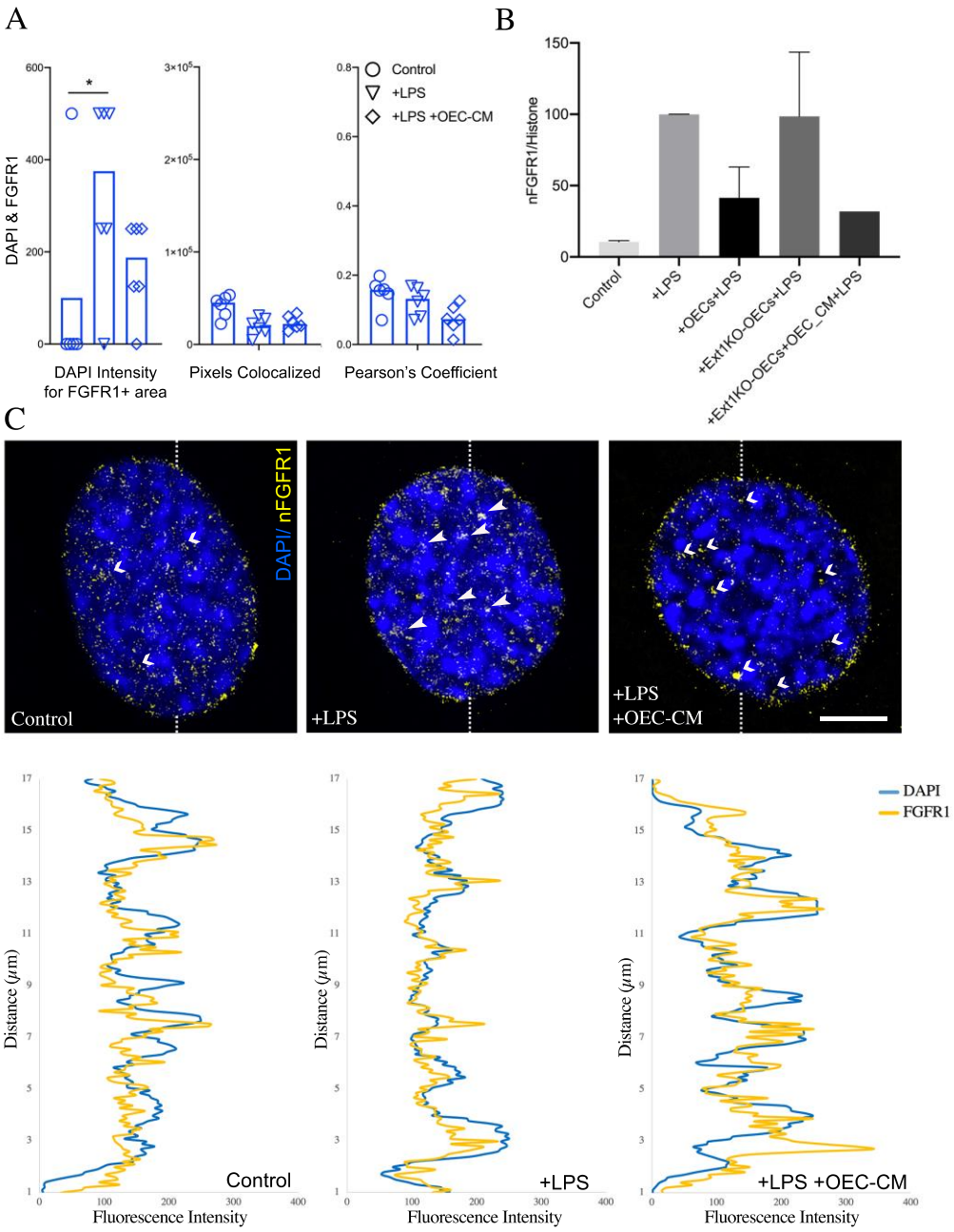

Figure 12: OEC-HSPGs limit intracellular FGFR1 trafficking to the euchromatin in astrocytes. (A) Intensity of the DAPI signal that overlaps with FGFR1 showed a significant increase following LPS treatment, and this increase was suppressed by the presence of OEC-CM (left panel). In contrast, when the colocalization of FGFR1 and DAPI was quantified by pixels colocalized (middle) or Pearson's colocalization coefficient (right), no difference between treatments was observed. Astrocytes were treated with OECs or OEC-CM for 24 hours. Cells were exposed to 1μg/ml LPS for the last 2 hours of this treatment. Nuclear fractions of astrocytes were analyzed via quantitative immunoblotting for FGFR1. (B) Astrocytes cocultured with WT OECs, but not Ext1KO-OECs, attenuated nuclear accumulation of FGFR1. Addition of WT OEC-CM to HSPG-devoid OECs was sufficient

to prevent nFGFR1 accumulation, proposing a role for OEC-HSPGs in intracellular FGFR1 trafficking in astrocytes (N≤2). (C) Immunofluorescence staining for FGFR1 localized in nuclear region of astrocyte was assigned to yellow signal via Imaris. In the control group, FGFR1 signal was mostly located in heterochromatin loci (arrowheads) where DAPI signal is weaker (left image). Signal was observed to colocalize with bright euchromatin regions following LPS treatment, indicating active transcription associated with FGFR1 and self-renewal (middle image). Whereas in the presence of OEC-CM; signal showed a similar pattern to control group where FGFR1 did not correlate with euchromatin loci completely, suggesting limited active transcription and a more differentiated state (right image). (D) Quantification of the fluorescence intensity for DAPI (blue) and FGFR1 (orange) on the planes shown with dashed lines on C, show overlap in FGFR1 signal and DAPI rich euchromatin loci.

3.5 Discussion

FGF signaling is important for mediating astrocyte reactivity, but the respective contribution of downstream signaling components is unclear due to compensation/feedback mechanisms between FGFRs and other signaling pathways. In this study, we used OEC-astrocyte crosstalk as a reliable *in vitro* system that can be manipulated to determine FGFR1 downstream targets that take part in astrocyte reactivity. Our results suggest that OECs-secrete factors not only suppress astrocyte reactivity but also induce the expression of differentiation and neuro-repair promoting transcripts in astrocytes, both via FGFR1 in a HSPG-dependent mechanism.

FGFRs have cell–specific functions and show diverse distribution patterns in the nervous system. FGFR1 and FGFR2 knockout mice don't survive past embryonic day (E)7.5-9.5, and E10-11, respectively (Ornitz & Itoh, 2015), and loss-of-function mutations in either gene lead to a reduction in the number of neural progenitors and neurons (Ohkubo *et al.*, 2004). While FGFR3 null animals are viable, these animals show an increased GFAP expression in astrocytes and deficiencies in oligodendrocyte differentiation (Ornitz & Itoh, 2015). In fact, astrocyte specific deletion of FGFR1, FGFR2, and FGFR3 results in embryonic lethality due to severe reduction of cortical progenitors (Kang *et al.*, 2009). In contrast, FGFR4 knockout

mice are viable (Ornitz & Itoh, 2015) and FGFR4 expression in the brain is detectable only in early stages of development (Yazaki *et al.*, 1994, Fuhrmann *et al.*, 1999).

Upregulation of FGFR2 (Maric *et al.*, 2007), and FGFR3 (Zhang *et al.*, 2015; Cahoy *et al.*, 2008) correlates with glial and astrocyte lineage commitment, respectively. The role of FGFR3 is the most characterized FGFR subtype in astrocytes. Astrocytes overexpressing FGFR3 adopt reactive astrocyte characteristics such as increased size, number of branches, and GFAP expression, whereas suppression of FGFR3 activity reverses this phenotype (Kang *et al.*, 2009). Notably, FGFR3 null mice also exhibit reactive astrocyte phenotype with high GFAP expression, indicating an optimal FGFR3 activity or ratio between FGFR subtypes is required for normal development of astrocytes (Oh *et al.*, 2003; Pringle *et al.*, 2003). Hence, astrocyte differentiation requires a balanced signaling via different FGFR subunits.

FGFRs are equipped with different functional domains and binding specificities that can be activated by distinct ligands, along with HSPG coreceptors. FGF signaling, via FGFR1, displays four distinct transduction pathways: 1. the Janus kinase/signal transducer and activator of transcription (JAK/STAT), 2. phospholipase C (PLC)/calcium, 3. phosphatidylinositol 3-kinase (PI3K)/AKT, and 4. mitogen-activated protein kinase/ extracellular signal-regulated kinase (MAPK/ERK) pathways (Dailey *et al.,* 2005). Activation of MAP kinases is a common response to all FGFRs, which turns on a number of TF families. Expectedly, abnormal MAPK signaling is detected in a wide range of cancers and inflammatory diseases. RAS protein activation regulates two downstream pathways: ERK1/2 and JNK & p38. These pathways can directly or indirectly regulate numerous genes via activation of TFs. The balance between MAPK phosphorylation levels induces the gene expression for cell proliferation, survival, and differentiation, in a cell type- and stimulus-

dependent manner (Zarubin & Han., 2005). In primary astrocyte cultures, the proinflammatory activity of transcription factor NFκB, which turns on genes associated with neurotoxic reactive astrocytes, is mediated by p38 (Roy Choudhury *et al.*, 2014). However, stress-activated signal transduction together with nuclear translocation of NFκB is a coordinated event and, in addition to p38, is regulated/balanced by other MAP kinases. In most instances, NFκB translocation inhibits cellular differentiation and also apoptosis, increasing the number of undifferentiated cells (Joyce *et al.*, 2001). In contrast, STAT3 pathway is essential for the maturation of astrocytes during early brain development (He *et al.,* 2005; Kanski *et al.*, 2014; Hong *et al.*, 2014). STAT3 pathway possibly mediate the activation of neurorepair-promoting reactive astrocytes (Liddelow & Barres, 2017).

Here we show that astrocytes cocultured with OECs upregulate STAT3 and downregulate NFκB expression. Under stress, the presence of OECs upregulated all FGFR subunits in astrocytes, except FGFR4, suggesting that OECs secrete factors that not only suppress astrocyte reactivity but also induce the expression of differentiation and neuro-repair promoting transcripts in astrocytes. Our experiments targeting FGFR1 RTK activity indicate membrane signaling to have a role in astrocyte-OEC crosstalk. HSPGs play a regulatory role on FGFR pathway and also on cell-cell communication as secreted ECM proteins. Our experiments investigating the role of FGFR/HSPG pathway in OEC-astrocyte crosstalk show that astrocytes cultured with HSPG-deficient ($Ext1^{BLBP}KO$) OECs remain reactive, measured by nuclear NFκB. Similarly, while OEC-CM was sufficient to block astrocyte reactivity, OEC-CM treated with heparinase failed to do so. These results suggest that OEC-HSPGs, or synthetic heparan sulfate oligosaccharides that mimic OEC-HSPGs, have a therapeutic potential after CNS injury by targeting neurotoxic reactive astrocytes.

HSPGs can be cleaved from the cell membrane and regulate a wide range of intercellular functions by binding to ECM proteins, ligands and also forming complexes with cell surface receptors (Coles *et al.*, 2011), impacting the duration and the strength of the RTK activity (Ornitz & Itoh, 2015). Astrocytes are highly susceptible to local signals coming from other neural niche cells, and accordingly go through morphological, physiological and functional changes; a concept referred to as astrocyte plasticity (reviewed in Prittimaki & Parri, 2013; Khakh & Deneen, 2019). Currently, the criteria that validate astrocyte differentiation are poorly defined and mostly rely on increased complexity in astrocyte morphology (Molofsky *et al.,* 2015). Structural analyses of OB astrocytes show an increasingly complex morphology towards the ONL layer (Chiu & Greer, 1996; Larriva-Sahd 2014; García-Marqués & López-Mascaraque., 2017); where astrocytes mingle with OECs (Beiersdorfer *et al.*, 2019). Our findings showing differential FGFR1 phosphorylation activated on the astrocyte membrane in the presence of OEC-CM demonstrates that, secreted OEC-HSPGs are important moderators of astrocyte reactivity. FGFR1 receptor activation, via FGF, induces phosphorylation of ERK1/2 kinases, which is required for proliferation and also lineage specification in a cell type specific manner (Lanner & Rossant, 2010, Li *et al.*, 2006; see Chan *et al.*, 2013 for a summary table of findings). FGFR1 pY766 doesn't affect proliferation (Mohammadi *et al.*, 1992; Peters *et al.*, 1992) but differentiation via activation of PLCγ (Cross *et al.*, 2002; Spivak-Kroizman *et al.*, 1994; Furdui *et al.*, 2006). Immunofluorescent staining of the activated receptor using antibodies against PLCγ site (pY766-FGFR1) revealed enhanced overall signal in both primary and immortalized astrocytes after treatment with OEC-CM. In contrast, antibodies against pY653/Y654, (associated with kinase activity and ERK1/2 phosphorylation) showed decreased overall signal after treatment with OEC-CM in astrocytes, in particular around the perinuclear area, yet the astrocyte membrane was still positive for

pY653/Y654 signal. Endocytosis in response to ligand binding, as well as subsequent trafficking and degradation of FGFR, are mechanisms for regulating receptor tyrosine kinase (RTK) signaling (von Zastrow & Sorkin, 2007; Le Roy & Wrana, 2005, Auciello *et al.,* 2013). Perinuclear staining of FGFR1 is associated with receptor recycling (Irschick *et al.,* 2013) therefore the observed differences in phospho-FGFR1 staining suggest differential activation of receptor degradation mechanisms. Indeed, FGFR1 pY766 has been shown to be important for the internalization and degradation of the receptor (Sorokin *et al.* 1994, Auciello *et al.*, 2013; Reilly & Maher, 2001).

Notably, previous studies show ERK1/2 phosphorylation to be persistent following FGF stimulation (up to 24 hours), while PLCγ tyrosine phosphorylation is transient (30 minutes) (Ma *et al.*, 2009); suggesting that OEC-secreted factors preferentially stabilize pY766. Furthermore, PLCγ activation may inhibit ERK phosphorylation (Ma *et al.*, 2009). Indeed, we observed a decrease in pY653/Y654 in +LPS +OECs group coincident with significantly lower ERK phosphorylation in astrocyte nuclei. Additionally, our results show that OECs normalize the mitogenic effect of FGF2 on astrocytes, in accordance with decreased pY653/654 and pERK activity.

Mature astrocytes are quiescent and do not proliferate in the intact brain (Buffo *et al.*, 2008; Bush *et al.*, 1999; Horner *et al.*, 2000). FGF1 subfamily (FGF1 and FGF2) are secreted FGFs are important regulators of injury response and recovery (Ornitz and Itoh, 2015, Woodbury & Ikezu, 2014). FGF2 was observed in the cytoplasm of quiescent astrocytes, and the nucleus of proliferating astrocytes (Joy *et al.*, 1997; Planque, 2006). FGF2 upregulation by astrocytes after injury (Clarke *et al.*, 2001; Kirby *et al.*, 2013) induce cell cycle reentry (Kleiderman *et al.*, 2016). These results imply that in astrocyte monocultures, Y653/654 is phosphorylated and

able to transduce signals in response to FGF2 (or FGF1) secreted by astrocytes in an autocrine manner. In response to LPS-induced stress signal, astrocytes suppress pY653/654 and upregulate pY766. However, for a significant increase in Y766 phosphorylation, astrocytes need to be stimulated with both OEC-HSPG and FGF2.

Curiously, a nuclear function has also been reported for FGF2/FGFR1 complexes (Stachowiak *et al.,* 1997; Carpenter *et al.,* 2003). Moreover, nuclear accumulation of FGFRs in glial cells increases after injury (Leadbeater *et al.,* 2006) and is associated with cell proliferation (Stachowiak *et al*., 1997, Reilly & Maher, 2001). However, we found that neither stimulation of membrane FGFR signaling by FGF2 nor the inhibition by FGFR inhibitor SU5402 induce nuclear accumulation, in consensus with previous studies (Irschick *et al.,* 2013, Auciello *et al.*, 2013; reviewed in Stachowiak *et al.,* 2016). Stachowiak and colleagues proposed a 2-pathway model in which FGFR1 is synthesized on ER-attached polyribosomes and then follows either the 'membrane pathway' or 'nuclear pathway'. While the membrane pathway involves extensive glycosylation of the receptor in Golgi for the generation of plasma membrane bound receptors, non-glycosylated FGFR1 may exit pre-Golgi vesicles into the cytosol and translocate into the nucleus (Stachowiak *et al*., 2015). The mechanisms for relaying FGFR1 from the membrane pathway into nucleus have not been clarified in detail yet. It has been postulated that the presence of the FGFR-bound HSPGs regulate receptor trafficking to subcellular compartments (Stewart & Sanderson, 2014; Leadbeater *et al.,* 2006). Remarkably, HSPGs are also upregulated and can be translocated to the nuclear region together with FGF2 and FGFR1 post-injury (Leadbeater *et al.,* 2006). Studies show that the majority of the nuclear FGFR1 is non-glycosylated (Dunham-Ems *et al.,* 2006; reviewed in Tuzon *et al.,* 2019) and this form of FGFR1 directly interacts with CREB binding protein (CBP) (Fang *et al.,* 2005;

reviewed in Stachowiak *et al.,* 2015). FGFR1 is in a dynamic equilibrium with CBP and pp90 Ribosomal S6 kinase-I (RSK1) (Stachowiak *et al*., 2015). Nuclear accumulation of non-glycosylated FGFR1 disrupts the inactive RSK1-CBP complex, activating CBP transactivation of genes as well as protein complexes with histone modifying enzymes (Cheung *et al.,* 2000). Notably, PKC can also dissociate RSK1-CBP complex (Peng *et al*., 2002; reviewed in Stachowiak *et al*., 2015). Thus, the CBP related transcriptional changes may be moderated by several mechanisms following FGFR1 membrane activity.

These results indicate that context dependent, differential FGF/FGFR1 signaling can directly and rapidly impact the binary choice of cells to proliferate or differentiate. These changes are mediated by membrane activity and may also reflect nuclear FGFR-mediated regulation of transcription. Interesting candidates for genes that may be induced by nuclear FGFR1 include the recent list of genes turned on by neuroprotective versus neurotoxic astrocytes (Liddelow *et al*., 2017).

Our studies suggest that non-glycosylated FGFR1 accumulates in astrocyte nuclei upon stress and OEC-secreted factors can diminish this accumulation. We investigated whether OEC-secreted HSPGs may be responsible for the observed change in FGFR1 trafficking and found that $Ext1^{BLBP}$KO-OECs failed to diminish nuclear FGFR1 accumulation. Our examination of the consequences of nuclear FGFR1 trafficking and the function of OEC-HSPGs in nucleus suggest that stress signal increases the association between euchromatin and nuclear FGFR1. In contrast, in the presence of OEC-CM nuclear FGFR1 is found in heterochromatin loci, similar to unstimulated control astrocytes. Heparan sulfation is shown to have a role in self renewal (Jung *et al.,* 2016). In contrast, OEC HSPGs are known to be less sulfated compared to HSPGs secreted by other glia (Higginson *et al*., 2012). Interestingly,

OECs are unusual in that they rarely form tumors (only 11 cases reported to date) (Murtaza *et al.*, 2019). Whether these observations on differential HSPG sulfation may be a mechanism for OEC-induced astrocyte differentiation is an open question.

Chapter 4: Implication of Results & Future Directions for Research

4.1 Discussion of Results

4.1.1 Novel observations regarding the role of OECs in CNS regeneration

In the adult mammalian nervous system, neurogenesis levels are the highest in the olfactory system (Hellström *et al.*, 2009). OB astrocytes contribute to the neurogenesis by promoting a microenvironment in the OB that allows regenerating OSNs to pass through the BBB and integrate into the CNS (Li *et al.*, 2005; 2012), a process that is not permitted in other parts of the brain (Smith *et al.*, 2012). OB astrocytes stand out from other CNS astrocytes exhibiting weaker S100ß and stronger GFAP expression (see Allen Mouse Brain Atlas). This observation is of importance since high GFAP-expression is associated with multipotency (Magnusson & Frisén, 2016) while S100ß is neuroprotective only when expressed at low levels (Villarreal *et al.*, 2014), being up-regulated later in mature astrocytes (Raponi *et al.*, 2007). Moreover, OB astrocytes show structural variation in OB cortex layers, with a gradient of increased complexity towards the ONL (García-Marqués & López-Mascaraque, 2017), where OECs meet astrocytes (Beiersdorfer *et al.*, 2019). These observations suggest that the OB must exhibit a delicate balance of factors to maintain these neurorepair-promoting astrocytes and our work shows that some of these factors are secreted by OECs. We determined that an anti-inflammatory protein, CryAB, secreted via OEC-exosomes, moderates astrocyte reactivity. This secretion is an active response that can be stimulated by stress signals or potential factors secreted by astrocytes. Moreover, we showed that CryAB can suppress activation of multiple genes that were previously associated with neurotoxic astrocyte reactivity (Figure 8). Notably, our results indicated that there are other OEC-secreted factors, in addition to CryAB, that can suppress this harmful reactivity.

Previous studies pointed out that both FGF (Fahmy & Moftah, 2010; Goldshmit *et al.*, 2014), FGFR (Kang *et al.*, 2014) and also the FGF coreceptor HSPGs (Higginson *et al.*, 2012) can moderate astrocyte reactivity. HSPGs can be cleaved from the cell membrane of the donor cell, initiating an intercellular signaling pathway in the host cell (Steward & Sanderson, 2014). FGF signaling pathways take crucial and contrasting roles during neurodevelopment and recovery (Lanner & Rossant, 2010), hence it is not surprising that their regulation is highly complicated. We used OEC-astrocyte cultures to characterize FGFR1 downstream targets that can block neurotoxic astrocyte reactivity. Our findings indicate that OEC-HSPGs may account for CryAB independent factors secreted by OECs, that can suppress neurotoxic astrocyte reactivity. Moreover, we identified a possible regulatory role for OEC-HSPGs in intracellular FGFR1 trafficking and astrocyte differentiation. As a consequence of differential FGFR1 trafficking to the astrocyte nuclei, its association with the transcriptional machinery may also be regulated. Hence, we suggest that future studies should determine whether OEC secreted HSPGs support expression of neurorepair-promoting genes in astrocytes.

4.1.2 Assessing the role of OECs for maintaining astrocytes of the OB in a neurogenesis supportive state

The work presented thus far, examining OEC-astrocyte crosstalk, exploited *in vitro* models. Thus, future work will determine whether OECs can maintain neurogenesis supportive astrocytes in an *in vivo* model. Astrocytes and OECs express many of the same glial markers such as GFAP, S100ß and BLBP. Yet, previous work from our lab revealed OECs are neural crest derivatives (Forni *et al.*, 2011). Therefore, we plan to use a transgenic mouse line floxed for the neural crest marker Sox10 to target OECs in the OB. We propose to deplete OECs using $Sox10^{flox/flox}$ mice (Finzsch *et al.,* 2010) via local injections of AAV-Cre into the OB of

adult mice. We hypothesize that the altered communication between astrocytes and OECs will shift astrocytes of the OB from neurorepair-promoting to neurotoxic.

While GFAP is the most widely used marker for pan-reactive astrocytes, recent transcriptomic studies revealed that complement component-3 (C3) is specifically upregulated in neurogenesis-inhibitory astrocytes (Liddelow *et al.*, 2017; Liddelow & Barres, 2017). Thus, in addition to glial fibrillary acidic protein (GFAP), we will analyze whether OEC depletion in the OB causes a change in C3 expression in astrocytes. Our preliminary studies using AAV-Cre mediated local Sox10 knockdown in the ONL suggest OEC depletion increases the number of C3 positive glia but not the number of Sox2 positive cells in the RMS (Figure 13). Similar to the Sox2 data, no difference was observed for Ki67 or PCNA positive cells across the RMS (Figure 14). Curiously, no change was observed for GFAP or Iba1 (a microglia marker) expression across the RMS (Figure 14), although there was a slight increase for both markers at the injury site (data not shown). No difference was observed for DCX positive NSCs (Figure 13), which represent a subpopulation of Sox2 positive cells. NSCs were also C3 positive (Figure 13) for either treatment. Following Sox10 knockdown, Sox2 positive, DCX negative cells that were positive for C3 increased 278% as measured by immunofluorescence. These cells represent oligodendrocyte and astrocyte populations, as evident by S100ß signal (Figure 13 B" and B"', insets, orange and blue). Notably, despite unchanged GFAP signal, the S100ß signal increased in glia following Sox10 knockdown (Figure 13), suggesting increased reactivity (Villareal *et al.*, 2014).

Characterization of C3 positive cells adjacent to the RMS following local Sox10 knockdown in the OB showed that C3 staining overlapped with GFAP positive astrocytes (Figure 15, open arrowheads), Olig2 positive oligodendrocytes (Figure 15, arrowheads) and Iba1 positive

microglia (Figure 15, asterisk). Both oligodendrocytes and astrocytes were also Sox2 positive (yellow), while microglia were not, consistent with previously shown data (Zhang *et al.,* 2014). The majority of C3 positive cells were found to be astrocytes. In particular, out of C3 positive cells, less than 10% overlapped with the microglia marker Iba1 (purple), around 20% overlapped with the oligodendrocyte marker Olig2 (red), while more than 45% overlapped with the astrocyte marker GFAP (magenta). Very few cells were positive for the neuronal marker NeuN (data not shown). Some C3 cells did not overlap with any of these markers, but were Sox2 positive (yellow), possibly indicating the radial glia (Emsley *et al.*, 2012).

4.2 Limitations of Experimental Approach

Previous studies report that zinc sulfate lesion (ZL) of the OE results in cell death in the OB (Kim et al, 2006). We observed no differences in GFAP or C3 expression in OB astrocytes 10 days after ZL, despite a significant increase in the number of OECs (data not shown), serving as a control for our studies. A minimum of one week is predicted for viral transduction to be efficient, and our preliminary studies indicates a difference in astrocyte reactivity 14 days after OEC depletion. Therefore, an optimum timeline needs to be established to observe the changes predicted in astrocytes following AAV-Cre injections with appropriate controls. In addition, it is important to remember that the OB is a highly regenerative system which is expected to be maintained by numerous neurogenic and gliogenic signals. Therefore, in addition to knockdown of OECs, it may be necessary to induce CNS injury to trigger the expected changes in astrocytes. For this purpose, experimental autoimmune encephalomyelitis (EAE) model could be used. Studies show improved recovery following OEC transplantation into the CNS in multiple mouse models of CNS injury, including EAE (Li *et al.*, 2015). However, the changes in astrocyte recovery in these models are often overlooked. EAE is the

primary mouse model for MS and in addition to the oligodendrocyte cell loss, it is characterized by activation of astrocytes, and loss of their end-feet around small blood vessels even at early stages (Brosnan & Raine., 2013). This standardized animal model for injury is advantageous because it provides multiple readouts without the need for any CNS-invasive techniques. Moreover, EAE increases neural progenitor and stem cell migration from the SVZ to the OB, while the proliferating GFAP positive cells at the cortical layers of the OB remained constant (Picard-Riera *et al.*, 2002). In collaboration with Dr. Vanja Lazarevic at NIH/NCI, we repeated these experiments on EAE mouse brains and confirmed the increased migration of several cell types 30 days p.i. (Figure 16). In EAE mice, the percentage of DCX positive cells and the percentage of GFAP positive cells increased significantly where the RMS entered the OB (Figure 16 C & D). The percentage of proliferating oligodendrocytes, determined by co-staining for the proliferative marker Ki67 and the oligodendrocyte marker GPR17, increased in the corpus callosum (Figure 16, E), although the difference did not reach significance in this first study. Thus, using this EAE model ± Sox10 ablation and examining the olfactory bulb, may reveal the dramatic astrocytic changes predicted from our earlier work, with OECs modulating astrocytic reactivity. Specifically, following OEC depletion, inducing the EAE model should attenuate the factors that maintain astrocytes in the OB and thereby enable us to observe a significant difference in astrocytes in the absence/scarcity of OEC secreted factors. Additionally, we expect that OE OECs would eventually proliferate and replace the dead OB OECs. This state could be used as an internal control via changing the timeline after the AAV-Cre injection.

4.3 Recommendations for Future Research

A significant gap in our knowledge lies in regulation of FGFR signaling by the immune system which determines, at least in part, the proliferative states of astrocytes that contribute to the formation of the glial scar and inhibit regeneration. Over the last years, it has become increasingly clear that the FGFR pathway has a regulatory role in astrocyte differentiation and response to injury (Fahmy & Moftah, 2010; Goldshmit *et al.*, 2014; Kang *et al.*, 2014; Liddelow *et al.*, 2017). Our results imply that in astrocyte monocultures, Y653/654 is phosphorylated and transduces signals in response to FGF2 (or FGF1) secreted by astrocytes in an autocrine manner. In response to LPS-induced stress signal, astrocytes suppress pY653/654 and upregulate pY766. However, for a significant increase in Y766 phosphorylation, astrocytes need to be also stimulated with OEC-HSPGs. One of the important questions that still remains is how FGFR1 nuclear trafficking is initiated by astrocytes in reaction to the LPS-induced stress signal. Secretory FGFs (FGF1 and FGF2) are known to be upregulated following injury (Goldshmit *et al.*, 2014; Woodbury & Ikezu, 2014; Ornitz & Itoh, 2015). Moreover, both FGF1 and 2 and FGFR1 can accumulate in nuclei after injury (Więdłocha *et al.*, 2005). Although FGFR1 protein doesn't have a nuclear localization signal, it has been suggested that it is co-transported with FGF2 (Stachowiak *et al.*, 2011; 2015; 2016). However, we found that FGF2 stimulation by itself doesn't induce nuclear accumulation. Hence there must be additional astrocyte regulated factors that induce FGFR1 activation and intracellular trafficking. One such candidate protein is Anosmin1, a heparan sulfate dependent extracellular matrix protein that binds to FGF/FGFR1 complex and regulates FGF signaling (Choy & Kim, 2010).

Anosmin1 is coded by ANOS1 (previously called KAL1) gene and its expression is required for neural outgrowth and targeting (Rugarli *et al.*, 1993). Yamada and colleagues studied Anosmin1 expression in chicken embryos and showed that Anosmin1 is essential for neural crest formation and that it regulates the activities of several growth factors, including FGF (Endo *et al.*, 2012). ANOS1 has been identified in human, chicken, zebrafish, and musk shrew (reviewed in Dellovade *et al.*, 2003). Although the whole mouse genome is annotated, an ANOS1 orthologue has not been identified suggesting that the gene has been lost (possibly due to redundancy of function by another molecule) or shows such significant sequence divergence that it cannot be detected (Hu & Bouloux, 2011; Rugarli *et al.*, 1993). Although the gene has also not been found in rat, immunocytochemistry for Anosmin1 revealed robust staining in the OB, and Anosmin1 has been shown to promote olfactory neuronal development during rat embryogenesis (Soussi-Yanicostas *et al.*, 2002; Clemente *et al.*, 2008). These results indicate existence of an orthologue gene in rat and mouse genome, possibly on an autosome (Hu & Bouloux, 2011). During development, the identity of the cells expressing Anosmin1 in nasal regions is still unclear – however in the cerebellum the majority of Anosmin1 positive cells were also S100ß positive, pointing to a glial source (Gianola *et al.*, 2009). In agreement, human brain RNAseq data shows the highest ANOS1 expression to be in mature astrocytes (Zhang *et al.*, 2016).

Anosmin1 is an extracellular regulator of FGFR1 and Anosmin1 binding to either FGF/FGFR/HSPG complex or to FGFR-alone can have opposing effects, such as proliferation versus differentiation (Hu & Bouloux, 2011; Hu *et al.*, 2009). Notably, the glucidic composition and structure of HSPGs varies with species, cell type, and age which could control the binding and function of the different Anosmin1 domains (reviewed in Hu &

Bouloux 2011). Our results indicate a significantly increased proliferation in immortalized astrocytes stimulated with Anosmin1 and LPS, exceeding that observed with either stimulation alone (Figure 17). Indeed, earlier studies indicate that Anosmin1 (Garcia-Gonzalez *et al.*, 2010) or inflammatory signals (Liddelow & Barres, 2017) alone has no/or little effect on cell proliferation *in vivo*.

In summary, Anosmin1 can regulate FGFR1 signaling by differentially binding to ligands as well as HSPG and/or FGFR1. We hypothesize that insufficient levels of the right HSPG in the ECM together with excessive Anosmin1 may: 1) block FGFR signaling and 2) cause nuclear FGFR1 accumulation and increased astrocyte proliferation. Thus, it would be interesting to investigate the role of Anosmin1 for OEC-astrocyte crosstalk both in vitro and in vivo.

Clearly, when working *in vivo*, multiple parameters can change including changes in other neural niche cells. The OB provides a unique neural niche that supports neuroregeneration, with OECs being an integral component of OB plasticity. Future work will utilize this system to extend our *in vitro* results to identify factors that support astrocyte health, and apply these cues to astrocytes outside of the neurogenic zones of the CNS to improve recovery following injuries.

APPENDIX A:

OEC depletion increases the number of C3 positive astrocytes along the RMS

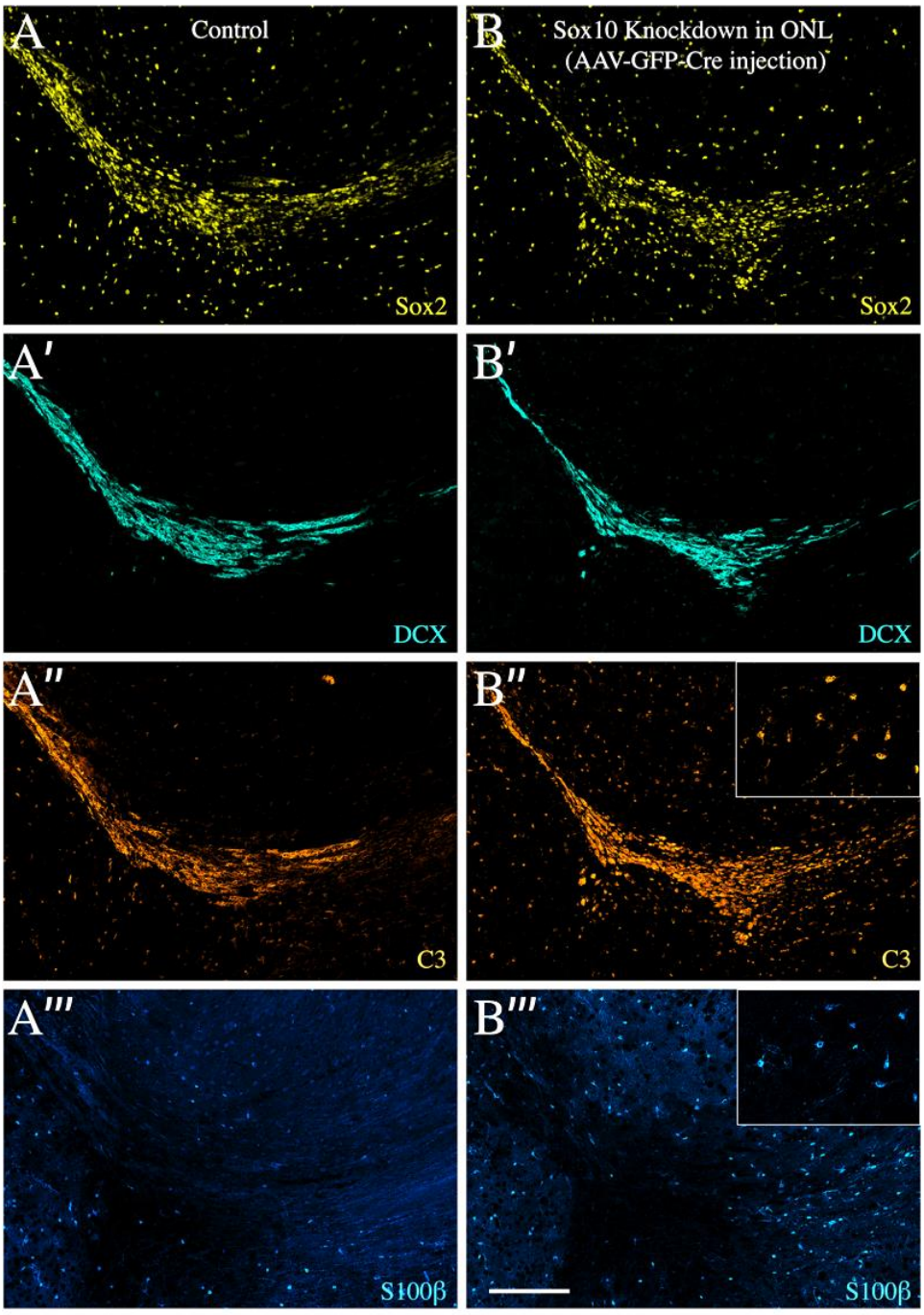

Figure 13: OEC depletion increases the number of C3 positive glia along the RMS. (A and B) Following Sox10 knockdown, Sox2 positive, DCX negative cells that are positive for C3 increased 278% (B", inset, orange). These cells represent oligodendrocyte and astrocyte population, as evident by S100ß signal (B" and B"', insets, orange and blue). Notably, S100ß signal was found to be increased in glia following Sox10 knockdown (A"' versus B"', blue).

AAV-Cre mediated local Sox10 knockdown in the ONL did not cause an increase in the number of Sox2 (A and B, yellow) positive cells along the RMS. No difference was observed for DCX positive NSCs (A' and B', cyan), which represent a subpopulation of Sox2 positive cells. NSCs were also C3 positive (A" and B", orange) for either treatments. Scale bar represents 100μm in low mag and 40μm in insets.

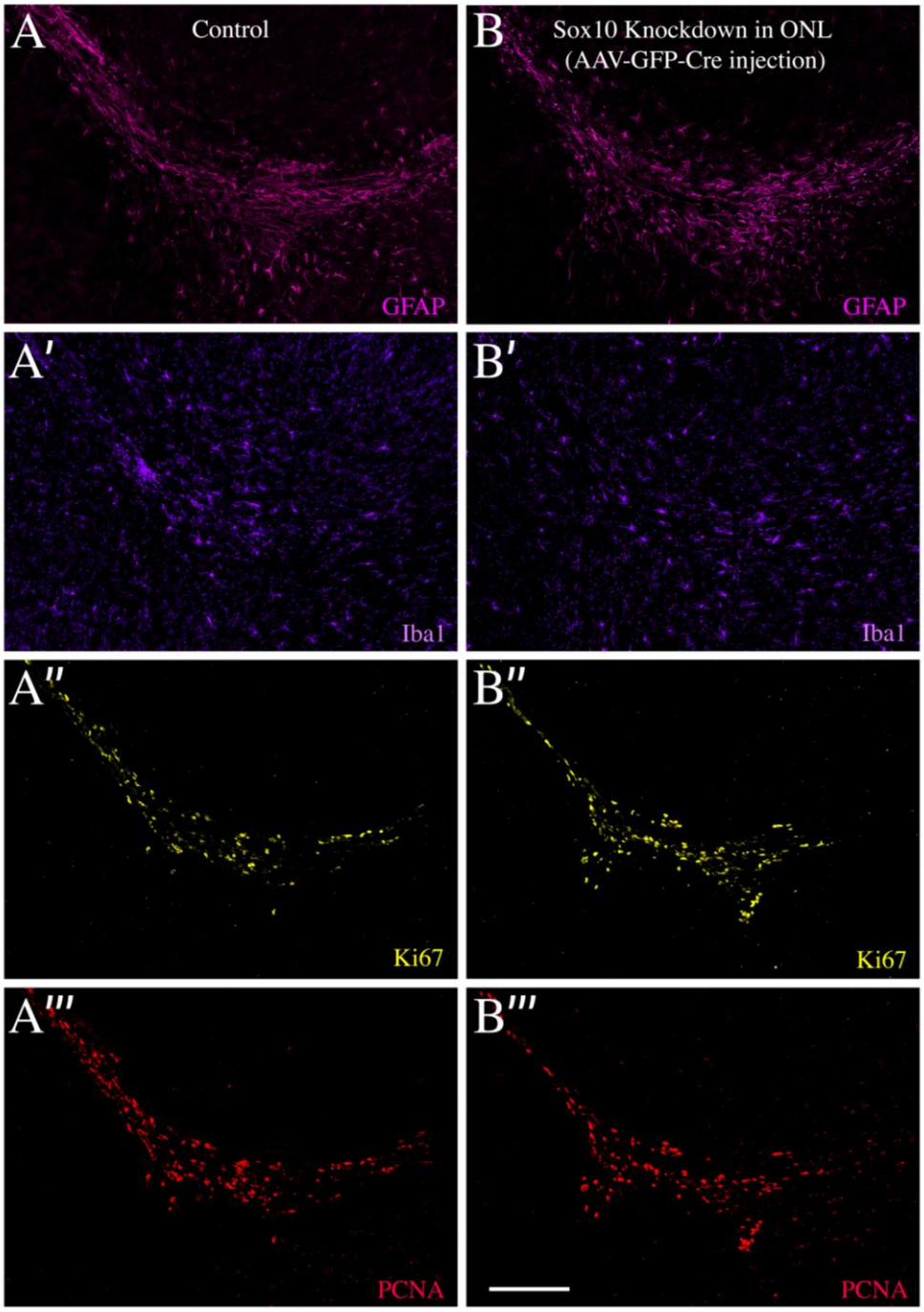

Figure 14: No difference was observed for GFAP, Iba1 or cell proliferation markers following OEC depletion. Scale bar represents 100μm.

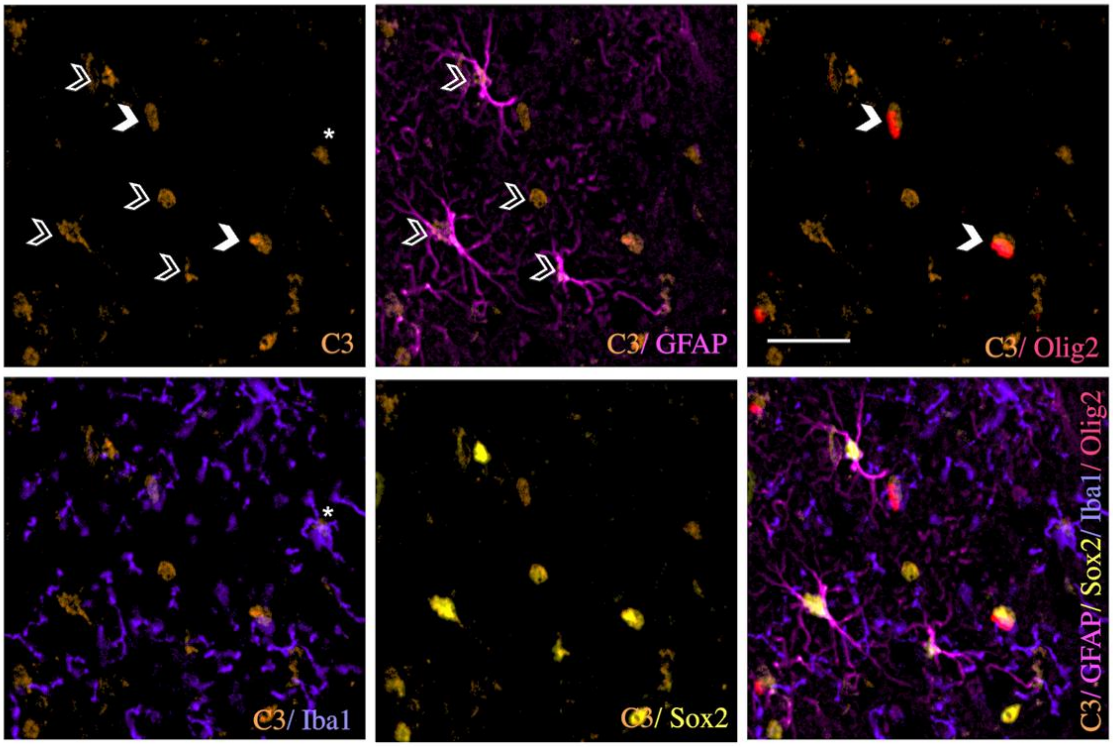

Figure 15: The majority of C3 positive cells are GFAP positive astrocytes. Characterization of C3 positive cells at the intersection of RMS and the OB. Following local Sox10 knockdown in the OB, C3 staining overlaps with GFAP positive astrocytes (magenta, open arrowheads), Olig2 positive oligodendrocytes (red, arrowheads) and Iba1 positive microglia (blue, asterisk). Oligodendrocytes and astrocytes, but not microglia are Sox2 positive (yellow). Less than 10% C3 positive cells overlapped with microglia marker Iba1 (purple), ~20% overlapped with oligodendrocyte marker Olig2 (red), > 45% overlapped with astrocyte marker GFAP (magenta). Some C3 cells did not overlap with any of these markers but were Sox2 positive (yellow). Scale bar represents 20μm.

APPENDIX B:

Experimental autoimmune encephalomyelitis increases the number of progenitors reaching to the OB from RMS

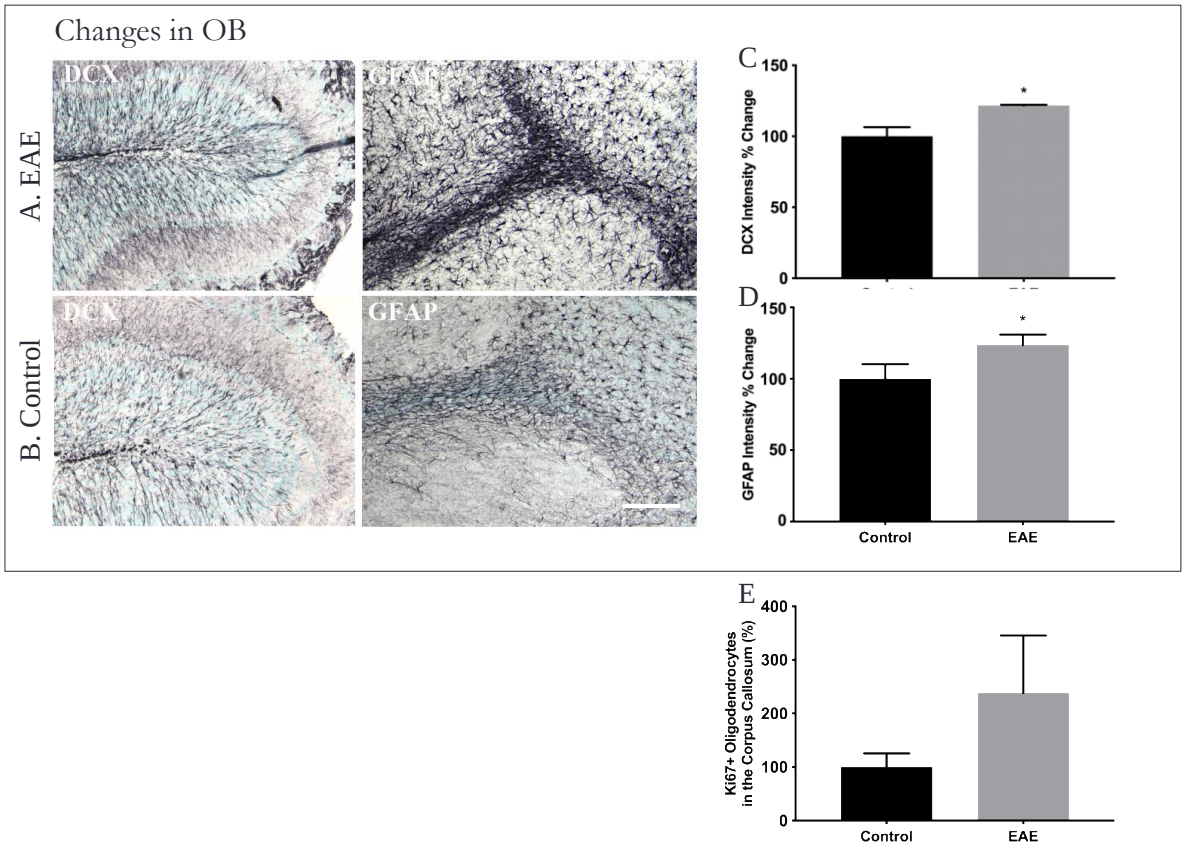

Figure 16: EAE increases the number of progenitors along RMS to the OB. (A) 30 days p.i. of EAE (B) and WT control adult mouse OBs immunostained for DCX on coronal sections (A and B, left images) and GFAP on sagittal sections (A and B, right images). In EAE mice, the percentage of DCX positive cells (C) and the percentage of GFAP positive cells (D) increased significantly at the intersection of RMS and the OB. (E) The percentage of proliferating oligodendrocytes, determined by the co-staining of proliferative marker Ki67 and oligodendrocyte marker GPR17, was increased in the corpus callosum (not significant, $p=0.0788$). $N = 3$; * $p \leq 0.05$; unpaired t-test. Scale bar represents 50µm.

APPENDIX C:
Co-stimulation of astrocytes with Anosmin1 and LPS increases astrocyte proliferation

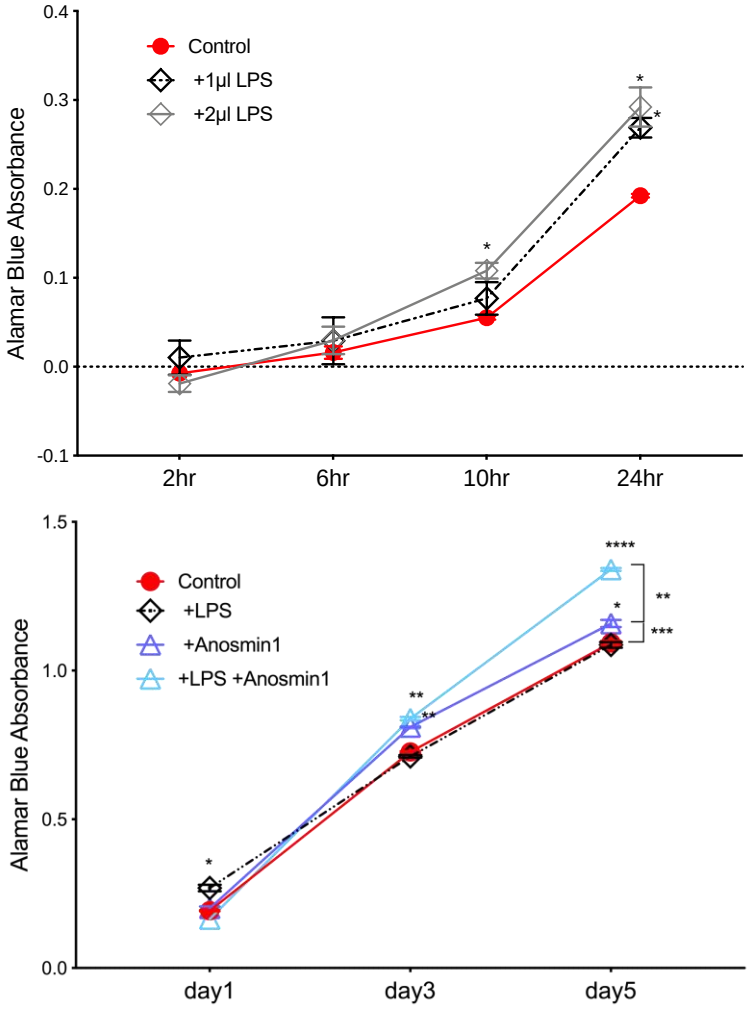

Figure 17: LPS and Anosmin1 have a combinational effect on astrocyte proliferation. Viability test on immortalized astrocyte line C8D30 shows significantly increased proliferation following 24hr 1µl LPS treatment (black dashed lines, rhombus) compared to untreated, control astrocytes (red lines, circle) (top image, 24hr, and bottom image, day1). 5ng/ml Anosmin1 significantly increased astrocyte proliferation on days 3 and 5, while no difference for LPS treated group was observed for these time points (bottom image). Compared to control group, combinational stimulation of LPS and Anosmin1 resulted in increased astrocyte proliferation on day5 (turquoise line, triangle) which was also significantly higher compared to either stimulation alone (bottom image, blue line, triangle, or black dashed line, rhombus) (N=3, * $p \leq 0.05$, ** $p \leq 0.01$, *** $p \leq 0.001$, **** $p \leq 0.0001$; two-way ANOVA).

Bibliography:

Addington, C. P., Roussas, A., Dutta, D., & Stabenfeldt, S. E. (2015). Endogenous repair signaling after brain injury and complementary bioengineering approaches to enhance neural regeneration. Biomarker Insights, 10(Suppl 1), 43–60. https://doi.org/10.4137/BMI.S20062

Adolf, A., Rohrbeck, A., Münster-Wandowski, A., Johansson, M., Kuhn, H. G., Kopp, M. A., … Höltje, M. (2019). Release of astroglial vimentin by extracellular vesicles: Modulation of binding and internalization of C3 transferase in astrocytes and neurons. Glia, 67(4), 703–717. https://doi.org/10.1002/glia.23566

Alvarez-Buylla, A., & Lim, D. A. (2004). For the long run: Maintaining germinal niches in the adult brain. Neuron. https://doi.org/10.1016/S0896-6273(04)00111-4

Arac, A., Brownell, S. E., Rothbard, J. B., Chen, C., Ko, R. M., Pereira, M. P., … Steinberg, G. K. (2011). Systemic augmentation of B-crystallin provides therapeutic benefit twelve hours post-stroke onset via immune modulation. Proceedings of the National Academy of Sciences. https://doi.org/10.1073/pnas.1107368108

Au, E., & Roskams, A. J. (2003). Olfactory ensheathing cells of the lamina propria in vivo and in vitro. GLIA, 41(3), 224–236. https://doi.org/10.1002/glia.10160

Au, W. W., Treloar, H. B., & Greer, C. A. (2002). Sublaminar organization of the mouse olfactory bulb nerve layer. Journal of Comparative Neurology. https://doi.org/10.1002/cne.10182

Auciello, G., Cunningham, D. L., Tatar, T., Heath, J. K., & Rappoport, J. Z. (2013). Regulation of fibroblast growth factor receptor signalling and trafficking by Src and Eps8. Journal of Cell Science, 126(Pt 2), 613–624. https://doi.org/10.1242/jcs.116228

Bachoo, R. M., Kim, R. S., Ligon, K. L., Maher, E. A., Brennan, C., Billings, N., … DePinho, R. A. (2004). Molecular diversity of astrocytes with implications for neurological disorders. Proceedings of the National Academy of Sciences of the United States of America. https://doi.org/10.1073/pnas.0402140101

Barnett, S. C., Alexander, C. L., Iwashita, Y., Gilson, J. M., Crowther, J., Clark, L., … Franklin, R. J. (2000). Identification of a human olfactory ensheathing cell that can effect transplant-mediated remyelination of demyelinated CNS axons. Brain: A Journal of Neurology, 123 (Pt 8, 1581–1588. https://doi.org/10.1093/brain/123.8.1581

Beiersdorfer, A., Wolburg, H., Grawe, J., Scheller, A., Kirchhoff, F., & Lohr, C. (2020). Sublamina-specific organization of the blood brain barrier in the mouse olfactory nerve layer. GLIA. https://doi.org/10.1002/glia.23744

Bignami, A., & Dahl, D. (1976). The Astroglial Response to Stabbing. Immunofluorescence Studies with Antibodies to Astrocyte-Specific Protein (GFAP) In Mammalian and Submammalian Vertebrates. Neuropathology and Applied Neurobiology. https://doi.org/10.1111/j.1365-2990.1976.tb00488.x

Boccazzi, M., & Ceruti, S. (2016). Where do you come from and what are you going to become, reactive astrocyte? Stem Cell Investig 2016; 3:15. https://doi.org/10.21037/sci.2016.05.02

Bohlen, C. J., Bennett, F. C., Tucker, A. F., Collins, H. Y., Mulinyawe, S. B., & Barres, B. A. (2017). Diverse Requirements for Microglial Survival, Specification, and Function Revealed by Defined-Medium Cultures. Neuron. https://doi.org/10.1016/j.neuron.2017.04.043

Brady, J. P., Garland, D. L., Green, D. E., Tamm, E. R., Giblin, F. J., & Wawrousek, E. F. (2001). B-Crystallin in Lens Development and Muscle Integrity: A Gene Knockout Approach. Investigative Ophthalmology & Visual Science (Vol. 42).

Brosnan, C. F., & Raine, C. S. (2013). The astrocyte in multiple sclerosis revisited. GLIA. https://doi.org/10.1002/glia.22443

Buffo, A., Rite, I., Tripathi, P., Lepier, A., Colak, D., Horn, A.-P., … Götz, M. (2008). Origin and progeny of reactive gliosis: A source of multipotent cells in the injured brain. Proceedings of the National Academy of Sciences of the United States of America, 105(9), 3581–3586. https://doi.org/10.1073/pnas.0709002105

Bush, T. G., Puvanachandra, N., Horner, C. H., Polito, A., Ostenfeld, T., Svendsen, C. N., … Sofroniew, M. V. (1999). Leukocyte infiltration, neuronal degeneration, and neurite outgrowth after ablation of scar-forming, reactive astrocytes in adult transgenic mice. Neuron. https://doi.org/10.1016/S0896-6273(00)80781-3

Cahoy, J. D., Emery, B., Kaushal, A., Foo, L. C., Zamanian, J. L., Christopherson, K. S., … Barres, B. A. (2008). A transcriptome database for astrocytes, neurons, and oligodendrocytes: A new resource for understanding brain development and function. Journal of Neuroscience. https://doi.org/10.1523/JNEUROSCI.4178-07.2008

Calof, A. L., & Guevara, J. L. (1993). Cell lines derived from retrovirus-mediated oncogene transduction into olfactory epithelium cultures. Methods in Neurosciences, 3, 222–231. Retrieved from https://doi.org/10.1006/ncmn.1993.1057

Calof, A. L., Hagiwara, N., Holcomb, J. D., Mumm, J. S., & Shou, J. (1996). Neurogenesis and cell death in olfactory epithelium. Journal of Neurobiology, 30(1), 67–81. https://doi.org/10.1002/(SICI)1097-4695(199605)30:1<67::AID-NEU7>3.0.CO;2-E

Carmen Martinez Garcia, M., Cuervas-Mons Finat, M., Latorre Macarron, E., Bullon Sopelana, M., & Gayoso Rodriguez, M. J. (1991). Responses of the astroglia in sensory deprived olfactory bulb of developing rats. Histology and Histopathology.

Carpenter, G. (2003). Nuclear localization and possible functions of receptor tyrosine kinases. Current Opinion in Cell Biology. https://doi.org/10.1016/S0955-0674(03)00015-2

Ceyzériat, K., Abjean, L., Carrillo-de Sauvage, M. A., Ben Haim, L., & Escartin, C. (2016). The complex STATes of astrocyte reactivity: How are they controlled by the JAK-STAT3 pathway? Neuroscience. https://doi.org/10.1016/j.neuroscience.2016.05.043

Chan, W. S., Sideris, A., Sutachan, J. J., Montoya G, J. V., Blanck, T. J. J., & Recio-Pinto, E. (2013). Differential regulation of proliferation and neuronal differentiation in adult rat spinal cord neural stem/progenitors by ERK1/2, Akt, and PLCγ. Frontiers in Molecular Neuroscience. https://doi.org/10.3389/fnmol.2013.00023

Chen, S., Wassenhove-McCarthy, D. J., Yamaguchi, Y., Holzman, L. B., Van Kuppevelt, T. H., Jenniskens, G. J., … McCarthy, K. J. (2008). Loss of heparan sulfate glycosaminoglycan assembly in podocytes does not lead to proteinuria. Kidney International. https://doi.org/10.1038/ki.2008.159

Cheung, P., Allis, C. D., & Sassone-Corsi, P. (2000). Signaling to chromatin through historic modifications. Cell. https://doi.org/10.1016/S0092-8674(00)00118-5

Choy, C., & Kim, S. H. (2010). Biological actions and interactions of Anosmin-1. In Kallmann Syndrome and Hypogonadotropic Hypogonadism (Vol. 39, pp. 78–93). https://doi.org/10.1159/000312695

Chuah, M. I., Hale, D. M., & West, A. K. (2011). Interaction of olfactory ensheathing cells with other cell types in vitro and after transplantation: Glial scars and inflammation. Experimental Neurology. https://doi.org/10.1016/j.expneurol.2010.08.012

Clarke, L. E., Liddelow, S. A., Chakraborty, C., Münch, A. E., Heiman, M., & Barres, B. A. (2018). Normal aging induces A1-like astrocyte reactivity. Proceedings of the National Academy of Sciences of the United States of America, 115(8), E1896–E1905. https://doi.org/10.1073/pnas.1800165115

Clarke, W. E., Berry, M., Smith, C., Kent, A., & Logan, A. (2001). Coordination of fibroblast growth factor receptor 1 (FGFR1) and fibroblast growth factor-2 (FGF-2) trafficking to nuclei of reactive astrocytes around cerebral lesions in adult rats. Molecular and Cellular Neuroscience. https://doi.org/10.1006/mcne.2000.0920

Clemente, D., Esteban, P. F., Del Valle, I., Bribián, A., Soussi-Yanicostas, N., Silva, A., & De Castro, F. (2008). Expression pattern of Anosmin-1 during pre- and postnatal rat brain development. Developmental Dynamics: An Official Publication of the American Association of Anatomists, 237(9), 2518–2528. https://doi.org/10.1002/dvdy.21659

Cross, M. J., Lu, L., Magnusson, P., Nyqvist, D., Holmqvist, K., Welsh, M., & Claesson-Welsh, L. (2002). The Shb adaptor protein binds to tyrosine 766 in the FGFR-1 and regulates the Ras/MEK/MAPK pathway via FRS2 phosphorylation in endothelial cells. Molecular Biology of the Cell. https://doi.org/10.1091/mbc.E02-02-0103

D'Agostino, M., Lemma, V., Chesi, G., Stornaiuolo, M., Serio, M. C., D'Ambrosio, C., … Bonatti, S. (2013). The cytosolic chaperone α-crystallin B rescues folding and compartmentalization of misfolded multispan transmembrane proteins. Journal of Cell Science, 126(18), 4160–4172. https://doi.org/10.1242/jcs.125443

Dailey, L., Ambrosetti, D., Mansukhani, A., & Basilico, C. (2005). Mechanisms underlying differential responses to FGF signaling. Cytokine & Growth Factor Reviews, 16(2), 233–247. https://doi.org/10.1016/j.cytogfr.2005.01.007

Dairaghi, L., Flannery, E., Giacobini, P., Saglam, A., Saadi, H., Constantin, S., … Wray, S. (2018). Reelin can modulate migration of olfactory ensheathing cells and gonadotropin releasing hormone neurons via the canonical pathway. Frontiers in Cellular Neuroscience. https://doi.org/10.3389/fncel.2018.00228

Dando, S. J., Ipe, D. S., Batzloff, M., Sullivan, M. J., Crossman, D. K., Crowley, M., … Ulett, G. C. (2016). Burkholderia pseudomallei capsule exacerbates respiratory melioidosis but does not afford protection against antimicrobial signaling or bacterial killing in human olfactory ensheathing cells. Infection and Immunity. https://doi.org/10.1128/IAI.01546-15

de Castro, F., Seal, R., & Maggi, R. (2017). ANOS1: A unified nomenclature for Kallmann syndrome 1 gene (KAL1) and Anosmin-1. Briefings in Functional Genomics, 16(4), 205–210. https://doi.org/10.1093/bfgp/elw037

De Cecco, M., Jeyapalan, J., Zhao, X., Tamamori-Adachi, M., & Sedivy, J. M. (2011). Nuclear protein accumulation in cellular senescence and organismal aging revealed with a novel single-cell resolution fluorescence microscopy assay. Aging. https://doi.org/10.18632/aging.100372

Dellovade, T. L., Hardelin, J. P., Soussi-Yanicostas, N., Pfaff, D. W., Schwanzel-Fukuda, M., & Petit, C. (2003). Anosmin-1 immunoreactivity during embryogenesis in a primitive eutherian mammal. Developmental Brain Research. https://doi.org/10.1016/S0165-3806(02)00544-8

Deumens, R., Koopmans, G. C., Honig, W. M. M., Hamers, F. P. T., Maquet, V., … Joosten, E. A. J. (2006). Olfactory ensheathing cells, olfactory nerve fibroblasts and biomatrices to promote long-distance axon regrowth and functional recovery in the dorsally hemisected adult rat spinal cord. Experimental Neurology, 200(1), 89–103. https://doi.org/10.1016/j.expneurol.2006.01.030

DM Hale. (2011). Olfactory ensheathing cells moderate astrocyte inflammatory activation.

Doetsch, F., Caille, I., Lim, D. A., Garcia-Verdugo, J. M., & Alvarez-Buylla, A. (1999). Subventricular zone astrocytes are neural stem cells in the adult mammalian brain. Cell. https://doi.org/10.1016/S0092-8674(00)80783-7

Donato, R. (2001). S100: a multigenic family of calcium-modulated proteins of the EF-hand type with intracellular and extracellular functional roles. The International Journal of Biochemistry & Cell Biology (Vol. 33). Retrieved from www.elsevier.com/locate/ijbcb*

Doucette, R., & Words, K. E. Y. (1990). Glial influences on axonal growth in the primary olfactory system. Glia, 3(6), 433–449. https://doi.org/10.1002/glia.440030602

Doyle, J. P., Dougherty, J. D., Heiman, M., Schmidt, E. F., Stevens, T. R., Ma, G., … Heintz, N. (2008). Application of a Translational Profiling Approach for the Comparative Analysis of CNS Cell Types. Cell. https://doi.org/10.1016/j.cell.2008.10.029

Dulle, J. E., & Fort, P. E. (2016). Crystallins and neuroinflammation: The glial side of the story. Biochimica et Biophysica Acta - General Subjects, 1860(1), 278–286. https://doi.org/10.1016/j.bbagen.2015.05.023

Dunham-Ems, S. M., Pudavar, H. E., Myers, J. M., Maher, P. A., Prasad, P. N., & Stachowiak, M. K. (2006). Factors Controlling Fibroblast Growth Factor Receptor-1's Cytoplasmic Trafficking and Its Regulation as Revealed by FRAP Analysis. Molecular Biology of the Cell. https://doi.org/10.1091/mbc.E05-08-0749

Dye, D. E., Medic, S., Ziman, M., & Coombe, D. R. (2013). Melanoma biomolecules: Independently identified but functionally intertwined. Frontiers in Oncology. https://doi.org/10.3389/fonc.2013.00252

Emsley, J. G., Menezes, J. R. L., Madeiro Da Costa, R. F., Martinez, A. M. B., & Macklis, J. D. (2012). Identification of radial glia-like cells in the adult mouse olfactory bulb. Experimental Neurology. https://doi.org/10.1016/j.expneurol.2012.05.012

Endo, Y., Ishiwata-Endo, H., & Yamada, K. M. (2012). Extracellular Matrix Protein Anosmin Promotes Neural Crest Formation and Regulates FGF, BMP, and WNT Activities. Developmental Cell, 23(2), 305–316. https://doi.org/10.1016/j.devcel.2012.07.006

Fahmy, G. H., & Moftah, M. Z. (2010). FGF-2 in astroglial cells during vertebrate spinal cord recovery. Frontiers in Cellular Neuroscience. https://doi.org/10.3389/fncel.2010.00129

Faiz, M., Sachewsky, N., Gascón, S., Bang, K. W. A., Morshead, C. M., & Nagy, A. (2015). Adult Neural Stem Cells from the Subventricular Zone Give Rise to Reactive Astrocytes in the Cortex after Stroke. Cell Stem Cell, 17(5), 624–634. https://doi.org/10.1016/j.stem.2015.08.002

Fang, X., Stachowiak, E. K., Dunham-Ems, S. M., Klejbor, I., & Stachowiak, M. K. (2005). Control of CREB-binding protein signaling by nuclear fibroblast growth factor receptor-1: A novel mechanism of gene regulation. Journal of Biological Chemistry. https://doi.org/10.1074/jbc.M504400200

Faulkner, J. R., Herrmann, J. E., Woo, M. J., Tansey, K. E., Doan, N. B., & Sofroniew, M. V. (2004). Reactive Astrocytes Protect Tissue and Preserve Function after Spinal Cord Injury. Journal of Neuroscience. https://doi.org/10.1523/JNEUROSCI.3547-03.2004

Finzsch, M., Schreiner, S., Kichko, T., Reeh, P., Tamm, E. R., Bösl, M. R., … Wegner, M. (2010). Sox10 is required for Schwann cell identity and progression beyond the immature Schwann cell stage. Journal of Cell Biology. https://doi.org/10.1083/jcb.200912142

Foo, L. C., Allen, N. J., Bushong, E. A., Ventura, P. B., Chung, W. S., Zhou, L., … Barres, B. A. (2011). Development of a method for the purification and culture of rodent astrocytes. Neuron. https://doi.org/10.1016/j.neuron.2011.07.022

Forni, P. E., Bharti, K., Flannery, E. M., Shimogori, T., & Wray, S. (2013). The indirect role of fibroblast growth factor-8 in defining neurogenic niches of the olfactory/GnRH systems. Journal of Neuroscience, 33(50), 19620–19634. https://doi.org/10.1523/JNEUROSCI.3238-13.2013

Franssen, E. H. P., De Bree, F. M., Essing, A. H. W., Ramon-Cueto, A., & Verhaagen, J. (2008). Comparative gene expression profiling of olfactory ensheathing glia and Schwann cells indicates distinct tissue repair characteristics of olfactory ensheathing glia. GLIA, 56(12), 1285–1298. https://doi.org/10.1002/glia.20697

Fuhrmann, V., Kinkl, N., Leveillard, T., Sahel, J., & Hicks, D. (1999). Fibroblast growth factor receptor 4 (FGFR4) is expressed in adult rat and human retinal photoreceptors and neurons. Journal of Molecular Neuroscience. https://doi.org/10.1385/jmn:13:1-2:187

Furdui, C. M., Lew, E. D., Schlessinger, J., & Anderson, K. S. (2006). Autophosphorylation of FGFR1 kinase is mediated by a sequential and precisely ordered reaction. Molecular Cell. https://doi.org/10.1016/j.molcel.2006.01.022

García-González, D., Clemente, D., Coelho, M., Esteban, P. F., Soussi-Yanicostas, N., & de Castro, F. (2010). Dynamic roles of FGF-2 and Anosmin-1 in the migration of neuronal precursors from the subventricular zone during pre- and postnatal development. Experimental Neurology. https://doi.org/10.1016/j.expneurol.2010.01.006

García-Marqués, J., & López-Mascaraque, L. (2017). Clonal Mapping of Astrocytes in the Olfactory Bulb and Rostral Migratory Stream. Cerebral Cortex (New York, N.Y. : 1991). https://doi.org/10.1093/cercor/bhw071

Gianola, S., de Castro, F., & Rossi, F. (2009). Anosmin-1 stimulates outgrowth and branching of developing Purkinje axons. Neuroscience, 158(2), 570–584. https://doi.org/10.1016/j.neuroscience.2008.10.022

Girouard, H., & Iadecola, C. (2006). Neurovascular coupling in the normal brain and in hypertension, stroke, and Alzheimer disease. Journal of Applied Physiology (Bethesda, Md. : 1985), 100(1), 328–335. https://doi.org/10.1152/japplphysiol.00966.2005

Göktaş, Ö., Cao Van, H., Fleiner, F., Lacroix, J. S., & Landis, B. N. (2010). Chemosensory function in Wegener's granulomatosis: A preliminary report. European Archives of Oto-Rhino-Laryngology. https://doi.org/10.1007/s00405-009-1184-4

Goldshmit, Y., Frisca, F., Pinto, A. R., Pébay, A., Tang, J. K. K. Y., Siegel, A. L., … Currie, P. D. (2014). Fgf2 improves functional recovery-decreasing gliosis and increasing radial glia and neural progenitor cells after spinal cord injury. Brain and Behavior. https://doi.org/10.1002/brb3.172

Gómez-Pinilla, F., Vu, L., & Cotman, C. W. (1995). Regulation of astrocyte proliferation by FGF-2 and heparan sulfate in vivo. The Journal of Neuroscience : The Official Journal of the Society for Neuroscience, 15(March), 2021–2029.

Gómez, R. M., Sánchez, M. Y., Portela-Lomba, M., Ghotme, K., Barreto, G. E., Sierra, J., & Moreno-Flores, M. T. (2018). Cell therapy for spinal cord injury with olfactory ensheathing glia cells (OECs). Glia, 66(7), 1267–1301. https://doi.org/10.1002/glia.23282

Grimpe, B., Pressman, Y., Bunge, M. B., & Silver, J. (2005). The role of proteoglycans in Schwann cell/astrocyte interactions and in regeneration failure at PNS/CNS interfaces. Molecular and Cellular Neuroscience. https://doi.org/10.1016/j.mcn.2004.06.010

Gulbenkian, S., Uddman, R., & Edvinsson, L. (2001). Neuronal messengers in the human cerebral circulation. Peptides, 22(6), 995–1007. https://doi.org/10.1016/S0196-9781(01)00408-9

Guntinas-Lichius, O., Angelov, D. N., Tomov, T. L., Dramiga, J., Neiss, W. F., & Wewetzer, K. (2001). Transplantation of olfactory ensheathing cells stimulates the collateral sprouting from axotomized adult rat facial motoneurons. Experimental Neurology, 172(1), 70–80. https://doi.org/10.1006/exnr.2001.7774\rS0014-4886(01)97774-X [pii]

Guo, Y. S., Liang, P. Z., Lu, S. Z., Chen, R., Yin, Y. Q., & Zhou, J. W. (2019). Extracellular αB-crystallin modulates the inflammatory responses. Biochemical and Biophysical Research Communications, 508(1), 282–288. https://doi.org/10.1016/j.bbrc.2018.11.024

Gupta, A., & Pulliam, L. (2014). Exosomes as mediators of neuroinflammation. Journal of Neuroinflammation, 11, 1–10. https://doi.org/10.1186/1742-2094-11-68

György, B., Szabó, T. G., Pásztói, M., Pál, Z., Misják, P., Aradi, B., … Buzás, E. I. (2011). Membrane vesicles, current state-of-the-art: Emerging role of extracellular vesicles. Cellular and Molecular Life Sciences. https://doi.org/10.1007/s00018-011-0689-3

Hale, D. M., Ray, S., Leung, J. Y., Holloway, A. F., Chung, R. S., West, A. K., & Chuah, M. I. (2011). Olfactory ensheathing cells moderate nuclear factor kappaB translocation in astrocytes. Molecular and Cellular Neuroscience. https://doi.org/10.1016/j.mcn.2010.09.004

Hamby, M. E., Coppola, G., Ao, Y., Geschwind, D. H., Khakh, B. S., & Sofroniew, M. V. (2012). Inflammatory Mediators Alter the Astrocyte Transcriptome and Calcium Signaling Elicited by Multiple G-Protein-Coupled Receptors. Journal of Neuroscience. https://doi.org/10.1523/JNEUROSCI.1256-12.2012

He, F., Ge, W., Martinowich, K., Becker-Catania, S., Coskun, V., Zhu, W., … Sun, Y. E. (2005). A positive autoregulatory loop of Jak-STAT signaling controls the onset of astrogliogenesis. Nature Neuroscience. https://doi.org/10.1038/nn1440

Hegedus, B., Dasgupta, B., Shin, J. E., Emnett, R. J., Hart-Mahon, E. K., Elghazi, L., … Gutmann, D. H. (2007). Neurofibromatosis-1 Regulates Neuronal and Glial Cell Differentiation from Neuroglial Progenitors In Vivo by Both cAMP- and Ras-Dependent Mechanisms. Cell Stem Cell. https://doi.org/10.1016/j.stem.2007.07.008

Hellström, N. A. K., Björk-Eriksson, T., Blomgren, K., & Kuhn, H. G. (2009). Differential Recovery of Neural Stem Cells in the Subventricular Zone and Dentate Gyrus After Ionizing Radiation. Stem Cells. https://doi.org/10.1634/stemcells.2008-0732

Herrmann, J. E., Imura, T., Song, B., Qi, J., Ao, Y., Nguyen, T. K., … Sofroniew, M. V. (2008). STAT3 is a critical regulator of astrogliosis and scar formation after spinal cord injury. Journal of Neuroscience. https://doi.org/10.1523/JNEUROSCI.1709-08.2008

Higginson, J. R., Thompson, S. M., Santos-Silva, A., Guimond, S. E., Turnbull, J. E., & Barnett, S. C. (2012). Differential Sulfation Remodelling of Heparan Sulfate by Extracellular 6-O-Sulfatases Regulates Fibroblast Growth Factor-Induced Boundary Formation by Glial Cells: Implications for Glial Cell Transplantation. Journal of Neuroscience. https://doi.org/10.1523/JNEUROSCI.6340-11.2012

Holt, L. M., Stoyanof, S. T., & Olsen, M. L. (2019). Magnetic Cell Sorting for In Vivo and In Vitro Astrocyte, Neuron, and Microglia Analysis. Current Protocols in Neuroscience. https://doi.org/10.1002/cpns.71

Hong, S., & Song, M. R. (2014). STAT3 but not STAT1 is required for astrocyte differentiation. PLoS ONE, 9(1), 1–9. https://doi.org/10.1371/journal.pone.0086851

Horner, P. J., & Palmer, T. D. (2003). New roles for astrocytes: The nightlife of an "astrocyte". La vida loca! Trends in Neurosciences. https://doi.org/10.1016/j.tins.2003.09.010

Horner, P. J., Power, A. E., Kempermann, G., Kuhn, H. G., Palmer, T. D., Winkler, J., … Gage, F. H. (2000). Proliferation and differentiation of progenitor cells throughout the intact adult rat spinal cord. Journal of Neuroscience. https://doi.org/10.1523/jneurosci.20-06-02218.2000

Hu, Y., & Bouloux, P. M. (2011). X-linked GnRH deficiency: Role of KAL-1 mutations in GnRH deficiency. Molecular and Cellular Endocrinology. https://doi.org/10.1016/j.mce.2011.04.001

Hu, Y., Butts, T., Poopalasundaram, S., Graham, A., & Bouloux, P. M. (2019). Extracellular matrix protein anosmin-1 modulates olfactory ensheathing cell maturation in chick olfactory bulb development. European Journal of Neuroscience, 50(9), 3472–3486. https://doi.org/10.1111/ejn.14483

Hu, Y., Guimond, S. E., Travers, P., Cadman, S., Hohenester, E., Turnbull, J. E., … Bouloux, P.-M. (2009). Novel mechanisms of fibroblast growth factor receptor 1 regulation by extracellular matrix protein anosmin-1. The Journal of Biological Chemistry, 284(43), 29905–29920. https://doi.org/10.1074/jbc.M109.049155

Huang, Z. H., Wang, Y., Cao, L., Su, Z. Da, Zhu, Y. L., Chen, Y. Z., … He, C. (2008). Migratory properties of cultured olfactory ensheathing cells by single-cell migration assay. Cell Research. https://doi.org/10.1038/cr.2008.38

Huart, C., Rombaux, P., & Hummel, T. (2019). Neural plasticity in developing and adult olfactory pathways – focus on the human olfactory bulb. Journal of Bioenergetics and Biomembranes. https://doi.org/10.1007/s10863-018-9780-x

Imaizumi, T., Lankford, K. L., Burton, W. V., Fodor, W. L., & Kocsis, J. D. (2000). Xenotransplantation of transgenic pig olfactory ensheathing cells promotes axonal regeneration in rat spinal cord. Nature Biotechnology. https://doi.org/10.1038/79432

Inatani, M., Irie, F., Plump, A. S., Tessier-Lavigne, M., & Yamaguchi, Y. (2003). Mammalian Brain Morphogenesis and Midline Axon Guidance Require Heparan Sulfate. Science. https://doi.org/10.1126/science.1090497

Irie, F., Badie-Mahdavi, H., & Yamaguchi, Y. (2012). Autism-like socio-communicative deficits and stereotypies in mice lacking heparan sulfate. Proceedings of the National Academy of Sciences of the United States of America, 109(13), 5052–5056. https://doi.org/10.1073/pnas.1117881109

Irschick, R., Trost, T., Karp, G., Hausott, B., Auer, M., Claus, P., & Klimaschewski, L. (2013). Sorting of the FGF receptor 1 in a human glioma cell line. Histochemistry and Cell Biology. https://doi.org/10.1007/s00418-012-1009-1

Jeppesen, D. K., Fenix, A. M., Franklin, J. L., Higginbotham, J. N., Zhang, Q., Zimmerman, L. J., … Coffey, R. J. (2019). Reassessment of Exosome Composition. Cell, 177(2), 428-445.e18. https://doi.org/10.1016/j.cell.2019.02.029

Johansson, S., Lee, I. H., Olson, L., & Spenger, C. (2005). Olfactory ensheathing glial co-grafts improve functional recovery in rats with 6-OHDA lesions. Brain, 128(12), 2961–2976. https://doi.org/10.1093/brain/awh644

John, G. R., Lee, S. C., Song, X., Rivieccio, M., & Brosnan, C. F. (2005). IL-1-regulated responses in astrocytes: Relevance to injury and recovery. GLIA. https://doi.org/10.1002/glia.20109

Joy, A., Moffett, J., Neary, K., Mordechai, E., Stachowiak, E. K., Coons, S., … Stachowiak, M. K. (1997). Nuclear accumulation of FGF-2 is associated with proliferation of human astrocytes and glioma cells. Oncogene. https://doi.org/10.1038/sj.onc.1200823

Joyce, D., Albanese, C., Steer, J., Fu, M., Bouzahzah, B., & Pestell, R. G. (2001). NF-kB and cell-cycle regulation: The cyclin connection. Cytokine and Growth Factor Reviews. https://doi.org/10.1016/S1359-6101(00)00018-6

Jung, S. H., Lee, H. C., Yu, D. M., Kim, B. C., Park, S. M., Lee, Y. S., … Lee, J. S. (2016). Heparan sulfation is essential for the prevention of cellular senescence. Cell Death and Differentiation. https://doi.org/10.1038/cdd.2015.107

Kalra, H., Simpson, R. J., Ji, H., Aikawa, E., Altevogt, P., Askenase, P., … Mathivanan, S. (2012). Vesiclepedia: A Compendium for Extracellular Vesicles with Continuous Community Annotation. PLoS Biology. https://doi.org/10.1371/journal.pbio.1001450

Kanda, T. (2013). Biology of the blood-nerve barrier and its alteration in immune mediated neuropathies. Journal of Neurology, Neurosurgery and Psychiatry. https://doi.org/10.1136/jnnp-2012-302312

Kang, W., Balordi, F., Su, N., Chen, L., Fishell, G., & Hebert, J. M. (2014). Astrocyte activation is suppressed in both normal and injured brain by FGF signaling. Proceedings of the National Academy of Sciences. https://doi.org/10.1073/pnas.1320401111

Kang, W., Wong, L. C., Shi, S.-H., & Hébert, J. M. (2009). The transition from radial glial to intermediate progenitor cell is inhibited by FGF signaling during corticogenesis. The Journal of Neuroscience: The Official Journal of the Society for Neuroscience, 29(46), 14571–14580. https://doi.org/10.1523/JNEUROSCI.3844-09.2009

Kanski, R., Van Strien, M. E., Van Tijn, P., & Hol, E. M. (2014). A star is born: New insights into the mechanism of astrogenesis. Cellular and Molecular Life Sciences. https://doi.org/10.1007/s00018-013-1435-9

Keerthikumar, S., Chisanga, D., Ariyaratne, D., Al Saffar, H., Anand, S., Zhao, K., … Mathivanan, S. (2016). ExoCarta: A Web-Based Compendium of Exosomal Cargo. Journal of Molecular Biology. https://doi.org/10.1016/j.jmb.2015.09.019

Khakh, B. S., & Deneen, B. (2019). The Emerging Nature of Astrocyte Diversity. Annual Review of Neuroscience. https://doi.org/10.1146/annurev-neuro-070918-050443

Kim, D. K., Lee, J., Kim, S. R., Choi, D. S., Yoon, Y. J., Kim, J. H., … Gho, Y. S. (2015). EVpedia: A community web portal for extracellular vesicles research. Bioinformatics. https://doi.org/10.1093/bioinformatics/btu741

Kim, H. H., Puche, A. C., & Margolis, F. L. (2006). Odorant deprivation reversibly modulates transsynaptic changes in the NR2B-mediated CREB pathway in mouse piriform cortex. Journal of Neuroscience. https://doi.org/10.1523/JNEUROSCI.1727-06.2006

Kirby, E. D., Muroy, S. E., Sun, W. G., Covarrubias, D., Leong, M. J., Barchas, L. A., & Kaufer, D. (2013). Acute stress enhances adult rat hippocampal neurogenesis and activation of newborn neurons via secreted astrocytic FGF2. ELife. https://doi.org/10.7554/eLife.00362

Klenke, U., & Taylor-Burds, C. (2012). Culturing embryonic nasal explants for developmental and physiological study. Current Protocols in Neuroscience. https://doi.org/10.1002/0471142301.ns0325s59

Klopstein, A., Santos-Nogueira, E., Francos-Quijorna, I., Redensek, A., David, S., Navarro, X., & López-Vales, R. (2012). Beneficial effects of αB-crystallin in spinal cord contusion injury. Journal of Neuroscience, 32(42), 14478–14488. https://doi.org/10.1523/JNEUROSCI.0923-12.2012

Kore, R. A., & Abraham, E. C. (2014). Inflammatory cytokines, interleukin-1 beta and tumor necrosis factor-alpha, upregulated in glioblastoma multiforme, raise the levels of CRYAB in exosomes secreted by U373 glioma cells. Biochemical and Biophysical Research Communications. https://doi.org/10.1016/j.bbrc.2014.09.068

Kore, R. A., & Abraham, E. C. (2016). Phosphorylation negatively regulates exosome mediated secretion of CryAB in glioma cells. Biochimica et Biophysica Acta - Molecular Cell Research, 1863(2), 368–377. https://doi.org/10.1016/j.bbamcr.2015.11.027

Kuipers, H. F., Yoon, J., Van Horssen, J., Han, M. H., Bollyky, P. L., Palmer, T. D., & Steinman, L. (2017). Phosphorylation of αB-crystallin supports reactive astrogliosis in demyelination. Proceedings of the National Academy of Sciences of the United States of America, 114(9), E1745–E1754. https://doi.org/10.1073/pnas.1621314114

Lakatos, A., Barnett, S. C., & Franklin, R. J. M. (2003). Olfactory ensheathing cells induce less host astrocyte response and chondroitin sulphate proteoglycan expression than Schwann cells following transplantation into adult CNS white matter. Experimental Neurology. https://doi.org/10.1016/S0014-4886(03)00270-X

Lakatos, A., Franklin, R. J. M., & Barnett, S. C. (2000). Olfactory ensheathing cells and Schwann cells differ in their in vitro interactions with astrocytes. GLIA. https://doi.org/10.1002/1098-1136(200012)32:3<214::AID-GLIA20>3.0.CO;2-7

Lanner, F., & Rossant, J. (2010). The role of FGF/Erk signaling in pluripotent cells. Development. https://doi.org/10.1242/dev.050146

Larriva-Sahd, J. (2014). Structural variation and interactions among astrocytes of the rostral migratory stream and olfactory bulb: II. Golgi and electron microscopic study of the adult rat. Neuroscience Research. https://doi.org/10.1016/j.neures.2014.08.011

Le Roy, C., & Wrana, J. L. (2005). Clathrin- and non-clathrin-mediated endocytic regulation of cell signalling. Nature Reviews Molecular Cell Biology. https://doi.org/10.1038/nrm1571

Leadbeater, W. E., Gonzalez, A. M., Logaras, N., Berry, M., Turnbull, J. E., & Logan, A. (2006). Intracellular trafficking in neurones and glia of fibroblast growth factor-2, fibroblast growth factor receptor 1 and heparan sulphate proteoglycans in the injured adult rat cerebral cortex. Journal of Neurochemistry, 96(4), 1189–1200. https://doi.org/10.1111/j.1471-4159.2005.03632.x

Li, J., Chen, W., Li, Y., Chen, Y., Ding, Z., Yang, D., & Zhang, X. (2015). Transplantation of olfactory ensheathing cells promotes partial recovery in rats with experimental autoimmune encephalomyelitis. International Journal of Clinical and Experimental Pathology.

Li, Y., Decherchi, P., & Raisman, G. (2003). Transplantation of olfactory ensheathing cells into spinal cord lesions restores breathing and climbing. The Journal of Neuroscience: The Official Journal of the Society for Neuroscience, 23(3), 727–731. https://doi.org/23/3/727 [pii]

Li, Y., Field, P. M., & Raisman, G. (2005). Olfactory ensheathing cells and olfactory nerve fibroblasts maintain continuous open channels for regrowth of olfactory nerve fibres. GLIA, 52(3), 245–251. https://doi.org/10.1002/glia.20241

Li, Y., Field, P. M., & Raisman, G. (1997). Repair of adult rat corticospinal tract by transplants of olfactory ensheathing cells. Science, 277(5334), 2000–2002. https://doi.org/10.1126/science.277.5334.2000

Li, Y., Li, D., Ibrahim, A., & Raisman, G. (2012). Repair involves all three surfaces of the glial cell. In Progress in Brain Research. https://doi.org/10.1016/B978-0-444-59544-7.00010-X

Li, Z., Theus, M. H., & Wei, L. (2006). Role of ERK 1/2 signaling in neuronal differentiation of cultured embryonic stem cells. Development Growth and Differentiation. https://doi.org/10.1111/j.1440-169X.2006.00889.x

Li, Z., Theus, M. H., & Wei, L. (2006). Role of ERK 1/2 signaling in neuronal differentiation of cultured embryonic stem cells. Development Growth and Differentiation. https://doi.org/10.1111/j.1440-169X.2006.00889.x

Lian, H., Yang, L., Cole, A., Sun, L., Chiang, A. C. A., Fowler, S. W., … Zheng, H. (2015). NFκB-Activated Astroglial Release of Complement C3 Compromises Neuronal Morphology and Function Associated with Alzheimer's Disease. Neuron. https://doi.org/10.1016/j.neuron.2014.11.018

Liddelow, S. A., & Barres, B. A. (2017). Reactive Astrocytes: Production, Function, and Therapeutic Potential. Immunity, 46(6), 957–967. https://doi.org/10.1016/j.immuni.2017.06.006

Liddelow, S. A., Guttenplan, K. A., Clarke, L. E., Bennett, F. C., Bohlen, C. J., Schirmer, L., … Barres, B. A. (2017). Neurotoxic reactive astrocytes are induced by activated microglia. Nature, 541(7638), 481–487. https://doi.org/10.1038/nature21029

Lu, J., Féron, F., Mackay-Sim, A., & Waite, P. M. E. (2002). Olfactory ensheathing cells promote locomotor recovery after delayed transplantation into transected spinal cord. Brain, 125(1), 14–21. https://doi.org/10.1093/brain/awf014

Ma, D. K., Ponnusamy, K., Song, M. R., Ming, G. L., & Song, H. (2009). Molecular genetic analysis of FGFR1 signalling reveals distinct roles of MAPK and PLC1 activation for self-renewal of adult neural stem cells. Molecular Brain, 2(1), 1–14. https://doi.org/10.1186/1756-6606-2-16

Mackay-Sim, A., & Kittel, P. (1991). Cell dynamics in the adult mouse olfactory epithelium: A quantitative autoradiographic study. Journal of Neuroscience. https://doi.org/10.1523/jneurosci.11-04-00979.1991

Magnusson, J. P., & Frisen, J. (2016). Stars from the darkest night: unlocking the neurogenic potential of astrocytes in different brain regions. Development. https://doi.org/10.1242/dev.133975

Magnusson, J. P., Göritz, C., Tatarishvili, J., Dias, D. O., Smith, E. M. K., Lindvall, O., … Frisén, J. (2014). A latent neurogenic program in astrocytes regulated by Notch signaling in the mouse. Science. https://doi.org/10.1126/science.346.6206.237

Maric, D., Fiorio Pla, A., Chang, Y. H., & Barker, J. L. (2007). Self-renewing and differentiating properties of cortical neural stem cells are selectively regulated by basic fibroblast growth factor (FGF) signaling via specific FGF receptors. The Journal of Neuroscience: The Official Journal of the Society for Neuroscience, 27(8), 1836–1852. https://doi.org/10.1523/JNEUROSCI.5141-06.2007

McKhann, G. M., D'Ambrosio, R., & Janigro, D. (1997). Heterogeneity of astrocyte resting membrane potentials and intercellular coupling revealed by whole-cell and gramicidin-perforated patch recordings from cultured neocortical and hippocampal slice astrocytes. The Journal of Neuroscience: The Official Journal of the Society for Neuroscience, 17(18), 6850–6863. https://doi.org/MO1

Mohammadi, M., Dionne, C. A., Li, W., Li, N., Spivak, T., Honegger, A. M., … Schlessinger, J. (1992). Point mutation in FGF receptor eliminates phosphatidylinositol hydrolysis without affecting mitogenesis. Nature. https://doi.org/10.1038/358681a0

Molofsky, A.V., Glasgow, S.M., Chaboub, L.S., Tsai, H.H., Murnen, A.T., Kelley, K.W., Fancy, S.P.J., Yuen, T.J., Madireddy, L., Baranzini, S., et al. (n.d.). Expression profiling of Aldh1l1-precursors in the developing spinal cord reveals glial lineage-specific genes and direct Sox9-Nfe2l1 interactions. Glia 61, 1518–1532.

Molofsky, A. V., & Deneen, B. (2015). Astrocyte development: A Guide for the Perplexed. Glia, 63(8), 1320–1329. https://doi.org/10.1002/glia.22836

Müller, G. (2012). Microvesicles/exosomes as potential novel biomarkers of metabolic diseases. Diabetes, Metabolic Syndrome and Obesity: Targets and Therapy. https://doi.org/10.2147/dmso.s32923

Muranova, L. K., Sudnitsyna, M. V., & Gusev, N. B. (2018). αB-Crystallin Phosphorylation: Advances and Problems. Biochemistry (Moscow). https://doi.org/10.1134/S000629791810005X

Murtaza, M., Chacko, A., Delbaz, A., Reshamwala, R., Rayfield, A., McMonagle, B., … Ekberg, J. A. K. (2019). Why are olfactory ensheathing cell tumors so rare? Cancer Cell International. https://doi.org/10.1186/s12935-019-0989-5

Nash, H. H., Borke, R. C., & Anders, J. J. (2001). New Method of Purification for Establishing Primary Cultures of Ensheathing Cells from the Adult Olfactory Bulb. GLIA (Vol. 34).

Nato, G., Caramello, a., Trova, S., Avataneo, V., Rolando, C., Taylor, V., … Luzzati, F. (2015). Striatal astrocytes produce neuroblasts in an excitotoxic model of Huntington's disease. Development, 142(5), 840–845. https://doi.org/10.1242/dev.116657

Nazareth, L., Chen, M., Shelper, T., Shah, M., Tello Velasquez, J., Walkden, H., … Ekberg, J. A. K. (2019). Novel insights into the glia limitans of the olfactory nervous system. Journal of Comparative Neurology, 527(7), 1228–1244. https://doi.org/10.1002/cne.24618

Nikolaychik, V. V., Samet, M. M., & Lelkes, P. I. (1996). A new method for continual quantitation of viable cells on endothelialized polyurethanes. Journal of Biomaterials Science, Polymer Edition. https://doi.org/10.1163/156856296X00057

O'Toole, D. A., West, A. K., & Chuah, M. I. (2007). Effect of olfactory ensheathing cells on reactive astrocytes in vitro. Cellular and Molecular Life Sciences. https://doi.org/10.1007/s00018-007-7106-y

Ohkubo, Y., Uchida, A. O., Shin, D., Partanen, J., & Vaccarino, F. M. (2004). Fibroblast growth factor receptor 1 is required for the proliferation of hippocampal progenitor cells and for hippocampal growth in mouse. The Journal of Neuroscience: The Official Journal of the Society for Neuroscience, 24(27), 6057–6069. https://doi.org/10.1523/JNEUROSCI.1140-04.2004

Ornitz, D. M., & Itoh, N. (2015). Advanced Review: The Fibroblast Growth Factor Signaling Pathway. WIREs Dev Biol, 4, 215–266. https://doi.org/WIREs Dev Biol2015, 4:215–266. doi: 10.1002/wdev.176

Ousman, S. S., Tomooka, B. H., Van Noort, J. M., Wawrousek, E. F., O'Conner, K., Hafler, D. A., … Steinman, L. (2007). Protective and therapeutic role for αB-crystallin in autoimmune demyelination. Nature. https://doi.org/10.1038/nature05935

Peng, H., Myers, J., Fang, X., Stachowiak, E. K., Maher, P. A., Martins, G. G., … Stachowiak, M. K. (2002). Integrative nuclear FGFR1 signaling (INFS) pathway mediates activation of the tyrosine hydroxylase gene by angiotensin II, depolarization and protein kinase C. Journal of Neurochemistry. https://doi.org/10.1046/j.1471-4159.2002.00833.x

Perego, C., Vanoni, C., Bossi, M., Massari, S., Basudev, H., Longhi, R., & Pietrini, G. (2000). The GLT-1 and GLAST glutamate transporters are expressed on morphologically distinct astrocytes and regulated by

neuronal activity in primary hippocampal cocultures. Journal of Neurochemistry. https://doi.org/10.1046/j.1471-4159.2000.0751076.x

Peters, K. G., Marie, J., Wilson, E., Ives, H. E., Escobedo, J., Rosario, M. Del, … Williams, L. T. (1992). Point mutation of an FGF receptor abolishes phosphatidylinositol turnover and Ca2+ flux but not mitogenesis. Nature. https://doi.org/10.1038/358678a0

Petersen, E. R., Ammitzbøll, C., Søndergaard, H. B., Oturai, A. B., Sørensen, P. S., Nilsson, A. C., … Sellebjerg, F. (2019). Expression of melanoma cell adhesion molecule-1 (MCAM-1) in natalizumab-treated multiple sclerosis. Journal of Neuroimmunology, 337. https://doi.org/10.1016/j.jneuroim.2019.577085

Picard-Riera, N., Decker, L., Delarasse, C., Goude, K., Nait-Oumesmar, B., Liblau, R., … Evercooren, A. B.-V. (2002). Experimental autoimmune encephalomyelitis mobilizes neural progenitors from the subventricular zone to undergo oligodendrogenesis in adult mice. Proceedings of the National Academy of Sciences. https://doi.org/10.1073/pnas.192314199

Pirttimaki, T. M., & Parri, H. R. (2013). Astrocyte plasticity: Implications for synaptic and neuronal activity. Neuroscientist. https://doi.org/10.1177/1073858413504999

Planque, N. (2006). Nuclear trafficking of secreted factors and cell-surface receptors: New pathways to regulate cell proliferation and differentiation, and involvement in cancers. Cell Communication and Signaling. https://doi.org/10.1186/1478-811X-4-7

Poopalasundaram, S., Knott, C., Shamotienko, O. G., Foran, P. G., Dolly, J. O., Ghiani, C. A., … Wilkin, G. P. (2000). Glial heterogeneity in expression of the inwardly rectifying K+ channel, Kir4.1, in adult rat CNS. GLIA. https://doi.org/10.1002/(SICI)1098-1136(200006)30:4<362: AID-GLIA50>3.0.CO;2-4

Pringle, N. P., Yu, W.-P., Howell, M., Colvin, J. S., Ornitz, D. M., & Richardson, W. D. (2003). Fgfr3 expression by astrocytes and their precursors: evidence that astrocytes and oligodendrocytes originate in distinct neuroepithelial domains. Development (Cambridge, England), 130(1), 93–102. https://doi.org/10.1242/dev.00184

Probert, L., Akassoglou, K., Kassiotis, G., Pasparakis, M., Alexopoulou, L., & Kollias, G. (1997). TNF-α transgenic and knockout models of CNS inflammation and degeneration. In Journal of Neuroimmunology (Vol. 72, pp. 137–141). https://doi.org/10.1016/S0165-5728(96)00184-1

Qiu, J., Yan, Z., Tao, K., Li, Y., Li, Y., Li, J., … Chen, H. (2016). Sinomenine activates astrocytic dopamine D2 receptors and alleviates neuroinflammatory injury via the CRYAB/STAT3 pathway after ischemic stroke in mice. Journal of Neuroinflammation, 13(1). https://doi.org/10.1186/s12974-016-0739-8

Quach, Q. L., Metz, L. M., Thomas, J. C., Rothbard, J. B., Steinman, L., & Ousman, S. S. (2013). CRYAB modulates the activation of CD4+ T cells from relapsing-remitting multiple sclerosis patients. Multiple Sclerosis Journal, 19(14), 1867–1877. https://doi.org/10.1177/1352458513489853

Raisman, G., & Li, Y. (2007). Repair of neural pathways by olfactory ensheathing cells. Nature Reviews. Neuroscience, 8(4), 312–319. https://doi.org/10.1038/nrn2099

Ramer, L. M., Au, E., Richter, M. W., Liu, J., Tetzlaff, W., & Roskams, A. J. (2004). Peripheral Olfactory Ensheathing Cells Reduce Scar and Cavity Formation and Promote Regeneration after Spinal Cord Injury. Journal of Comparative Neurology. https://doi.org/10.1002/cne.20049

Raponi, E., Agenes, F., Delphin, C., Assard, N., Baudier, J., Legraverend, C., & Deloulme, J. C. (2007). S100ß expression defines a state in which GFAP-expressing cells lose their neural stem cell potential and acquire a more mature developmental stage. GLIA. https://doi.org/10.1002/glia.20445

Reddy, V. S., Madala, S. K., Trinath, J., & Reddy, G. B. (2018, May 1). Extracellular small heat shock proteins: exosomal biogenesis and function. Cell Stress and Chaperones. Cell Stress and Chaperones. https://doi.org/10.1007/s12192-017-0856-z

Reilly, J. F., & Maher, P. A. (2001). Importin β-mediated nuclear import of fibroblast growth factor receptor: Role in cell proliferation. Journal of Cell Biology. https://doi.org/10.1083/jcb.152.6.1307

Reilly, J. F., Mizukoshi, E., & Maher, P. A. (2004). Ligand dependent and independent internalization and nuclear translocation of fibroblast growth factor (FGF) receptor 1. DNA and Cell Biology. https://doi.org/10.1089/dna.2004.23.538

Richter M, Au E, Liu J, Kwon B, Tetzlaff W, R. A. (2003). Neoangiogenesis in an ensheathing cell matrix: a trinity of mechanisms to promote spinal cord regeneration. Washington, DC: Society for Neuroscience: Abstract Viewer/Itinerary Planner.

Roet, K. C. D., & Verhaagen, J. (2014). Understanding the neural repair-promoting properties of olfactory ensheathing cells. Experimental Neurology. Academic Press Inc. https://doi.org/10.1016/j.expneurol.2014.05.007

Rossi, D. J., Brady, J. D., & Mohr, C. (2007, November). Astrocyte metabolism and signaling during brain ischemia. Nature Neuroscience. https://doi.org/10.1038/nn2004

Rothhammer, V., Mascanfroni, I. D., Bunse, L., Takenaka, M. C., Kenison, J. E., Mayo, L., … Quintana, F. J. (2016). Type I interferons and microbial metabolites of tryptophan modulate astrocyte activity and central nervous system inflammation via the aryl hydrocarbon receptor. Nature Medicine, 22(6), 586–597. https://doi.org/10.1038/nm.4106

Roy Choudhury, G., Ryou, M. G., Poteet, E., Wen, Y., He, R., Sun, F., … Yang, S. H. (2014). Involvement of p38 MAPK in reactive astrogliosis induced by ischemic stroke. Brain Research, 1551, 45–58. https://doi.org/10.1016/j.brainres.2014.01.013

Rugarli EI, Lutz B, Kuratani SC, Wawersik S, Borsani G, Ballabio A, E. G. (1993). Expression pattern of the Kallmann syndrome gene in the olfactory system suggests a role in neuronal targeting. Nat Genet.

Ruitenberg MJ, Plant GW, Hamers FP, Wortel J, Blits B, Dijkhuizen PA, Gispen WH, Boer GJ, V. J. (2003). Ex vivo adenoviral vector-mediated neurotrophin gene transfer to olfactory ensheathing glia: effects on rubrospinal tract regeneration, lesion size, and functional recovery after implantation in the injured rat spinal cord. J. Neurosci.

Santos-Silva. (2007). FGF/Heparin Differentially Regulates Schwann Cell and Olfactory Ensheathing Cell Interactions with Astrocytes: A Role in Astrocytosis.

Seftalioglu, A., & Karakoc, L. (2000). Expression of CD146 adhesion molecules (MUC18 or MCAM) in the thymic microenvironment. acta histochem (Vol. 102). Urban & Fischer Verlag. Retrieved from http://www.urbanfischer.de/journals/actahist

Shao, W., Zhang, S. Z., Tang, M., Zhang, X. H., Zhou, Z., Yin, Y. Q., … Zhou, J. W. (2013). Suppression of neuroinflammation by astrocytic dopamine D2 receptors via αb-crystallin. Nature, 494(7435), 90–94. https://doi.org/10.1038/nature11748

Shi, Q., Chowdhury, S., Ma, R., Le, K. X., Hong, S., Caldarone, B. J., … Lemere, C. A. (2017). Complement C3 deficiency protects against neurodegeneration in aged plaque-rich APP/PS1 mice. Science Translational Medicine. https://doi.org/10.1126/scitranslmed.aaf6295

Silver, J., Schwab, M. E., & Popovich, P. G. (2015). Central nervous system regenerative failure: Role of oligodendrocytes, astrocytes, and microglia. Cold Spring Harbor Perspectives in Biology, 7(3). https://doi.org/10.1101/cshperspect.a020602

Singh, J. P., Kumar, R. R., Goswami, S., Rai, G. K., Sakhare, A., Kumar, S., … Praveen, S. (2019). A putative heat-responsive transcription factor (TaHD97) and its targets in wheat (Triticum aestivum) providing thermotolerance. Indian Journal of Biotechnology.

Smith, G. M., Falone, A. E., & Frank, E. (2012). Sensory axon regeneration: Rebuilding functional connections in the spinal cord. Trends in Neurosciences. https://doi.org/10.1016/j.tins.2011.10.006

Smithson, L. J., & Kawaja, M. D. (2010). Microglial/macrophage cells in mammalian olfactory nerve fascicles. Journal of Neuroscience Research. https://doi.org/10.1002/jnr.22254

Sofroniew, M. V., & Vinters, H. V. (2010, January). Astrocytes: Biology and pathology. Acta Neuropathologica. https://doi.org/10.1007/s00401-009-0619-8

Sorokin, A., Mohammadi, M., Huang, J., & Schlessinger, J. (1994). Internalization of fibroblast growth factor receptor is inhibited by a point mutation at tyrosine 766. Journal of Biological Chemistry.

Soussi-Yanicostas, N., De Castro, F., Julliard, A. K., Perfettini, I., Chédotal, A., & Petit, C. (2002). Anosmin-1, defective in the X-linked form of Kallmann syndrome, promotes axonal branch formation from olfactory bulb output neurons. Cell (Vol. 109). https://doi.org/10.1016/S0092-8674(02)00713-4

Spivak-Kroizman, T., Mohammadi, M., Hu, P., Jaye, M., Schlessinger, J., & Lax, I. (1994). Point mutation in the fibroblast growth factor receptor eliminates phosphatidylinositol hydrolysis without affecting neuronal differentiation of PC12 cells. Journal of Biological Chemistry.

Sreekumar, P. G., Kannan, R., Kitamura, M., Spee, C., Barron, E., Ryan, S. J., & Hinton, D. R. (2010). αB crystallin is apically secreted within exosomes by polarized human retinal pigment epithelium and provides neuroprotection to adjacent cells. PLoS ONE, 5(10). https://doi.org/10.1371/journal.pone.0012578

Stachowiak, E. K., Maher, P. A., Tucholski, J., Mordechai, E., Joy, A., Moffett, J., … Stachowiak, M. K. (1997). Nuclear accumulation of fibroblast growth factor receptors in human glial cells - Association with cell proliferation. Oncogene. https://doi.org/10.1038/sj.onc.1201057

Stachowiak, M. K., Birkaya, B., Aletta, J. M., Narla, S. T., Benson, C. A., Decker, B., & Stachowiak, E. K. (2015). "Nuclear FGF Receptor-1 and CREB binding protein: An integrative signaling module." Journal of Cellular Physiology. https://doi.org/10.1002/jcp.24879

Stachowiak, M. K., & Stachowiak, E. K. (2016). Evidence-Based Theory for Integrated Genome Regulation of Ontogeny-An Unprecedented Role of Nuclear FGFR1 Signaling. Journal of Cellular Physiology, 231(6), 1199–1218. https://doi.org/10.1002/jcp.25298

Stachowiak, M. K., Stachowiak, E. K., Aletta, J. M., & Tzanakakis, E. S. (2011). A common integrative nuclear signaling module for stem cell development. In Stem Cells: From Mechanisms to Technologies. https://doi.org/10.1142/9789814317931_0004

Stevens, B., & Muthukumar, A. K. (2016). Cellular neuroscience. Differences among astrocytes. Science (New York, N.Y.). https://doi.org/10.1126/science.aaf2849

Stewart, M. D., & Sanderson, R. D. (2014). Heparan sulfate in the nucleus and its control of cellular functions. Matrix Biology. https://doi.org/10.1016/j.matbio.2013.10.009

Tanık, N., Serin, H. I., Celikbilek, A., Inan, L. E., & Gündoğdu, F. (2015). Olfactory bulb and olfactory sulcus depths are associated with disease duration and attack frequency in multiple sclerosis patients. Journal of the Neurological Sciences. https://doi.org/10.1016/j.jns.2015.09.016

Tuzon, C. T., Rigueur, D., & Merrill, A. E. (2019). Nuclear Fibroblast Growth Factor Receptor Signaling in Skeletal Development and Disease. Current Osteoporosis Reports. https://doi.org/10.1007/s11914-019-00512-2

van Noort, J. M., Bsibsi, M., Nacken, P. J., Verbeek, R., & Venneker, E. H. G. (2015). Therapeutic intervention in multiple sclerosis with alpha B-crystallin: A randomized controlled phase IIa trial. PLoS ONE, 10(11). https://doi.org/10.1371/journal.pone.0143366

Verkhratsky, A., Sofroniew, M. V., Messing, A., deLanerollei, N. C., Rempe, D., Rodríguez, J. J., & Nedergaard, M. (2012). Neurological diseases as primary gliopathies: A reassessment of neurocentrism. ASN Neuro. https://doi.org/10.1042/AN20120010

Villarreal, A., Seoane, R., Torres, A. G., Rosciszewski, G., Angelo, M. F., Rossi, A., … Ramos, A. J. (2014). S100ß protein activates a RAGE-dependent autocrine loop in astrocytes: Implications for its role in the propagation of reactive gliosis. Journal of Neurochemistry. https://doi.org/10.1111/jnc.12790

von Zastrow, M., & Sorkin, A. (2007). Signaling on the endocytic pathway. Current Opinion in Cell Biology. https://doi.org/10.1016/j.ceb.2007.04.021

Wheeler, M. A., Clark, I. C., Tjon, E. C., Li, Z., Zandee, S. E. J., Couturier, C. P., … Quintana, F. J. (2020). MAFG-driven astrocytes promote CNS inflammation. Nature, 578(7796), 593–599. https://doi.org/10.1038/s41586-020-1999-0

Więdłocha, A., Nilsen, T., Wesche, J., Sørensen, V., Małecki, J., Marcinkowska, E., & Olsnes, S. (2005). Phosphorylation-regulated nucleocytoplasmic trafficking of internalized fibroblast growth factor-1. Molecular Biology of the Cell. https://doi.org/10.1091/mbc.E04-05-0389

Williams, S. K., Franklin, R. J. M., & Barnett, S. C. (2004). Response of Olfactory Ensheathing Cells to the Degeneration and Regeneration of the Peripheral Olfactory System and the Involvement of the Neuregulins. Journal of Comparative Neurology, 470(1), 50–62. https://doi.org/10.1002/cne.11045

Woodbury, M. E., & Ikezu, T. (2014). Fibroblast growth factor-2 signaling in neurogenesis and neurodegeneration. Journal of Neuroimmune Pharmacology. https://doi.org/10.1007/s11481-013-9501-5

Yaldızlı, Penner, I. K., Yonekawa, T., Naegelin, Y., Kuhle, J., Pardini, M., … Sprenger, T. (2016). The association between olfactory bulb volume, cognitive dysfunction, physical disability and depression in multiple sclerosis. European Journal of Neurology. https://doi.org/10.1111/ene.12891

Yamaguchi, Y., Inatani, M., Matsumoto, Y., Ogawa, J., & Irie, F. (2010). Roles of heparan sulfate in mammalian brain development: Current views based on the findings from ext1 conditional knockout studies. Progress in Molecular Biology and Translational Science, 93(C), 133–152. https://doi.org/10.1016/S1877-1173(10)93007-X

Yazaki, N., Hosoi, Y., Kawabata, K., Miyake, A., Minami, M., Satoh, M., … Itoh, N. (1994). Differential expression patterns of mRNAs for members of the fibroblast growth factor receptor family, FGFR-1–FGFR-4, in rat brain. Journal of Neuroscience Research. https://doi.org/10.1002/jnr.490370403

Zamanian, J. L., Xu, L., Foo, L. C., Nouri, N., Zhou, L., Giffard, R. G., & Barres, B. A. (2012). Genomic Analysis of Reactive Astrogliosis. Journal of Neuroscience. https://doi.org/10.1523/JNEUROSCI.6221-11.2012

Zarubin, T., & Han, J. (2005). Activation and signaling of the p38 MAP kinase pathway. Cell Research, 15(1), 11–18. https://doi.org/10.1038/sj.cr.7290257

Zhang, Y., Chen, Y., Wu, J., Manaenko, A., Yang, P., Tang, J., … Zhang, J. H. (2015). Activation of Dopamine D2 Receptor Suppresses Neuroinflammation Through αb-Crystalline by Inhibition of NF-κB Nuclear Translocation in Experimental ICH Mice Model. Stroke, 46(9), 2637–2646. https://doi.org/10.1161/STROKEAHA.115.009792

Zhang, Y., Sloan, S. A., Clarke, L. E., Caneda, C., Plaza, C. A., Blumenthal, P. D., … Barres, B. A. (2016). Purification and Characterization of Progenitor and Mature Human Astrocytes Reveals Transcriptional and Functional Differences with Mouse. Neuron. https://doi.org/10.1016/j.neuron.2015.11.013